In presenting the dissertation as a partial fulfillment of the requirements for an advanced degree from the Georgia Institute of Technology, I agree that the Library of the Institute shall make it available for inspection and circulation in accordance with its regulations governing materials of this type. I agree that permission to copy from, or to publish from, this dissertation may be granted by the professor under whose direction it was written, or, in his absence, by the Dean of the Graduate Division when such copying or publication is solely for scholarly purposes and does not involve potential financial gain. It is understood that any copying from, or publication of, this dissertation which involves potential financial gain will not be allowed without written permission.

[redacted]

[redacted]

THE ROLE OF SEDIMENT GRADATION ON CHANNEL ARMORING

A THESIS

Presented to

The Faculty of the Graduate Division

by

William Campbell Little

In Partial Fulfillment

of the Requirements for the Degree

Doctor of Philosophy

in the School of Civil Engineering

Georgia Institute of Technology

May 1972

THE ROLE OF SEDIMENT GRADATION

ON CHANNEL ARMORING

Approved:

Paul G. Mayer, Chairman

Marion R. Carstens

George M. Slaughter

Date approved by Chairman: June 6, 1972

ACKNOWLEDGMENTS

The author gratefully acknowledges the advice and assistance of his thesis advisor, Dr. Paul G. Mayer, who provided constant guidance and encouragement. Drs. M. R. Carstens, G. M. Slaughter, and C. S. Martin are thanked for their suggestions in the preparation of the final draft.

Special thanks are given to Drs. W. M. Sangster and S. C. Webb for permitting this research to be done off campus.

The author is indebted to the U. S. Department of Agriculture for financial assistance through the "Employees' Training Act." Appreciation is also expressed to the staff of the Southern Piedmont Conservation Research Center, Watkinsville, Georgia, for their assistance. Special thanks are given to William F. Whitehead, Jr., for the construction of all equipment used in this study and the many extra hours in performing these experiments.

The author's wife, Stephanie, is acknowledged for her patience and understanding during this study.

Permission has been granted by the Graduate Division for special pagination and margin widths in order that this dissertation may be published as a report of the Environmental Resources Center, Georgia Institute of Technology.

TABLE OF CONTENTS

TABLE OF CONTENTS (Continued)

LIST OF TABLES

LIST OF TABLES (Continued)

LIST OF ILLUSTRATIONS

Figure Page

TEXT

LIST OF ILLUSTRATIONS (Continued)

APPENDIX

NOMENCLATURE

Symbol	Quantity	Dimensions (F,L,T)
a	constant	none
A	flow area	L^2
b	constant	none
B	width of flume	L
c	constant	none
d_g	geometric mean diameter of sediment particles	L
d_t	arithmetic mean diameter of transported sediment particles	L
$d_{05}, d_{75}, d_{84.1}, d_{95}$	particle size for which 5, 75, $d_{84.1}$, and 95 percent by weight is finer	L
g	acceleration due to gravity	LT^{-2}
n	Mannings' roughness coefficient	$L^{1/6}$
q_s	mass sediment transport rate, unit width	$FT^{-1}L^{-1}$
Q_s	total mass sediment transport rate	FT^{-1}
Q	water volume rate of flow	L^3T^{-1}
r	mass density of sediment	FT^2L^{-4}
R	hydraulic radius	L
$R_*=\frac{u_* d_g}{\upsilon}$	particle Reynolds number	none
$s=\frac{\gamma_s}{\gamma}=\frac{r}{\rho}$	specific gravity of sediment	none
S	slope of energy grade line	none
SP	Shields' parameter	none

NOMENCLATURE (Continued)

Symbol	Quantity	Dimensions (F,L,T)
$u_* = \sqrt{gRS}$	bed shear velocity	LT^{-1}
$\bar{U} = Q/A$	time-areal average flow velocity	LT^{-1}
u_{dc}	fluid velocity 0.35_d from theoretical bed	LT^{-1}
X	a variable	none
y	depth of flow	L
α	angle bed makes with horizontal	none
γ	specific weight of water	FL^{-3}
γ_s	specific weight of sediment	FL^{-3}
μ	dynamic viscosity of fluid	FTL^{-2}
ν	kinematic viscosity of fluid	L^2T^{-1}
ρ	mass density of fluid	FT^2L^{-4}
σ_g	geometric standard deviation of bed particle diameter	none
σ_t	arithmetic standard deviation of transported particle diameter	L
$\sigma_{\tau_c/\bar{\tau}}$	arithmetic standard deviation of the dimensionless shear stress $\tau_c/\bar{\tau}$	none
$\frac{d_{ga}}{d_{go}\ \sigma_{go}}$	dimensionless sediment term from dimensional analysis	none
τ	average boundary shear stress	FL^{-2}
Φ	angle of repose of sediment	none
Ψ_*	dimensionless sediment transport rate	none

NOMENCLATURE (Continued)

Symbol	Quantity	Dimensions (F,L,T)
	Subscripts not Defined Above	
a	refers to armored bed particles	
c	refers to critical state of incipient motion	
e	refers to eroded bed particles	
f	refers to final flow properties	
i	refers to initial flow properties	
o	refers to the original bed particles	

SUMMARY

The objective of this study was to systematically investigate the effects of sediment gradation on channel armoring. The primary variable was gradation of the sediment material. A geometric mean diameter of 1.00 millimeter was used for all sediments with geometric standard deviations, σ_{go}, of 1.12, 1.50, 2.00, 2.50, and 3.00. These mixtures of crushed quartz were placed in a recirculating flume with a sediment bed 1.97 feet wide, 40.0 feet long, and approximately 0.15 foot deep. Arbitrarily selected flows, to purposely induce armoring, were kept constant throughout each experiment. Bed slope was initially set at 0.002. Depth of flow was held constant throughout each experimental run by a sluice gate. The armoring process was considered to be stable when the final sediment transport rate was not more than one percent of the initial transport rate. The surface layer of particles was then removed by the wax method and the distribution of the armored particles determined.

An empirical equation was developed through dimensional analysis relating the sediment properties of the original and armored distributions to the flow properties, when the sediment bed had become stable because of the armoring process. The equation is

$$\frac{d_{ga}}{d_{go}\,\sigma_{go}} = 0.908 \left[\frac{u_{*c}^{3}}{\nu(s-1)g}\right]^{0.353} \qquad (1)$$

where d_{ga} and d_{go} are geometric mean diameters of the armored and original sediment mixtures, respectively, σ_{go} is the geometric standard

deviation of the original sediment mixture, u_* is the bed shear velocity defined by $u_* = \sqrt{gRS}$ where g is the acceleration of gravity, R is the hydraulic radius and S is the slope of the energy grade line, ν is the kinematic viscosity of the water, and s is the specific gravity of the sediment (2.65). From the equation, for the given flow conditions and original sediment properties in a channel, the geometric mean diameter of the armored material, d_{ga}, can be calculated. The armored diameter calculated from this equation is applicable only if the channel would armor.

Another criterion was developed to determine, for the given sediment and flow properties, if the sediment bed could armor. If the calculated geometric mean diameter of the armored surface material was between the d_{05} and d_{95} (that size for which 5 and 95 percent, respectively, by weight is finer) size of the original material, the original bed material would armor for those flow conditions.

With the broadly graded materials, $\sigma_{go} \geq 2.00$, where channel armoring occurred, the bed degraded uniformly in depth along the length of the bed. However, for uniform materials, $\sigma_{go} < 1.50$, little or no armoring could be induced, and the bed did not degrade uniformly in depth but degraded more at the beginning of the reach and less at the outlet end resulting in a reduced bed slope.

Dunes formed initially and as they moved off, armoring was immediately observable. Armoring of the surface had no significant change on the average bed shear stress throughout the armoring process.

After an "armor coat" had developed, a very low sediment transport rate continued for long periods of time. This transport was by local

scour of fine material around larger particles. Fine material could be observed "hiding" in the wake or zone of separation of the large particles. Turbulence caused shifting of the zone of separation and sporadic movement of fine material.

The results of this study were compared with the calculated armored distributions by a method developed by Gessler. The geometric mean diameters calculated by Gessler's method were consistently lower than the measured values of this study and differed from 3.5 to 29.0 percent with an average difference of approximately 20 percent.

CHAPTER I

INTRODUCTION

Description of the Problem

The transport of uniformly graded sediments has been studied extensively. However, most investigators in sediment transport studies have chosen uniformly graded materials purposely in order to eliminate any effects of gradation upon transport. In fact, many investigators have used selected sands or glass beads so that the transport may be related only to the size (mass) of these particles.

When a mixture of sediment containing both fine and coarse material is subjected to a relatively low velocity, it is likely that the small grains will be moved while the large size material remains in place. This segregation of material, if permitted to continue, will eventually result in the accumulation of mostly coarser particles on the bed surface, called "armoring" or "armor-coat." The percentage of each size contained in the sediment mixture will determine how the segregation process occurs, which, in turn, will determine the distribution of grain sizes of the armor coat. As the fine material moves out, the rate of sediment being transported decreases since less and less of the "moveable" material is available for transport. If the flow conditions are kept constant, the sediment rate approaches zero, resulting in an armored surface. This armored surface protects material just below the surface from being eroded and, hence, for that flow condition a stable channel is formed.

There are two basic types of channel equilibria, that is, conditions when the channel is neither aggrading nor degrading. One type, termed "dynamic" equilibrium, occurs when an equal amount of sediment is being transported into and out of a given reach. The other type of equilibrium occurs when no sediment is being transported into nor out of a given reach. This is termed "static" equilibrium and is a special case of dynamic equilibrium. It is thus immediately obvious that static equilibrium represents conditions below incipient motion of all particles. Static equilibrium may be achieved in two ways: First, by having the flow conditions such that no particles in the bed mixture move or, second, for a given flow over a broadly-graded material, by allowing sufficient time for the material to segregate and the surface to become armored (static equilibrium). The problem to be studied in this thesis is the role sediment gradation plays in the process of sediment armoring to produce "static" equilibrium in open channels.

Purpose and Scope of the Investigation

The objective of this investigation is to determine quantitatively the effects of sediment gradation on channel armoring. Criteria for determining the distribution of particle sizes on an armored bed are to be formulated from experimental results. These results were to be obtained by carefully synthesizing known original distributions subjected to constant flow until sediment outflow had ceased. Armored particle size distributions were then to be analyzed.

CHAPTER II

REVIEW OF LITERATURE

In 1950 and 1952 Lane and Carlson (17) studied different reaches of irrigation canals in the San Luis Valley of Southern Colorado. These canals were constructed in the alluvial cone deposited by the Rio Grande River and had been in use since the late 1800's. These canals were extremely stable because of the armoring from the large particles.

Lane and Carlson expressed concisely and clearly the problem of canal design in widely graded coarse noncohesive materials where armoring occurs.

> Canals constructed through coarse, noncohesive material rarely, if ever, pass through a material of a narrow range of particle sizes. In practically every case the material covers a considerable range, usually extending from sand on up to gravel or cobbles. Unless the boundary shear values and velocities are very low, some material will be scoured out of such a canal when it is put into operation. Whether or not the results are satisfactory depends upon whether or not the amount moved out produces unsatisfactory conditions. In the San Luis Valley Canal sections on which measurements were made, the finer material had been removed from the top layer of the bed and a paving of coarser material was left. Between the larger particles, however, were found smaller ones; and even sand particles were present immediately under the top particles. It was hoped that substantially all of the material above a certain size would be found to have been removed from the bed so that this size could be used as an index of design, but this was found not to be the case; and no satisfactory analysis of the data based on a specific size left in the bed was found.

To make the results of his studies available for design purposes immediately, Lane arbitrarily selected d_{75} (size for which 75 percent by weight of the material was finer) to describe the natural material. The d_{75} Lane used was from the natural bank material (original material in

which the canal was constructed) and was plotted versus the tractive force (shear stress) of the maximum sustained flow. Lane stated his design criterion in words as follows:

> For ease in remembering this relation, it may be stated in English units as: the limiting tractive force in pounds per square foot recommended for design is equal to four-tenths of the particle size in inches of the sieve opening on which 25 percent of the weight of the natural bank material will be retained.

In 1950 Harrison (15) studied the process of segregation of particles which formed a "pavement" armoring in a degrading bed by using Einstein's (9) method of analysis. Three different bed materials were used supposedly having logarithmic normal distributions, but they could not be accurately described statistically by geometric means and standard deviations (s-curved lines on logarithmic-probability graph paper). Both "dynamic" and "static" equilibrium transport were studied. Harrison's major conclusions were:

1. The accumulation of non-moving particles on the bed surface causes an increase in its effective roughness.

2. It has been found that a layer of non-moving particles, the thickness of one particle, is effective in preventing scour. It is felt that a complete layer of non-moving particles is not necessary in all cases.

3. Non-moving particles in a pavement arrange themselves in a characteristic "shingled" formation.

4. The Einstein relationship for the rate of transport predicts very well the limiting grain size, i.e., a size larger than that for which there is no transport. Einstein's function for the limiting size was $\psi_* = 27$.

Limited measurements of the surface texture were made to determine the characteristics of the armored layer as a function of the flow parameters. All parameters used to describe the phenomenon of armoring were sediment parameters except the parameter ψ_*, defined by Einstein[1/] (9). Harrison stated that for $\psi_* = 27$ there was no sediment movement. For a given discharge and slope, a $\psi_* = 27$ defines a unique sediment size, below which there would be movement and above which there would be no movement. However, this is quite contrary to the results of Lane and Carlson (17) and Gessler (12) who found that in stable armored channels with no sediment movement, all particle sizes contained in the original distribution were found among the larger particles forming the armored layer.

In a study by Daranandana (8), the objectives were to determine differences in transport behavior between uniform and graded sands, and to determine how the graded sands would segregate during the establishment of a dynamic equilibrium. No attempt was made to study the problem of static equilibrium where the phenomenon of armoring predominated. He used only two sands, one nearly uniform ($d_g = 0.33$ mm, $\sigma_g = 1.25$), and one graded ($d_g = 0.33$ mm, $\sigma_g = 2.07$).

Daranandana found that of the total bed material transported, the ratio of the uniform to graded materials was very low for ripples and progressively increased approaching unity for violent antidunes. No significant difference of the resistance to flow with respect to grain

---

1/ ψ_* is a dimensionless parameter used in the calculation of bedload which is expressive of the ability of the flow to transport a given size of particle.

roughness was found. However, resistance to flow by form roughness of the graded sand was lower than for uniform bed materials as was also reported by Einstein (9). Sediment transport equations developed by Einstein (9), Colby and Hubbel (6), Kalinske (16), Bagnold (2), and Bishop (3) were tested and compared by Daranandana with actual measurements. The modified Einstein step method developed by Colby and Hubbell (6) appeared best for calculating the total sediment load for the uniform and graded materials. However, in order to use this method the suspended load concentration must be predetermined. Einstein's method, when based on one representative size range, gave good results for the graded material for the upper regime (of bed forms).

Daranandana concluded that for the same concentration of the total sediment load, less stream power (the product of shear stress and slope) was required to transport a given concentration of graded bed material than is the case with a uniform bed material. Perhaps this result was attributable to the fact that for a given median sediment size, larger percentages of finer material are contained in a graded sediment distribution than in a uniform sediment.

Coleman (7) conducted experiments using sediment beds with equal percentages of material in each of the size classes for a given distribution (arithmetic distribution). However, Coleman studied only the transportation of the segregated material and not the armoring process. No results were reported concerning the surface particle distribution after segregation had occurred. Coleman's results were

$$\frac{\sigma_t}{d_t} = R_*^{\frac{1}{2}} \left[\frac{\rho \mu_*^2}{(r-\rho)\ g\ d_t} \right]^{\frac{1}{2}} \qquad (1)$$

in which, σ_t is the standard deviation of transported distribution, d_t is the mean diameter of transported distribution, r is the mass density of sediment particles, ρ is the mass density of the fluid, g is the acceleration of gravity, u_* is the shear velocity, and R_* is the particle Reynolds number based on the shear velocity.

From the above, the coefficient of variability of the transported grains, σ_t/d_t, is a function of R_* and Shields' parameter. Considerable scatter occurred in the data as presented by Equation (1).

Garde and Hason (11) used two gradations, both with a mean diameter of 2.0 mm, in experimental studies carried out in order to determine the depth of flow and slope after the bed had armored. Their method followed closely the approach by Lane and Carlson (17). Both used Strickler's equation to compute Manning's "n" from the sediment size. Garde and Hason deduced that the original geometric standard deviation had little influence on the final bed roughness as expressed by Manning's "n." However, the scatter of data indicated errors up to 25 percent in predicting Manning's "n." Garde and Hason did not recognize the difference between parallel degradation for armored beds (equal depth of degradation along channel) and rotational degradation for uniform materials (degradation reduces bed slope).

Gessler (12) presented another approach to incipient motion. He utilized the armoring phenomenon to determine the probability with which a given particle will move and, through a priori reasoning, deduced that the mean bed shear stress does not have to exceed the "critical" shear stress in order to move sediment particles. He argued that the turbulent fluctuations of the bed shear stress may exceed the "critical"

shear stress of the particle even when the mean bed shear stress is well below the "critical" shear stress. He assumed the fluctuations of the bed shear stress to follow the normal error function with a standard deviation of 0.57, a value he determined as the best fit for his data. Einstein suggested earlier a value of 0.5. Gessler also assumed that the standard deviation was constant and did not vary with flow. However, Cheng (5) and Coleman (7) found that the standard deviation of the shear stress was a function of the fluid flow. Assuming a standard deviation of 0.57, Gessler stated that when the critical shear stress, τ_c, and the average bed shear stress, $\bar{\tau}$, were equal ($\tau_c = \bar{\tau}$), the probability of particle movement was 0.5 (equal probability of moving or remaining in place). However, as Chen (4) has pointed out, this would be correct only if a particle could respond (move and continue to be transported) instantaneously with an instantaneous excess of force on that particle. Of course, not only must the magnitude of the force exceed the weight of the particle, but the excess force must be present for at least some minimum duration in order to overcome the inertia of the particle.

To imply that the probability of a particle moving is 0.5 when the local instantaneous bed shear stress exceeds the critical shear stress 50 percent of the time is thus conditional. As Lane and Carlson (17) pointed out, even in stable armored channels, small amounts of all sizes in the original material can be found within the interstices of the armored layer. The geometrical arrangement of the armored layer, for each size of particle, is such that particles of any given size are present at different distances below the tops of the largest particles. This reasoning suggests that for a given original sediment distribution

and for given flow properties, a specific geometrical arrangement results. Any distrubance of this arrangement would produce further transport until another specific arrangement of particles has occurred. This argument also suggests that particle shape may be extremely important in armoring in that different particle shapes would "wedge" together in different geometrical arrangements.

CHAPTER III

DESIGN OF EXPERIMENT

Discussion of Armoring

There is presently no theory available with which to predict, for a given distribution of sediment and flow properties, (1) whether the sediment bed will armor, or (2) what the distribution of the armored surface layer will be if the bed armors.

The random forces acting on a mixture of sediment particles is a result of the spectrum of turbulence in the flow in which the turbulence is in turn modified by the distribution of sediment. These random forces result in sporadic and intermittent movement of sediment particles. The process of armoring is thus stochastic in nature with a statistical distribution of turbulence acting as the motivating force on a statistical distribution of sediment. The gross phenomena which sediment segregation and armoring display on a macro scale simply are the result of what is actually happening statistically on a micro scale. Even the transport of a uniform sediment is such a complicated phenomenon that no statistical solution has been obtained for this simplest case of sediment distribution. For this reason, the approach in this thesis will be that of using average parameters to describe the phenomenon of armoring. Of course, even these gross parameters must be thought of in a statistical sense since none are truly steady or uniform.

Since armoring results in a sediment bed that is in static

equilibrium (no sediment inflow and no sediment outflow), armoring is then basically an incipient motion problem. Martin (18), and others, have shown that Shields' parameter, when correlated with the particle Reynolds number, R_*, has considerable scatter from investigator to investigator. However, Martin pointed out that the apparent reason for the wide scatter of the data might be attributable to the different levels of turbulence which existed in the test apparatus of the various investigators. He developed an incipient motion criterion based upon a velocity, u_{dc}, defined as the velocity at a distance of 0.35 d from a theoretical wall, which is 0.20 d below the plane tangent to the top of the bed particles. This criterion was

$$\frac{u_{dc}}{\sqrt{(s-1)\ g\ d\ [\tan \Phi \cos \alpha + \sin \alpha]}} = \text{constant} \qquad (2)$$

where s is the specific gravity of the particles, g the acceleration of gravity, d the particle diameter, Φ the angle of repose of the sediment, and α the bed slope. The constant C as determined by Equation (2) using the data of Mavis et al. (19) and Schaffernak (also reported in reference 19) varied from 0.9 to 1.1. The value of C for White's (21) data was approximately 1.9. Martin concluded that for extremely low levels of turbulence, C = 1.9, for high levels of turbulence, C = 1.1. Martin's criterion for incipient motion is more difficult to use since a velocity distribution must be determined before calculating u_{dc}.

In order to simplify the problem of incipient motion, it is assumed in this thesis that a planar bed profile exists. That is, the bed is flat and no configuration exists other than the local irregularities

caused by the sediment particles. It is further assumed that the majority of voids around the largest particles are at least partially filled by smaller particles. Thus, surface irregularities are less than the radius of the largest particles contained in the mixture.

There might be only one average incipient motion condition for uniform sediments, whereas there can be many incipient motion points for graded mixtures where armoring occurs. The lowest incipient motion point for graded mixtures is the flow condition for which only the smallest particles contained in the mixture are about to be set in motion. The diameter under consideration is a function of the geometric standard deviation of the bed material and the point of movement is a function of the flow properties. This incipient motion point will be referred to hereafter as the "lower" incipient motion point.

Another important incipient motion condition with graded materials is the point (flow condition) at which the maximum size material contained in the mixture is about to be set in motion. Above this point, of course, there can be no armoring since all material will be in motion. The diameter under consideration here is a function of the geometric standard deviation, and the point of movement is a function of the flow properties. This point will hereafter be referred to as the "upper" incipient motion point.

Between the "lower" and "upper" incipient motion points, the particle size distribution left on the surface as an armor coat is a function of the original sediment distribution, fluid properties, and flow properties. The interrelationships between the properties of the armor coat, original sediment distribution, fluid and flow properties

is the objective of this study. The observed fact that a sediment bed, with a given distribution of particle sizes, can become stable at limited flow conditions as a result of armoring will be utilized in an effort to determine the particle size distribution of the armored surface as a function of the flow properties. Of course, a primary variable is the gradation of the original bed material.

Dimensional Analysis

Dimensional analysis will be used to formulate possible functional relationships and to investigate systematically the phenomenon of armoring. The results of the dimensional analysis, provided that the essential and pertinent variables have been included, will serve as a guide for the organization of the experimental work and for correlation of the pertinent variables.

The essential variables involved in this study are assumed to be:

u_* - bed shear velocity, ft/sec

ρ - mass density of water, lb-sec^2/ft^4

γ_s-γ - submerged weight of sediment, lb/ft^3

μ - dynamic viscosity of water, lb sec/ft^2

d_g - geometric mean diameter of sediment, ft

σ_g - geometric standard deviation of sediment distribution, dimensionless

The bed shear velocity, u_*, mass density of water, ρ, and d_g were chosen as repeating variables. Utilizing the above variables, the Buckingham-Pi theorem yields three π-terms.

These are,

$$\pi_1 = \frac{\rho u_* d_g}{\mu} \tag{3}$$

$$\pi_2 = \frac{\rho\, u_*^2}{(\gamma_s - \gamma) d_g} \tag{4}$$

$$\pi_3 = \sigma_g \tag{5}$$

The first Pi term is the particle Reynolds number based on the shear velocity. Thus,

$$\pi_1 = \frac{\rho u_* d_g}{\mu} = \frac{u_* d_g}{\nu} = R_* \tag{6}$$

In this dimensionless term, the length parameter d_g is reasoned to refer to the geometric mean diameter of those particles which are generating the turbulence in the stream (hydraulically rough boundary). For an armored surface, d_g must then be the geometric mean of the particles armoring the surface and is designated as d_{ga}. The first Pi term then becomes

$$\pi_1 = \frac{u_* d_{ga}}{\nu} \tag{7}$$

The length parameter d_g in the second Pi term is reasoned to refer to the geometric mean diameter of those particles which are about to be set in motion, which, in the case of a stable armored surface, is again the geometric mean diameter of the armored surface particles, d_{ga}.
Equation (4) then becomes

$$\pi_2 = \frac{\rho\, u_*^2}{(\gamma_s - \gamma) d_{ga}} \tag{8}$$

Since the shear velocity is

$$u_* = \sqrt{\frac{\tau}{\rho}} \tag{9}$$

and the armored surface is stable and critical conditions exist, $\tau = \tau_c$, then equation (8) becomes

$$\pi_2 = \frac{\tau_c}{(\gamma_s - \gamma) d_{ga}} \tag{10}$$

which is Shields' parameter.

Since σ_g is a dimensionless term and does not alone adequately describe a sediment distribution, some combination of dimensionless lengths must be used with the geometric standard deviation of the original material, σ_{go}, to form a meaningful dimensionless parameter. In the process of armoring, the fine material is selectively transported out, thus changing the original particle size distribution into some other distribution with a different geometric mean particle size. Therefore, a priori, it seems reasonable that the ratio of the armored particle size to another particle size describing the gradation of the original material should be significant. A statistical descriptor of the gradation of a sediment logarithmic-normally distributed is σ_g and may be expressed mathematically by

$$\sigma_g = \frac{d_{84.1}}{d_{50}} \tag{11}$$

or

$$d_{50}\, \sigma_g = d_{84.1} \tag{12}$$

where $d_{84.1}$ and d_{50} are the particle sizes for which 84.1 and 50 percent, respectively, of the material by weight is finer. If σ_g in Equation (12) refers to the geometric standard deviation of the original mixture, σ_{go}, then $d_{84.1}$ is a statistical descriptor of the gradation of the original material. From this discussion, then, one possible dimensionless parameter describing both the original mixture and armored mixture is

$$\frac{d_{ga}}{d_{84.1}} = \frac{d_{ga}}{d_{go}\,\sigma_{go}} \tag{13}$$

where the subscript 'ga' refers to armored particles, and 'go' refers to the original mixture of sediment. Equations (6), (8), and (13) will be used to attempt to relate the sediment properties to the fluid and flow properties where armoring occurs.

Control and Measurement of Variables

The bed shear velocity, u_*, can be calculated by

$$u_* = \sqrt{gRS} \tag{14}$$

where g is the acceleration of gravity, R is the hydraulic radius, and S is the energy gradient. Since the shear velocity, u_*, is proportional to the square root of the product RS, it is seen that u_* is a function of fluid, flow, and bed properties. For an experiment in armoring it is extremely important that the shear velocity remain constant throughout an entire experiment. This means that for satisfactory results, all fluid properties (controlled mainly by temperature), volume rate of flow, and energy gradient must remain constant throughout the experiment.

Equation (14) also shows that depth of flow and the bed and water surface elevations should be measured as accurately as possible.

Choice of Experimental Variables

In an experiment to study the effects of gradation of a material upon channel armoring, a primary variable must be the distribution of sediment. Daranandana (8) found that the statistical parameters of mean, standard deviation, skewness, and kurtosis give the most complete description of a sediment distribution. Vanoni et al. (20) reported that most rivers of the world contain sediments that are logarithmically normally distributed. In this study, logarithmic normal distributions were used, and the statistical parameters of first, second, third, and fourth moments (mean, variance, skewness, and kurtosis, respectively) were used to describe the sediments. The original distributions were composited such that there was no skewness nor kurtosis (logarithmic-symetrical distribution). Since only one geometric mean diameter, 1.00 millimeter, was used, the only variable involved with the different sediments was standard deviation. Since logarithmic normal distributions were used, this variable is known as the geometric standard deviation.

There were two main reasons for choosing 1.00 millimeter for the geometric-mean diameter. One reason involved the fact that a means of trapping all sediment that eroded from the flume was needed so that no sediment was reintroduced into the flume. For a geometric mean diameter of 1.00 millimeter as used, the minimum size of sediment for the most broadly graded distribution would be on the order of 0.1 millimeter. With small geometric mean diameters, the minimum size would be proportionately smaller. Sieve cloth could be used to screen the 0.1 millimeter sand and yet pass the water.

Another reason involved the fact that the finer the sediment, the more pronounced the dune formation would be in the initial stages of degradation. In studying armoring, which is the end result of the process of hydraulic segregation, the formation of dunes could only cause difficulties in the experimental techniques of controlling both channel bed and water surface elevations at the downstream control point in the flume (end sill and sluice gate, respectively). Thus, for these reasons, a geometric mean diameter of 1.00 millimeter was chosen for all sediments.

The shape of sediment particles is very important in any sediment transport study. Martin (18) showed the importance of particle shape as reflected by the angle of internal friction (repose). However, shape was not a primary variable in these studies, and the results will be applicable only to the shape of particles used. The crushed quartz used in this study is very similar in shape and angularity to those sands found in regions where granite is the parent mineral.

CHAPTER IV

EXPERIMENTAL EQUIPMENT AND PROCEDURES

Equipment

The major test apparatus for this study was a recirculating flume 60 feet in length with a sediment bed 1.969 feet wide, four inches deep, and 40 feet long as shown in Figure 1. The side walls, floor, pipe line, pump, and all other parts of the flume system in contact with the water, were constructed of stainless steel. Slope was continuously adjustable from zero to 0.0200 and was set by a mechanical counter previously calibrated to the slope.

Water was pumped from a sump tank by a centrifugal pump through a four-inch pipe line containing the flow control system shown in Figure 2. The flow control system converted the differential water pressure from a four-inch venturi meter to air pressure. This air pressure was fed to a pneumatic proportional controller which regulated a butterfly valve in the pipe line. The desired differential pressure on the venturi meter was monitored on an inclined differential manometer, also shown in Figure 1, and set by the proportional controller. An automatic flow control system was necessary because full flow filters were used and changes in head loss occurred across the filters.

The ambient temperature around the flume was not controlled and fluctuated from approximately 70-95 degrees fahrenheit. A small refrigeration compressor with a heat exchanger, placed in the sump tank, was

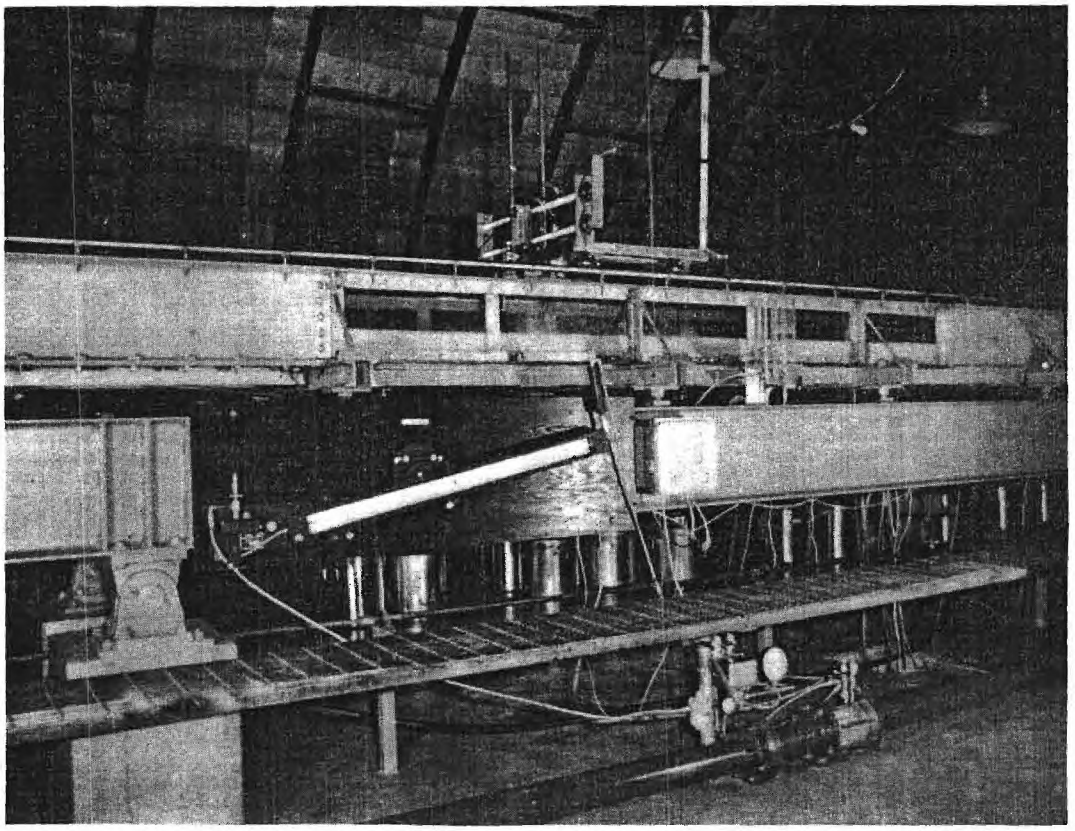

Figure 1. View of the Flume Used in the Armoring Experiments

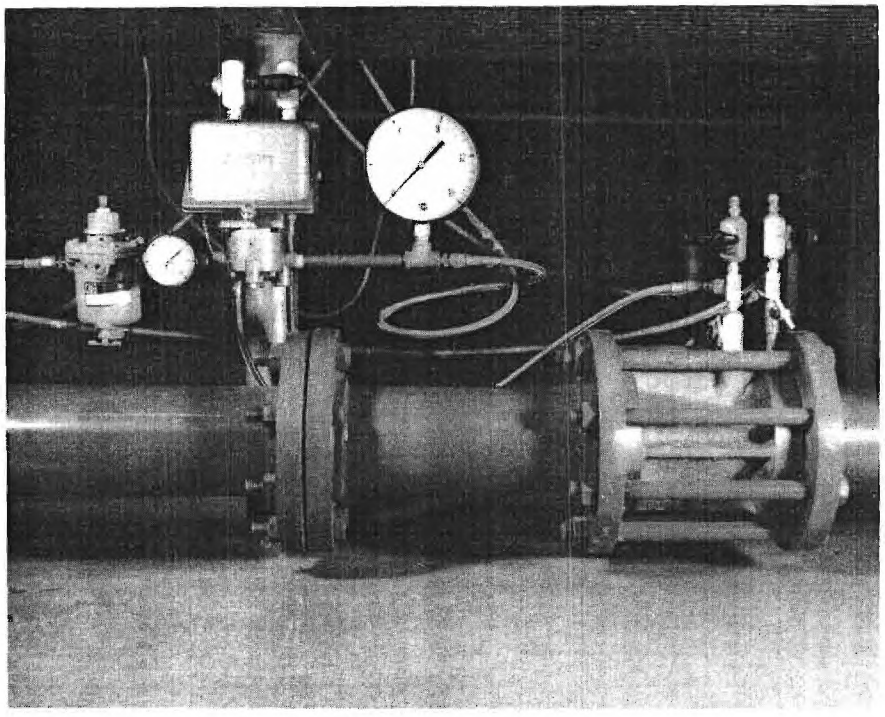

Figure 2. View of the Flow Control System

used to cool the water to maintain a constant temperature. During the summer months, the lowest constant temperature that could be maintained was 25 degrees centigrade (77 F) and, thus, the water temperature for experimental runs performed during the summer months was 25 degrees centigrade. A Calrod heating element was also installed in the sump tank, and the water temperature for experimental runs performed during the winter months was maintained at 20 degrees centigrade (68 F).

Located near the outlet end of the flume was a sluice gate and an end sill as shown in Figure 3. The end sill was formed by a vertical piece of lucite which fitted freely between two other pieces of lucite fastened to the floor of the flume. This piece of lucite was fastened to a stainless steel plate approximately four inches above the bottom of the flume. This plate was pivoted at the end of the flume and permitted the lucite plate to be raised and lowered by a set of jacks mounted underneath the steel plate. The purpose of the adjustable end sill was to follow the elevation of a degrading (or aggrading) sediment bed in the flume. A sluice gate was located approximately six inches downstream from the end sill to control the water surface elevation upstream. The sluice gate was placed downstream from the end sill (end of sediment bed) to avoid any local disturbance to the sediment bed from undulating waves near the sluice gate.

Screen separators, as shown in Figure 4, were located at the downstream end of the flume. The purpose of these separators was to catch all sediment and return only water to the sump and, thus, provide a means of collecting the total sediment load. Two separators, each with U. S. Standard 120-mesh (0.125 mm) stainless steel sieve cloth,

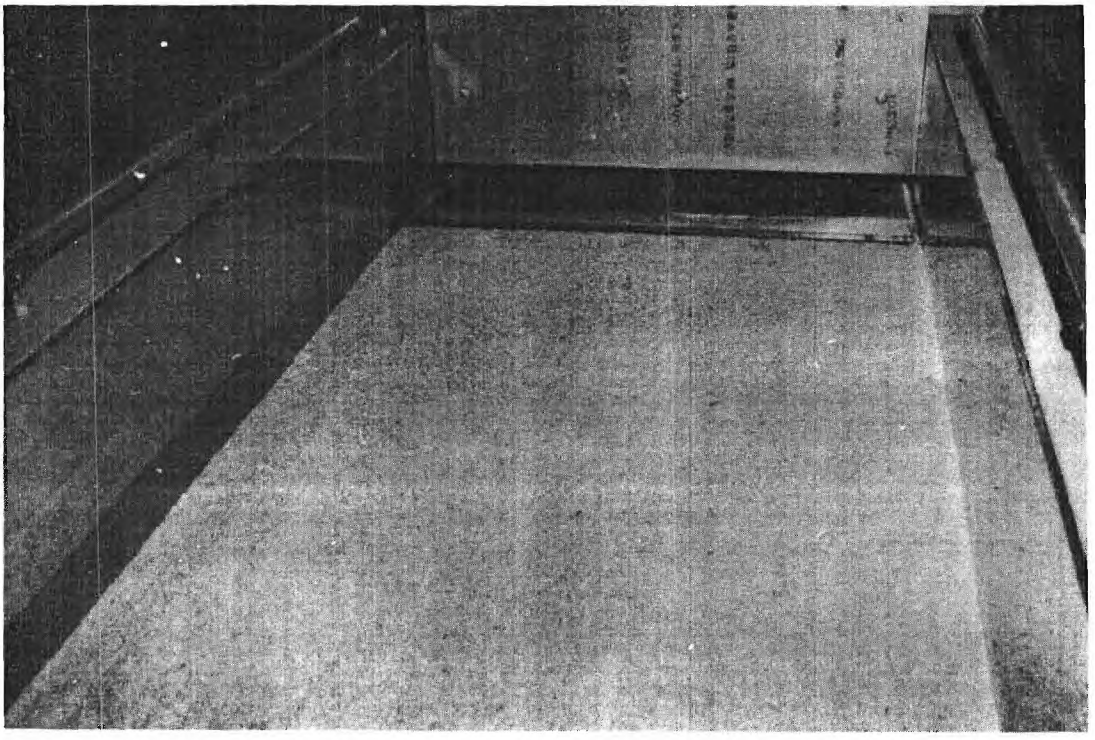

Figure 3. View of the Bed End Sill and Sluice Gate

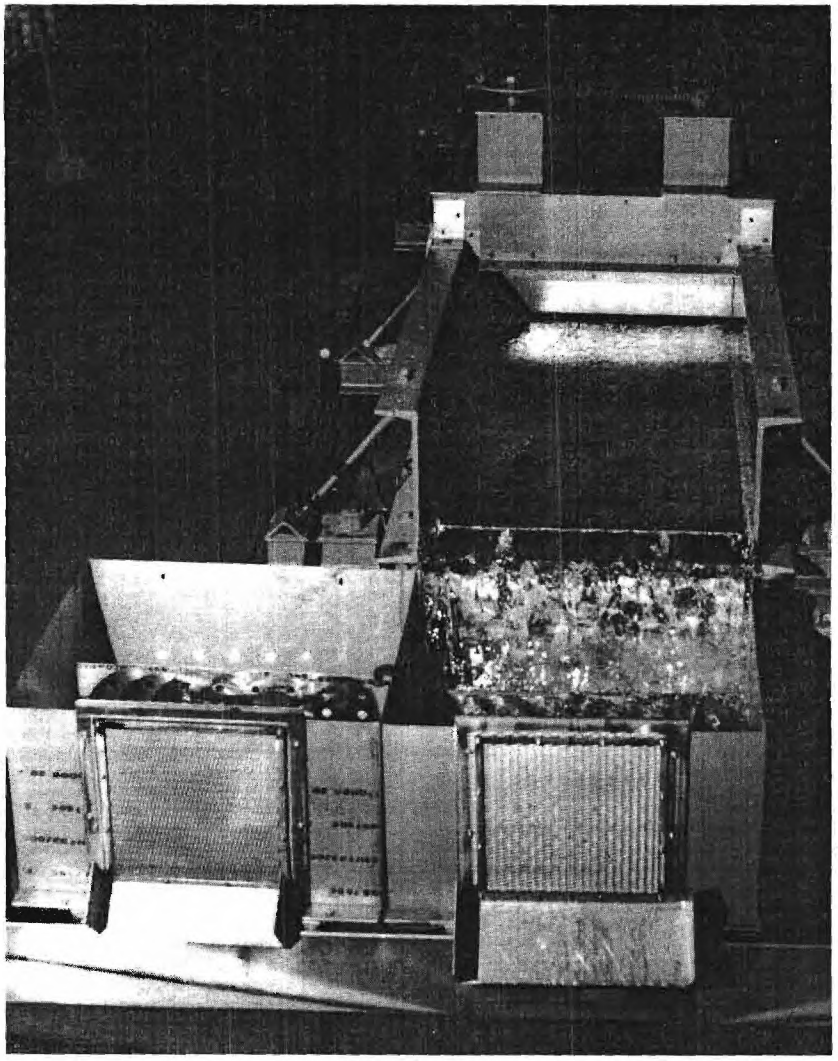

Figure 4. View of the Eroded Sediment Collectors

were used. While the sediment was being removed from one separator, the other was catching sediment from the flume so that total sediment load could be obtained in prescribed short time intervals.

Detailed Procedures

Material and Sieving

High purity crushed quartz was obtained in bulk quantities and sieved into 12 size ranges, six size ranges below 1.00 millimeter and size size ranges above 1.00 millimeter. The U. S. Standard square-root of two series of sieves was used. Specific gravity of each of the 12 size classes was measured and found to be 2.65.

A continuous flow industrial sieving machine, shown in Figure 5 with two precision sieves, was used such that one size range could be sieved with each set of sieves. All of the bulk sand was sieved, one size range at a time, and stored. However, the material stored for each size range was found to contain in most cases material that was finer than the indicated range. That is, for a given size range, finer material that should have passed the finer screen of the industrial sieving machine did not. This was characteristic of continuous flow sieving machines since retention time of the material was relatively short.

The Roto-tap laboratory sieving machine, with eight-inch diameter precision sieves, was used then as the standard to evaluate the actual contents of each size range sieved by the industrial sieving machine. A standard sieving time of five minutes was used for all samples as recommended by ASTM (1).

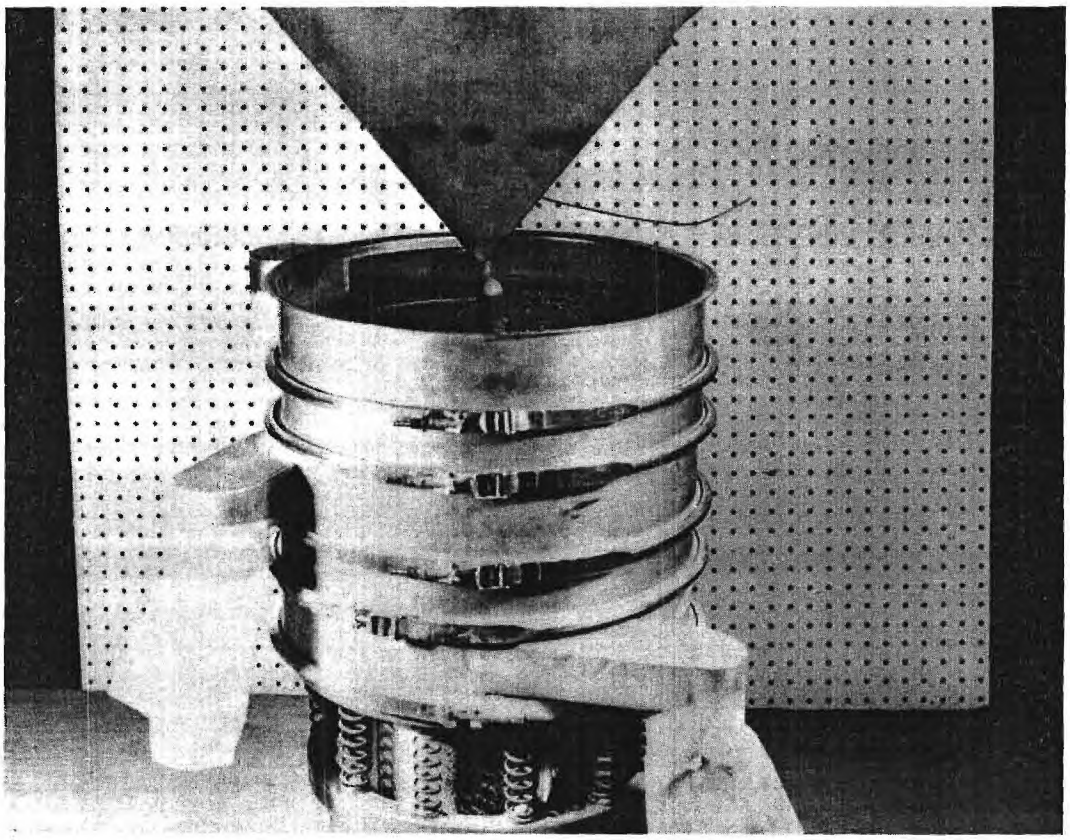

Figure 5. View of the Continuous-Flow Industrial Sieving Machine

Since each sieve size range stored contained material finer than the indicated range, this presented a problem with synthesizing a given distribution. Samples were obtained from each sieve size range of the stored material, and the contents for each particle size range were determined by sieving on the Roto-tap sieving machine. The weight of each size range necessary to synthesize a desired distribution with a total composited weight of 1500 grams was calculated by Equation (15), page 28. The example given by Equation (15) was for an original distribution with a geometric standard deviation, σ_{go}, equal 2.00.

The coefficient of X_1 in Equation (15) was the percentage of material, from 5.67 to 8.00 millimeters, contained in the material sieved by the industrial sieving machine and marked by the sieves used ($2\frac{1}{2}$-$3\frac{1}{2}$). The coefficient of X_2 was the percentage of material, from 4.00 to 5.67 millimeters, contained in the material sieved by the industrial sieving machine and marked by the sieves used ($3\frac{1}{2}$-5). The remainder of the coefficients corresponded similarly. The right-hand side of Equation (15) is the discrete density function of the desired distribution to be synthesized. The results of the solution to Equation (15) are summarized in Table 1, where the X-values are the weights of stored material, for the indicated size range, required to synthesize a composite mixture of 1.00 gram. The third column gives the weight in grams, for the indicated size range, necessary to synthesize the desired distribution with a total weight of 1500 grams.

A total of 320 samples, each containing 12 size ranges (a total of 3,840 subsamples), was needed to fill the flume to a depth of approximately two inches. Each subsample was weighed to the nearest 0.1 gram

Equation 15. Matrix of Percentages of Sand for Each Size Glass

$$
\begin{aligned}
65.8X_1 &= 0.60\\
34.2X_1+67.9X_2 &= 1.70\\
32.1X_2+53.3X_3 &= 4.20\\
46.7X_3+50.5X_4 &= 9.50\\
49.3X_4+64.9X_5 &= 15.00\\
0.2X_4+35.1X_5+97.0X_6 &= 19.00\\
3.0X_6+68.5X_7 &= 19.00\\
31.5X_7+70.1X_8 &= 15.00\\
29.9X_8+65.9X_9 &= 9.50\\
34.1X_9+59.7X_{10} &= 4.20\\
30.3X_{10}+87.1X_{11} &= 1.70\\
12.9X_{11}+88.0X_{12} &= 0.6
\end{aligned}
$$

Table 1. Weights Calculated by Equation (15)

Stored Material Sieve Range	X-Value gm	Weight for 1500 gm Composite Sample gm
$2\frac{1}{2}$-$3\frac{1}{2}$	0.00911	13.7
$3\frac{1}{2}$-5	.02044	30.6
5-7	.06649	99.5
7-10	.12664	189.6
10-14	.13493	202.2
14-18	.14679	219.7
18-25	.27094	405.6
25-35	.09223	138.2
35-45	.10231	153.2
45-60	.01191	17.8
60-80	.01537	23.0
80-120	.00456	6.9

and stored in paper cups. After all subsamples had been weighed and stored in cups, a complete distribution was composited by taking one cup from each size class and emptying it into a plastic bag. The plastic bags, each containing 1500 grams, were used to mix the composited distribution before loading into the flume.

This procedure was repeated for each of the five gradations used.

Loading the Flume

With broad gradations, mechanical segregation during loading was a problem. Figure 6 shows the metal grid with six-inch squares, which was used to load the sediment into the flume. Sand in the plastic bags, each containing approximately 1500 grams, was thoroughly mixed (dry) by closing the top of the plastic bag and inverting it several times. In emptying, a bag was inverted, the mouth of the bag was placed down into a square, and the sand was slowly removed. The surface of the sediment mixture was kept flat as the bag was removed from the slot. No further mixing of the material was attempted.

After the flume had been loaded with a sediment mixture, the formation of a planar smooth surface was attempted. A flat plate, the width of the flume, was attached vertically to the instrument carriage. The bottom edge of the plate was adjusted to the elevation of the bed, and the carriage was then pushed by hand at a constant speed to produce a smooth planar surface over the length of the sediment bed. However, the procedure proved to be unsatisfactory since it caused mechanical segregation of the sediment mixture and an accumulation of coarse material at the surface. After further consideration of the problem, a horizontal plate the width of the flume was sharpened to a knife edge.

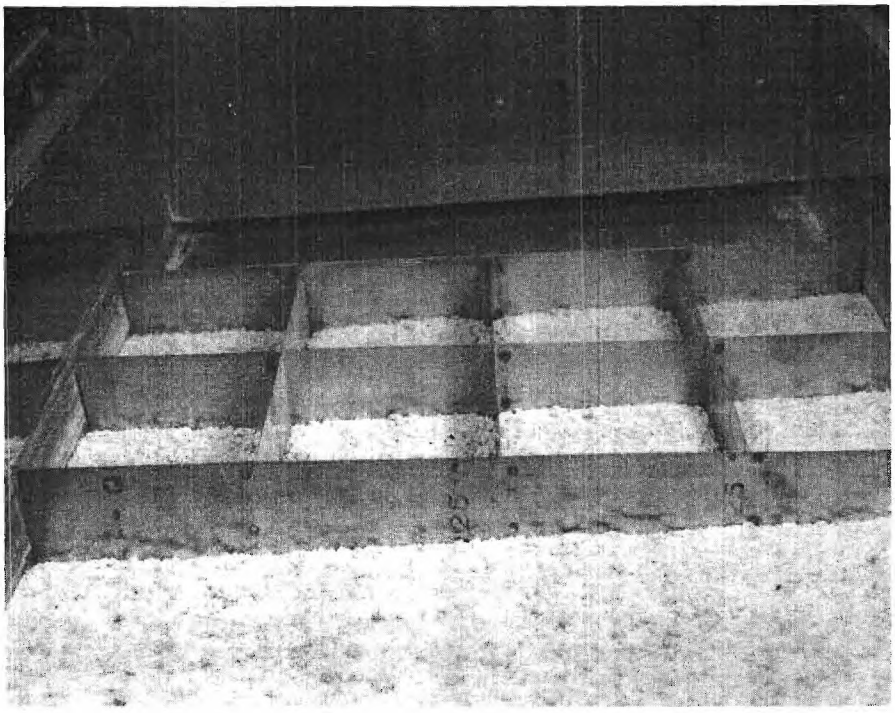

Figure 6. View of the Loading Grid

After the sediment bed had been wetted, the edge of this plate was laid on the end sill (at the desired initial elevation of the sediment bed), and the plate was secured to the instrument carriage by clamps. The instrument carriage was then manually towed, permitting the knife edge to slice through the sediment. Excess sediment was caught on the plate and removed from the flume and discarded. Since the sediment material was just wet enough to have near maximum capillary tension, there was no observable separation of grains. This technique proved to be quite successful in providing a smooth planar bed with a minimum of particle segregation.

Water and Bed Slope

The flume slope was calibrated by a point gage mounted on the instrument carriage. Both ends of the flume were blocked, and the flume was filled with water to a depth of approximately 0.5 foot. A digital counter was attached to the worm gear jacks which tilt the flume. The counter was set to zero when the difference between the point gage readings on the flume floor and water surface was constant. The flume was then tilted to some arbitrary amount on the counter, and point gage readings were taken at one-foot intervals. A least squares analysis of the point gage readings versus station was made. About ten counter settings with the same procedure were made. A least squares analysis was then made between counter reading and slope to give the slope calibration curve. This technique permitted the carriage rail to be used as the datum plane for all future water surface readings.

As described previously, the sediment bed was smoothed by a plate mounted on the instrument carriage which forced the bed to be parallel

to the instrument carriage rail. Thus, the instrument carriage rail was the datum plane for both measurements of bed slope and water slope. As long as all point gage measurements of both bed and water surface remained constant along the length of the flume, constant depth or "uniform" flow existed. Absolute slope of the bed was then determined by adding or subtracting differences in point gage readings along the length of the flume to the absolute slope of the carriage rails.

Surface Sample Determination

After the sediment bed had armored, it was necessary to obtain samples of the top layer of material only. A method using purified bee's wax was used. A six-inch square metal frame, as shown in Figure 7A, was imbedded into the sediment after all excess water had been drained from the sediment bed. Molten bee's wax at 65-68 degrees centigrade was poured into the metal frame until the particles were covered, as shown in Figure 7B. This temperature caused the wax to solidify before permeating any further than the top layer of particles. After cooling for five minutes, the frame, wax, and sediment were removed as shown in Figure 7C, and the underside was gently washed with warm water (35 C) to remove the sediment not adhering to the wax. The edges were trimmed to remove small clumps of wax that permeated around the edges of the metal frame. Each sample was then placed in a beaker and the wax remelted. As the wax became liquid, excess wax was decanted. After decanting, all other wax on the sand particles was removed by using chloroform as the solvent. The samples were then weighed and sieved on the Roto-tap to determine the size distribution of the armored particles. Three samples along the length of the flume were obtained for each run.

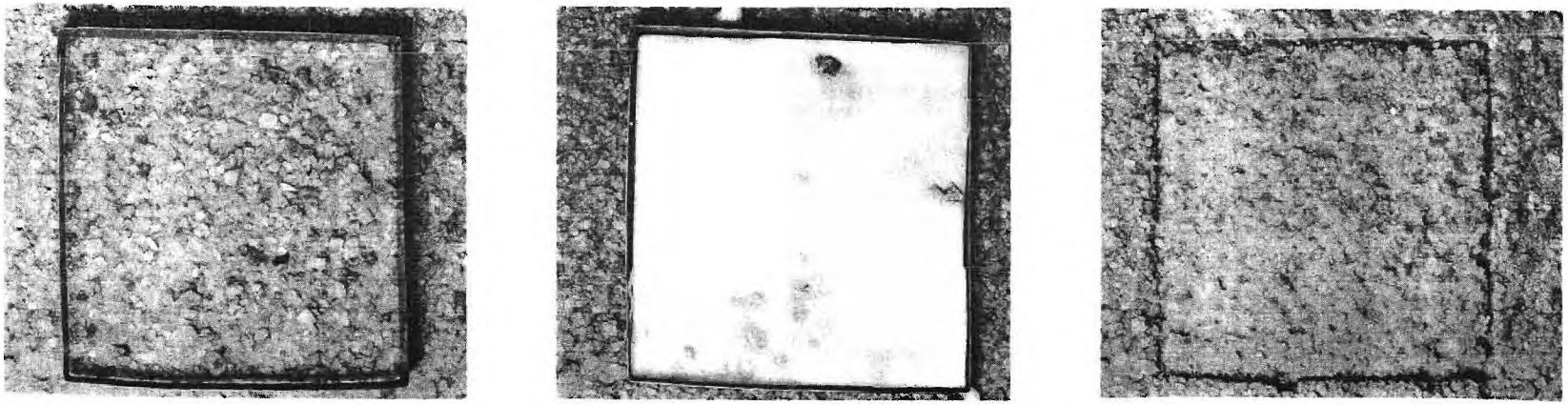

A B C

Figure 7. Technique for Determining Armored Particle Size Distribution

General Procedure

Quartz material was sieved into twelve size ranges by the square-root of two series of U. S. Standard sieves and stored by size class. The amount of each size class necessary to composite a desired distribution was weighed and composited. This distribution was carefully loaded into the flume to avoid mechanical segregation and then smoothed to a planar surface.

The sediment bed was then wetted very slowly as shown in Figure 8. After the sediment bed was saturated and had come to a temperature equilibrium with the water, the flow was increased to the desired rate of discharge over a two- to three-minute period. Constant depth flow was established by setting the sluice gate as soon as possible after full discharge was reached. When the discharge rate and depth of flow were constant, generally in less than five minutes, the beginning time of the experimental run was recorded.

From the starting time, total sediment discharge was caught by screen separators in short time intervals so that an estimate of sediment discharge rate could be determined. Sediment from each time interval was then dried, weighed, and stored for particle size distribution analysis.

As time progressed, the bed degraded since the sediment inflow rate into the flume was zero. Bed elevation was determined periodically, and the elevation of the end sill was adjusted to bed elevation. Of course, this also required readjustment of the sluice gate to maintain constant depth flow.

All measurements were continued until the sediment rate was not

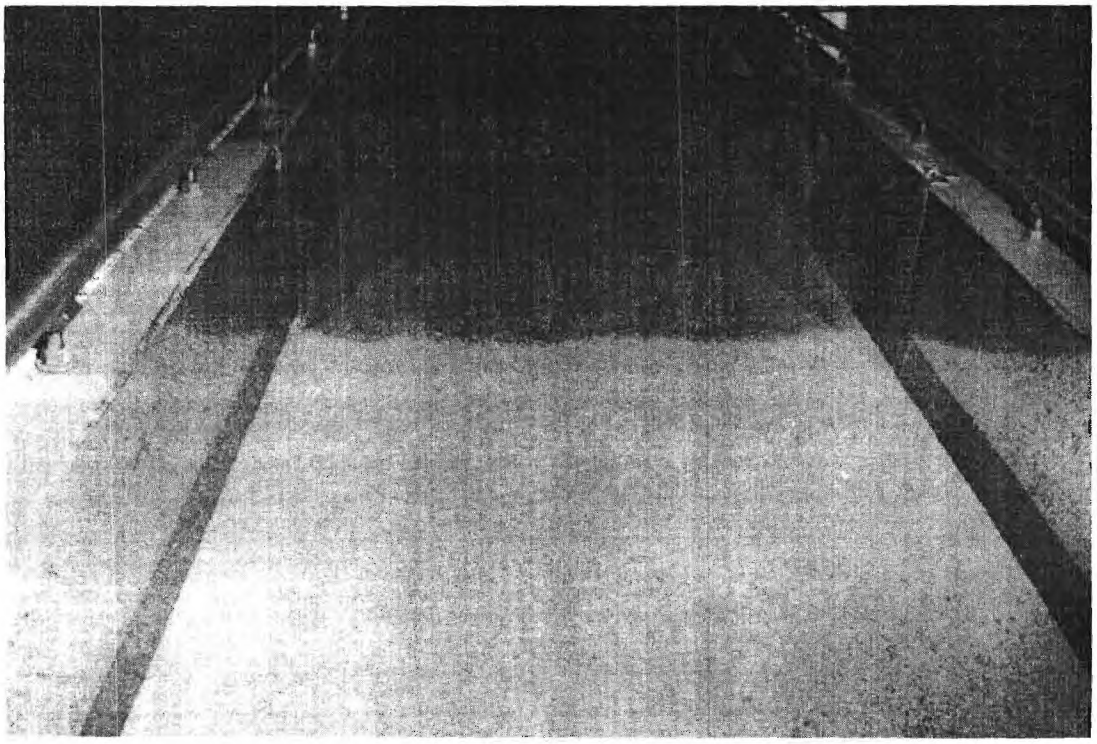

Figure 8. Initial Wetting of the Sediment Bed

more than one percent of the initial sediment transport rate. Flow was then stopped.

After the saturated bed was drained, samples of the top layer of sediment were obtained by the bee's-wax method. These samples were then processed to determine the distribution of particles which had armored the surface. The sediment bed, where the surface samples had been taken, was then patched with material similar to the armored distribution.

Measurements were then made to determine the final slope of the bed. This terminated what was called Part 1 of an experimental run.

The above procedure was then repeated at a higher discharge rate without changing the bed. This was then called Part 2. Further extensions of the experiments were designated similarly.

CHAPTER V

RESULTS

Table 2 gives the original geometric standard deviation, the discharge, and the starting condition of the bed surface for each of the experimental runs. After completing all measurements for Part 1 of each run, the armored surface was not disturbed, and Part 2 of the experimental run was immediately started with a higher discharge as shown in Table 2. As will be discussed in detail in Chapter VI, this technique proved to be as effective for the objectives of this study, as synthesizing a new mixture or removing the armored surface by the horizontal plate, described in Chapter IV. Parts 2 and 4 of Run 3 were used to verify this assumption. However, starting at a higher discharge after the surface had been armored at a lower discharge gave a very low sediment transport rate since most of the fine material had been transported out of the flume at the lower discharge rate. An exception to this was Run 3, Part 3, where the discharge of 0.668 cfs was high enough to totally destroy the armored surface that had developed at a discharge of 0.557 cfs. Once the largest particles were so much as even rolled over, fine material was exposed and the sediment transport rate increased considerably.

The original particle size distributions for each run are given in Table 3, and a composite of all gradations are plotted on Figure 9. As a matter of interest, approximately one man-year for each of these

Table 2. Arrangement of Experimental Runs

Run	Part	σ_{go}	Discharge cfs	Starting Condition of Bed
5	1	1.12	0.097	Original Distribution
5	2	1.12	.252	Original Distribution
5	3	1.12	.351	Original Distribution
5	4	1.12	.452	Original Distribution
5	5	1.12	.552	Original Distribution
5	6	1.12	.205	Original Distribution
4	1	1.50	.220	Original Distribution
4	2	1.50	.278	Original Distribution
4	3	1.50	.341	Original Distribution
2	1	2.05	.450	Original Distribution
2	2	2.05	.558	Armored Surface from Part 1
3	1	2.50	.446	Original Distribution
3	2	2.50	.557	Armored Surface from Part 1
3	3	2.50	.668	Armored Surface from Part 2
3	4	2.50	.572	Original Distribution
1	1	3.00	.440	Original Distribution
1	2	3.00	.555	Armored Surface from Part 1
6	1	3.05	.448	Original Distribution

Table 3. Original Bed Particle Size Distributions

U.S. Sieve No.	Sieve Opening mm	Geometric Standard Deviation					
		σ_{go}=1.12	σ_{go}=1.50	σ_{go}=2.05	σ_{go}=2.50	σ_{go}=3.00	σ_{go}=3.05
$2\frac{1}{2}$	8.000			99.85	98.93	96.99	96.99
$3\frac{1}{2}$	5.667			99.33	97.02	94.35	93.93
5	4.000		100.00	97.57	93.75	89.21	89.50
7	2.830		99.64	93.32	87.73	82.83	82.43
10	2.000	100.00	96.27	83.59	76.40	72.80	73.02
14	1.141	95.49	80.86	68.86	64.74	62.36	61.75
18	1.000	50.23	49.95	50.20	50.28	49.72	50.05
25	0.707	3.91	20.57	31.16	35.16	37.12	38.31
35	0.500	0.23	4.14	16.61	22.20	25.53	26.98
45	0.354	0.05	0.54	7.18	12.76	16.45	17.54
60	0.250		0.13	2.79	6.06	9.96	10.54
80	0.177			1.38	2.90	5.71	6.07
120	0.125			0.15	1.07	3.00	3.00

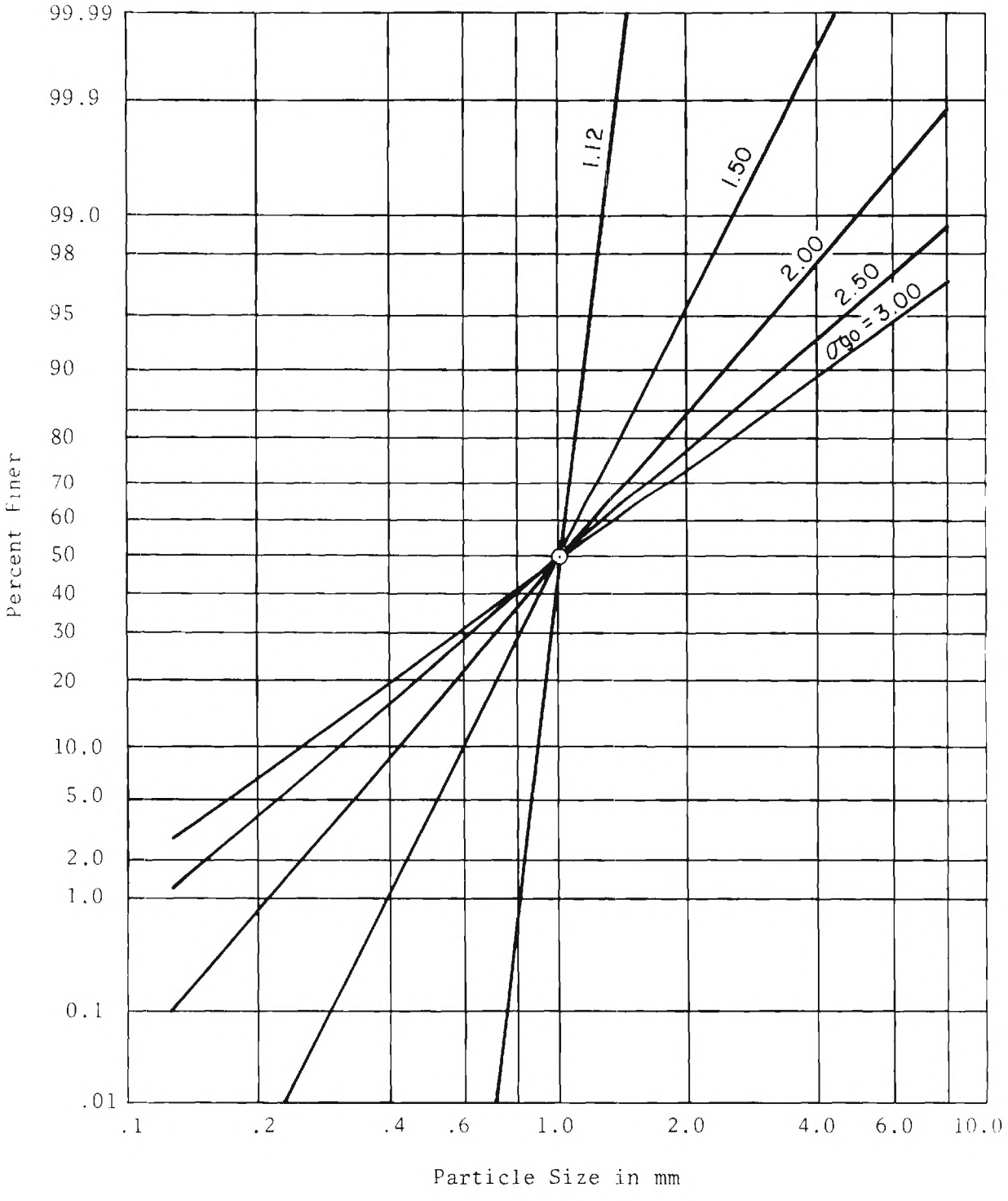

Figure 9. Original Particle Size Distributions

distributions was required to sieve, synthesize, and load the material into the flume.

Table 4 gives the armored surface particle size distributions for each run and part except for the uniform materials of Run 5 which would not armor. The values given are the average of three samples and was considered by the investigator to be the minimum number of samples for adequate results. Table 5 gives the eroded sediment particle size distributions. Only those runs are given in which the starting surface was the original mixture (see Table 2). Figures 10 through 20 are composite plots of the original, armored, and eroded distributions.

Table 6 gives a summary of the geometric mean particle size and geometric standard deviation for each of the original distributions, armored surface distributions, and the eroded particle size distributions. For all original mixtures, the geometric mean diameter was 1.00 millimeter.

Table 7 gives a summary of the measured and calculated flow parameters and the sediment properties necessary to calculate Shields' parameter, particle Reynolds number, and the sediment parameter $d_{ga}/d_{go}\ \sigma_{go}$ (the three Pi terms as developed in Chapter III).

The cumulative sediment transport as a function of cumulative time, is presented in the Appendix by Tables A.1 through A.8 and Figures A.1 through A.8. The sediment transport rate, which is the slope of the cumulative sediment transport versus cumulative time plot, was observed to be too low for Runs 1, 2, and 3. Apparently, the vertical plate used to smooth the channel bed prior to the run caused mechanical segregation of the surface material. There was less material that could be transported and, hence, a lower transport rate resulted.

Table 4. Armored Surface Particle Size Distributions

U.S. Sieve No.	Sieve Opening mm	Percent Finer										
		Run-Part Number										
		4-1	4-2	2-1	2-2	3-1	3-2	3-3	3-4	1-1	1-2	6-1
$2\frac{1}{2}$	8.00			100.0	100.0	100.0	100.0	100.0	100.0	97.0	97.0	97.0
$3\frac{1}{2}$	5.67			95.8	93.5	90.7	87.2	83.8	87.2	85.3	76.4	84.9
5	4.00	100.0	100.0	85.2	80.0	74.5	69.7	63.3	68.7	67.7	53.9	68.0
7	2.83	97.2	96.8	63.6	58.2	50.6	45.7	37.5	44.8	45.5	31.2	45.2
10	2.00	82.1	81.0	35.5	30.4	27.2	23.7	18.1	23.7	26.6	14.9	24.9
14	1.41	49.5	43.2	14.8	13.0	11.3	7.7	6.5	7.6	12.5	6.5	13.7
18	1.00	22.0	18.6	7.1	6.1	4.3	3.6	2.9	3.4	6.9	4.6	8.2
25	0.71	8.4	11.2	3.9	2.9	2.0	1.7	1.5	1.7	4.9	4.1	5.7
35	0.50	3.9	3.9	2.5	1.8	1.0	0.8	0.6	0.9	3.9	3.7	4.6
45	0.35	0.4	0.4	1.3	1.0	0.7	0.6	0.4	0.6	3.0	3.4	3.8
60	0.25										3.1	3.4
80	0.18										3.0	3.0
120	0.12											

Table 5. Eroded Sediment Particle Size Distributions

U.S. Sieve No.	Sieve Opening mm	Run Number 4-1	2-1	3-1	3-4	1-1	6-1
$2\frac{1}{2}$	8.000						
$3\frac{1}{2}$	5.667				100.0	100.0	
5	4.000		100.0	100.0	99.8	99.9	100.0
7	2.830	100.0	99.1	99.2	98.3	99.2	98.9
10	2.000	98.0	93.6	94.7	92.5	96.1	95.3
14	1.414	82.9	79.5	81.4	81.3	86.3	86.1
18	1.000	51.2	56.8	58.4	65.2	66.2	72.3
25	0.707	20.7	31.9	32.2	45.0	44.0	52.2
35	0.500	2.4	13.0	11.8	27.7	23.6	32.3
45	0.354	0.0	3.3	4.6	15.9	9.7	17.5
60	0.250		0.4	1.5	8.2	3.1	8.6
80	0.177		0.2	0.8	4.3	1.1	3.3
120	0.125		0.0	0.0	0.0	0.0	0.3

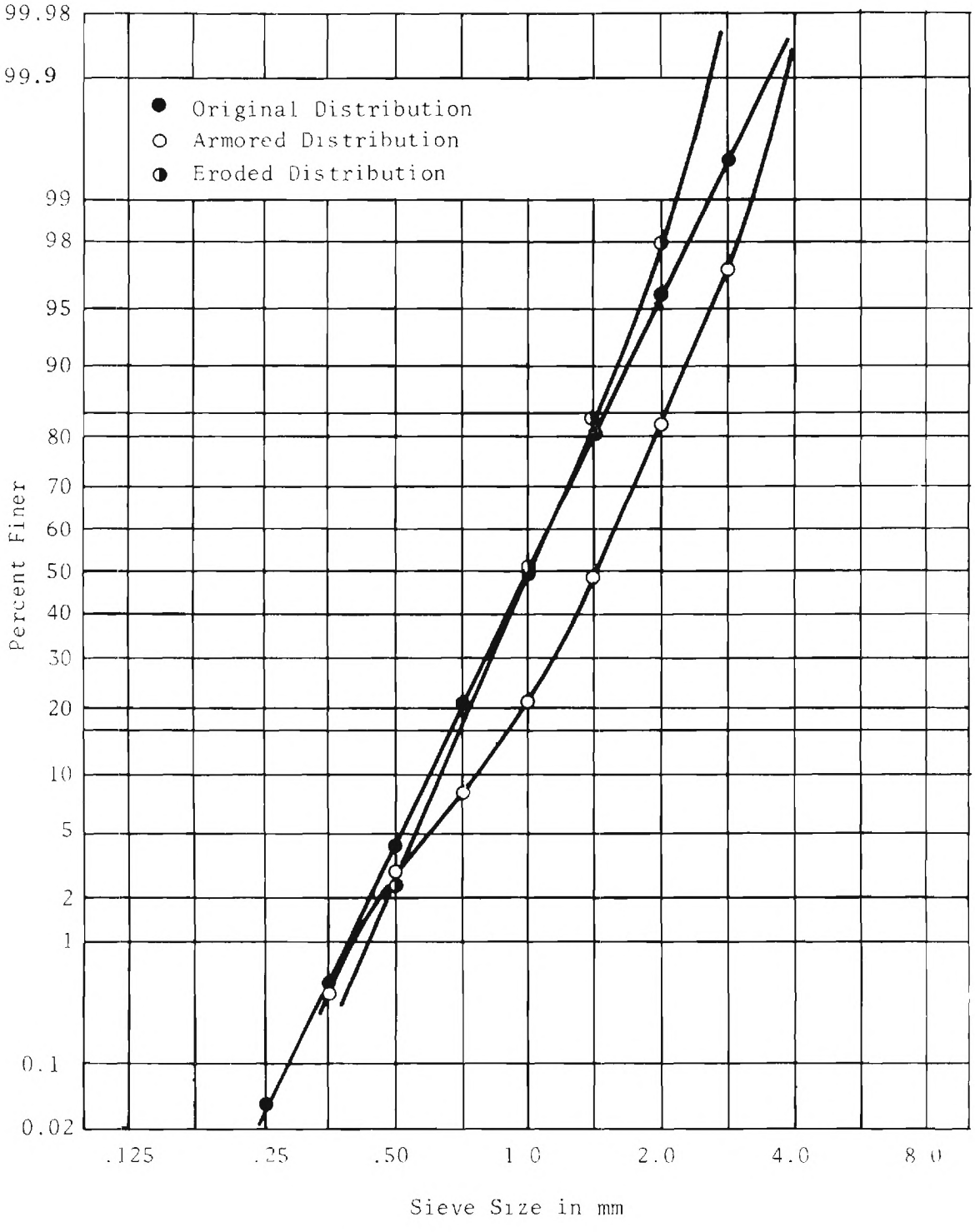

Figure 10. Plot of Original, Armored, and Eroded Distributions for Run 4-1

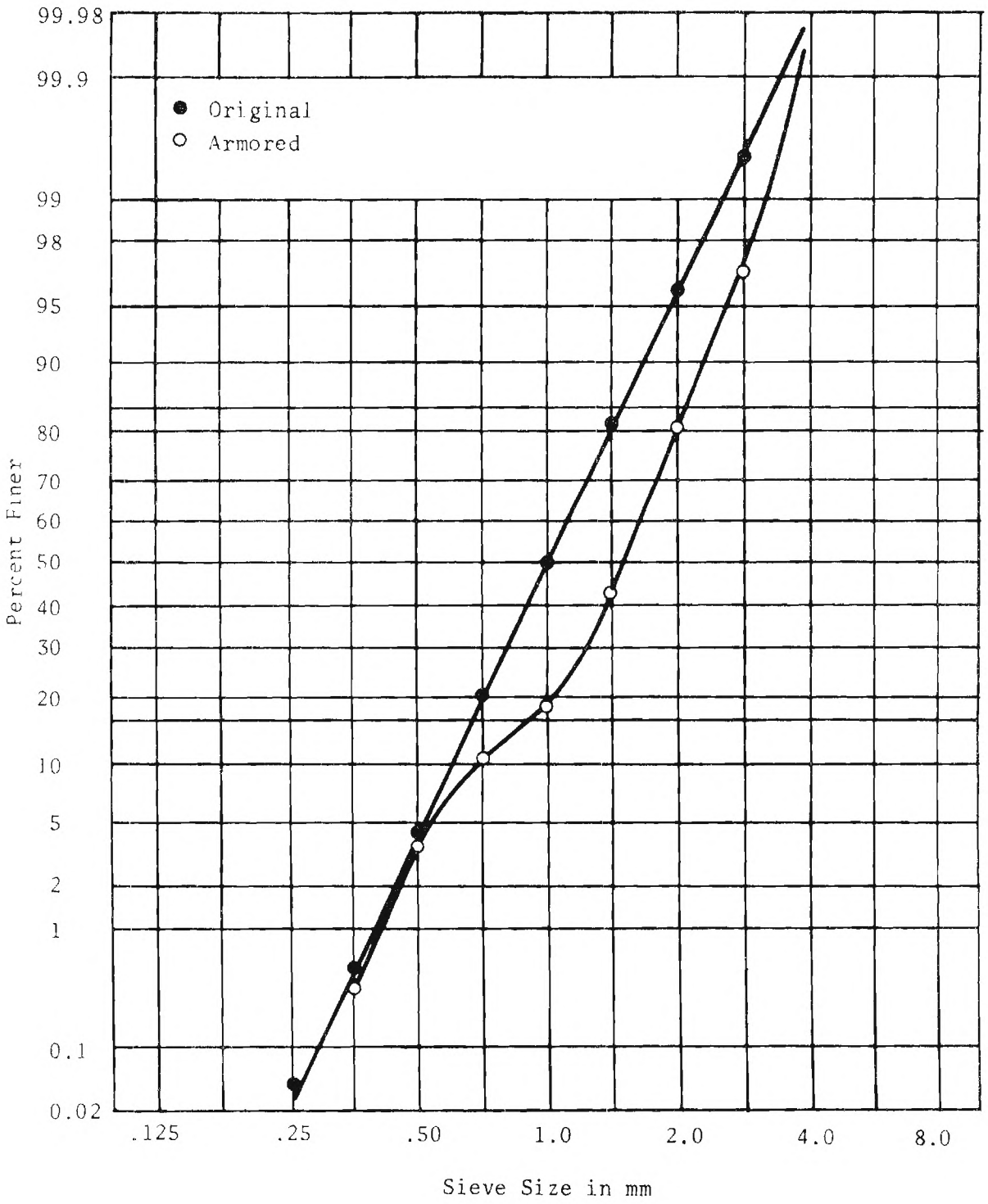

Figure 11. Plot of Original and Armored Distributions for Run 4-2

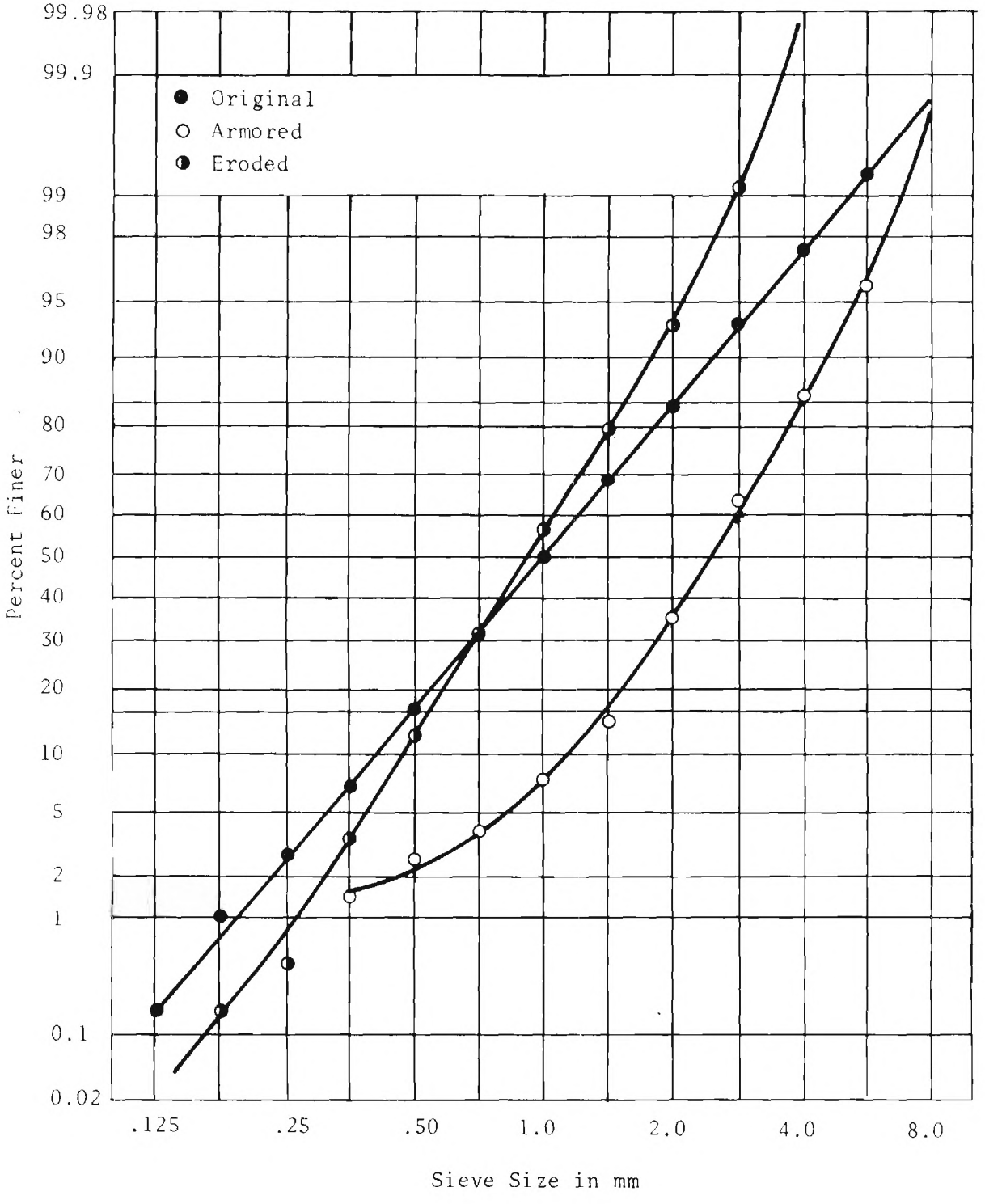

Figure 12. Plot of Original, Armored, and Eroded Distributions for Run 2-1

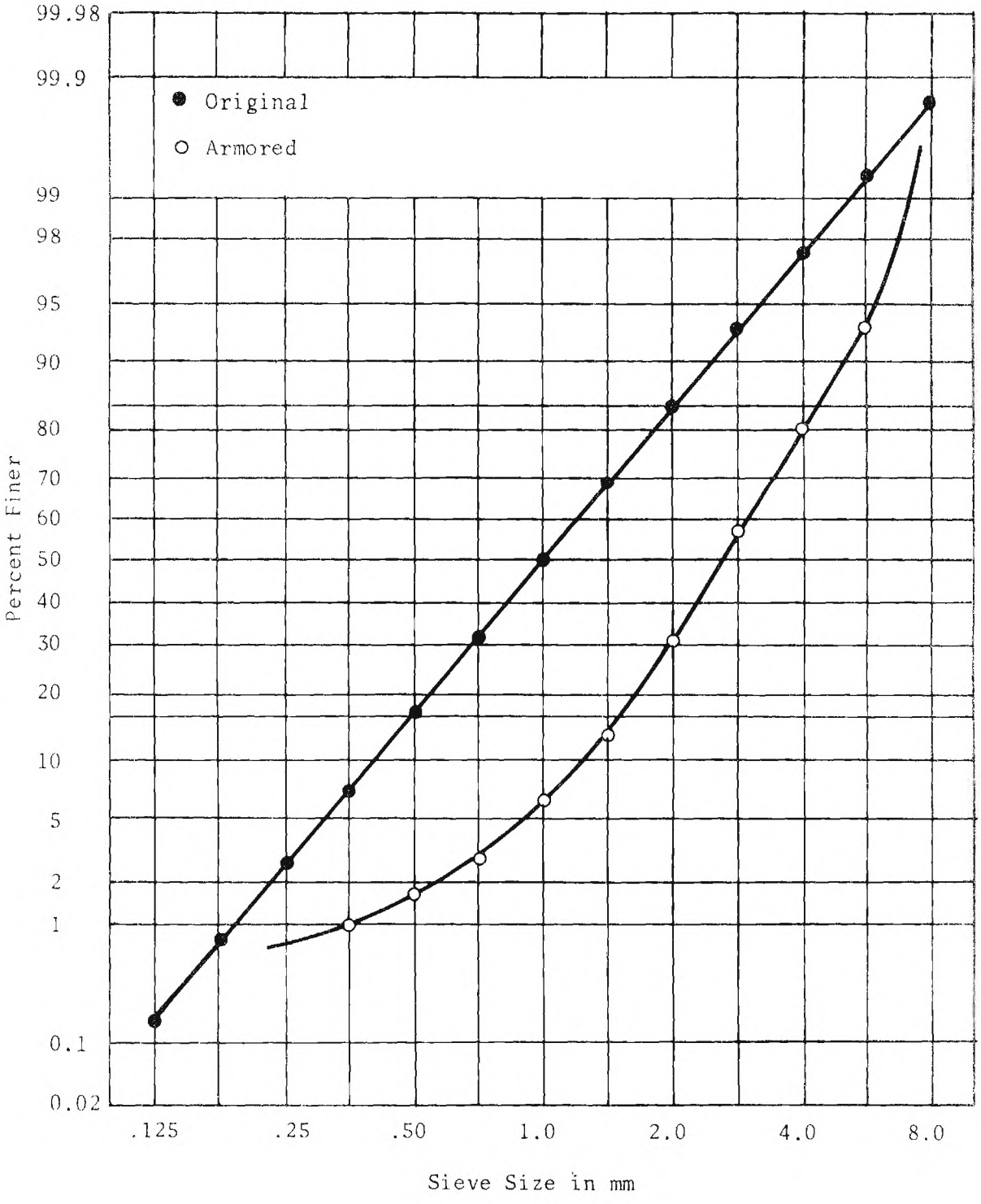

Figure 13. Plot of Original and Armored Distributions for Run 2-2

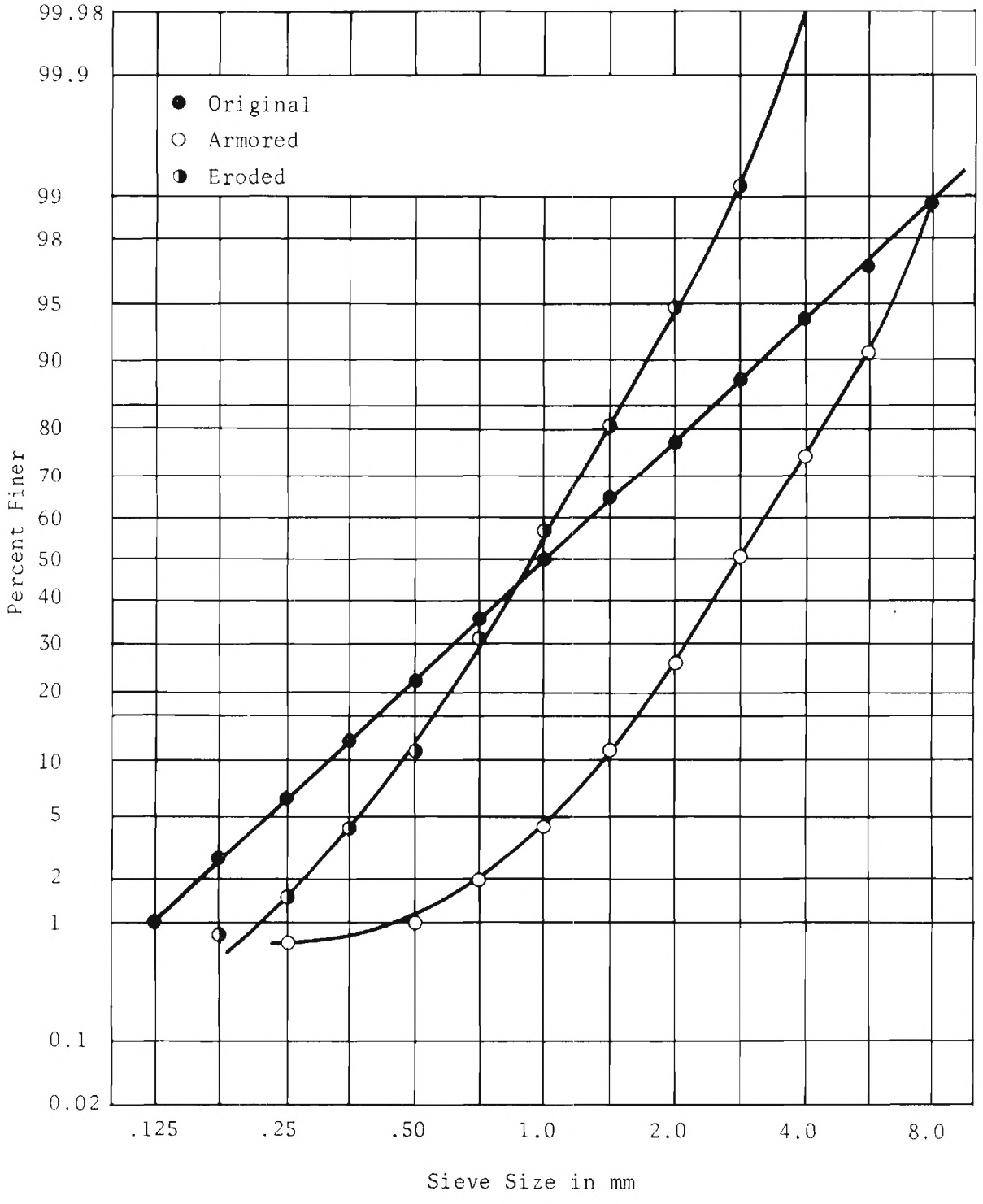

Figure 14. Plot of Original, Armored, and Eroded Distributions for Run 3-1

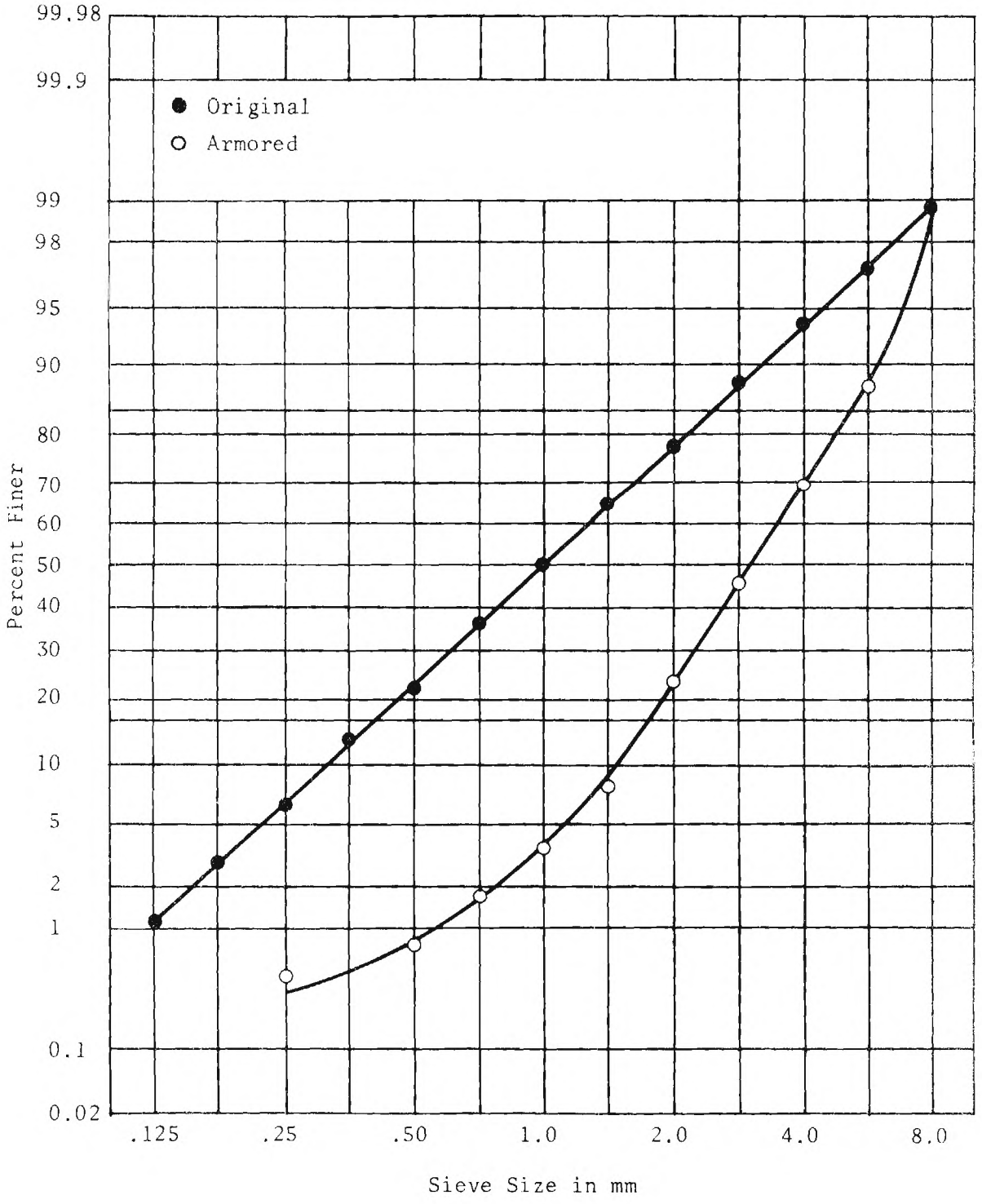

Figure 15. Plot of Original and Armored Distributions for Run 3-2

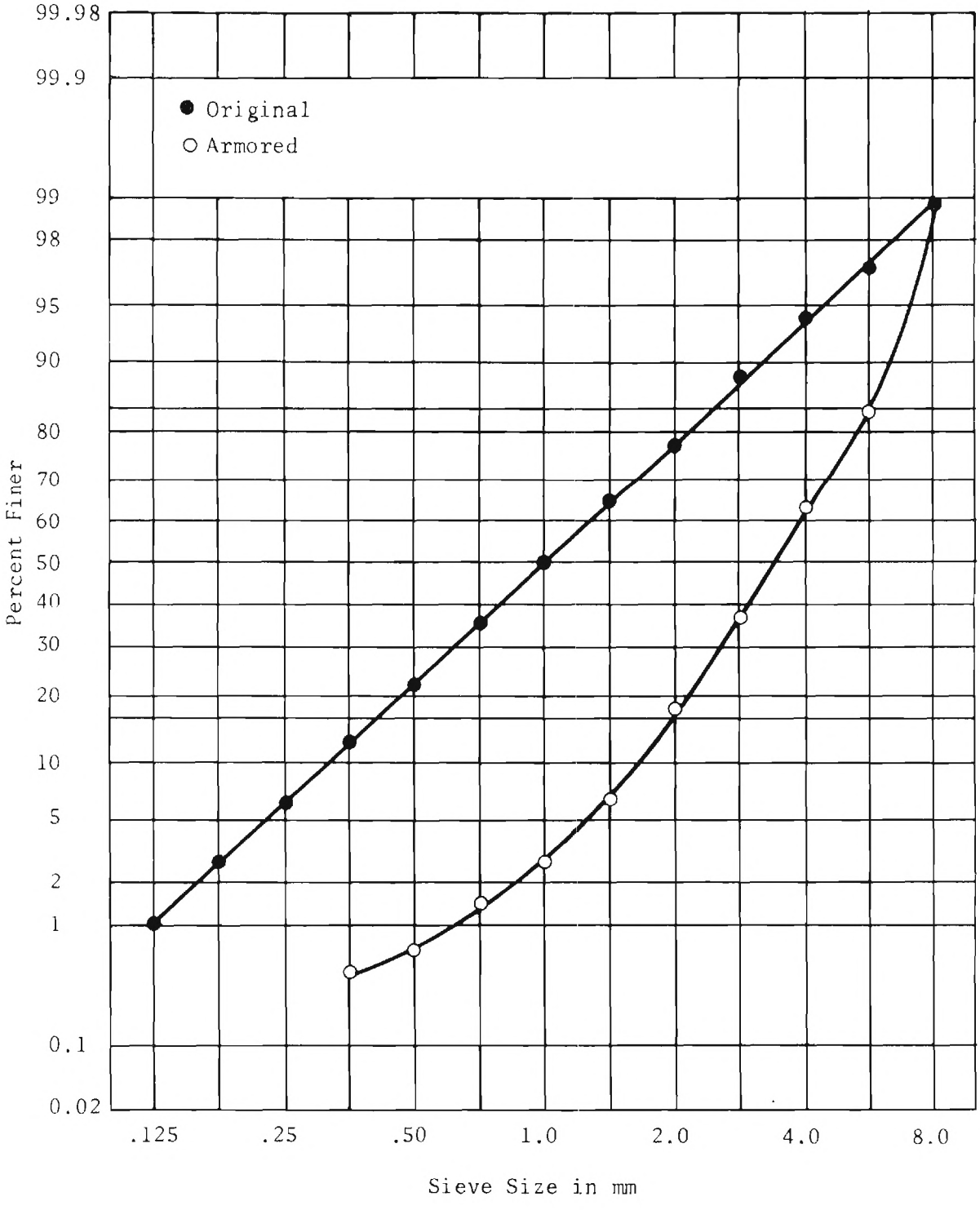

Figure 16. Plot of Original and Armored Distributions for Run 3-3

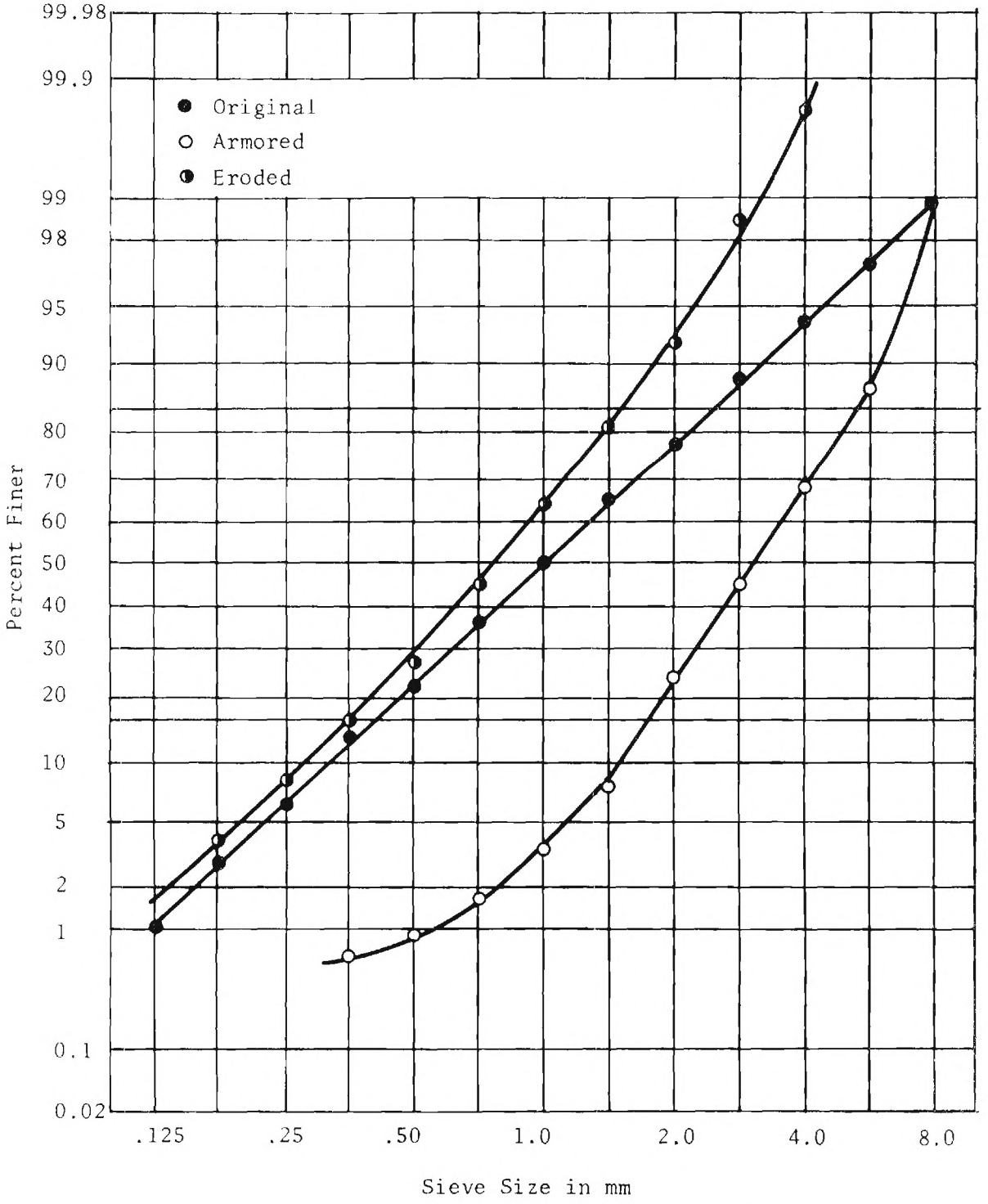

Figure 17. Plot of Original, Armored, and Eroded Distributions for Run 3-4

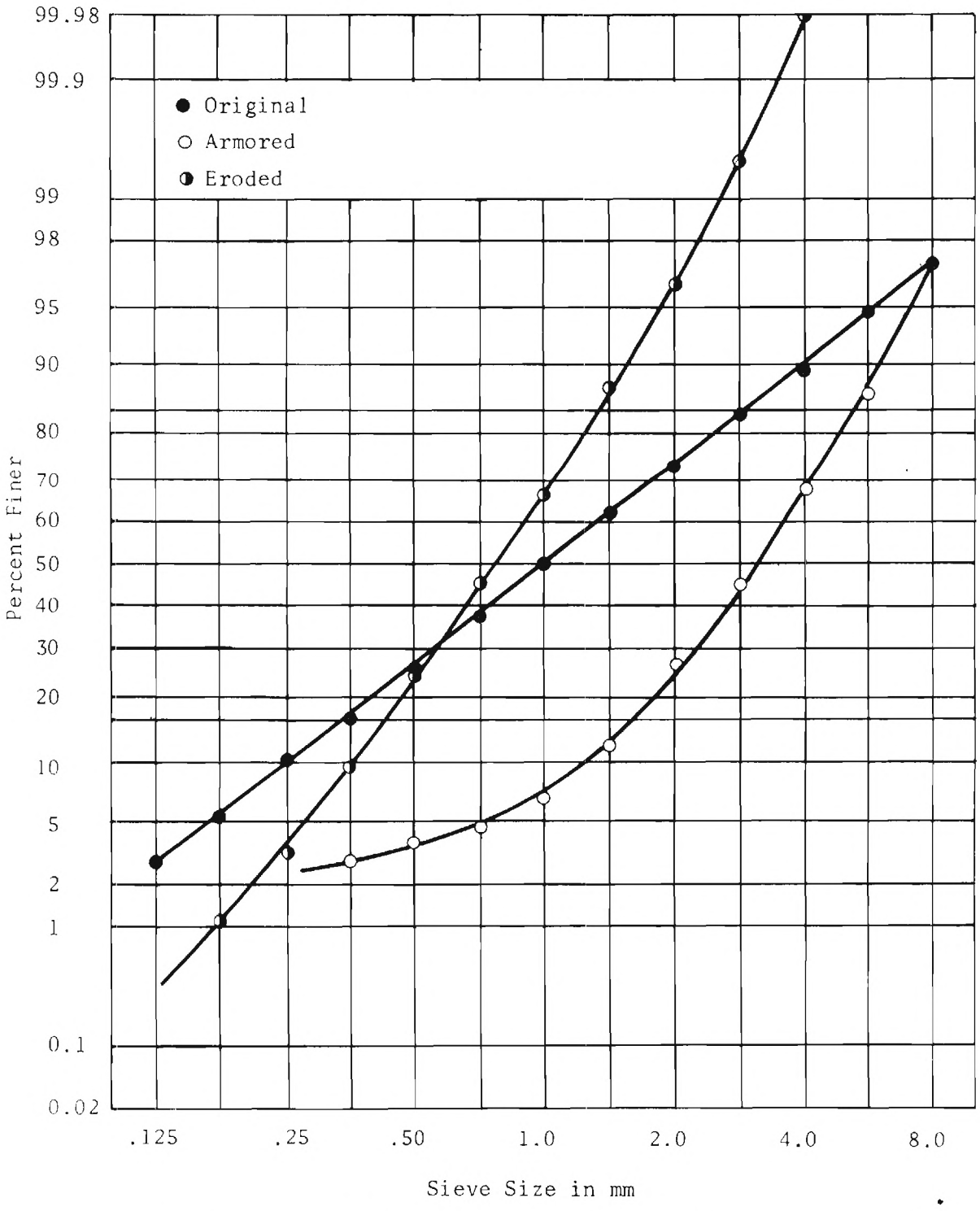

Figure 18. Plot of Original, Armored, and Eroded Distributions for Run 1-1

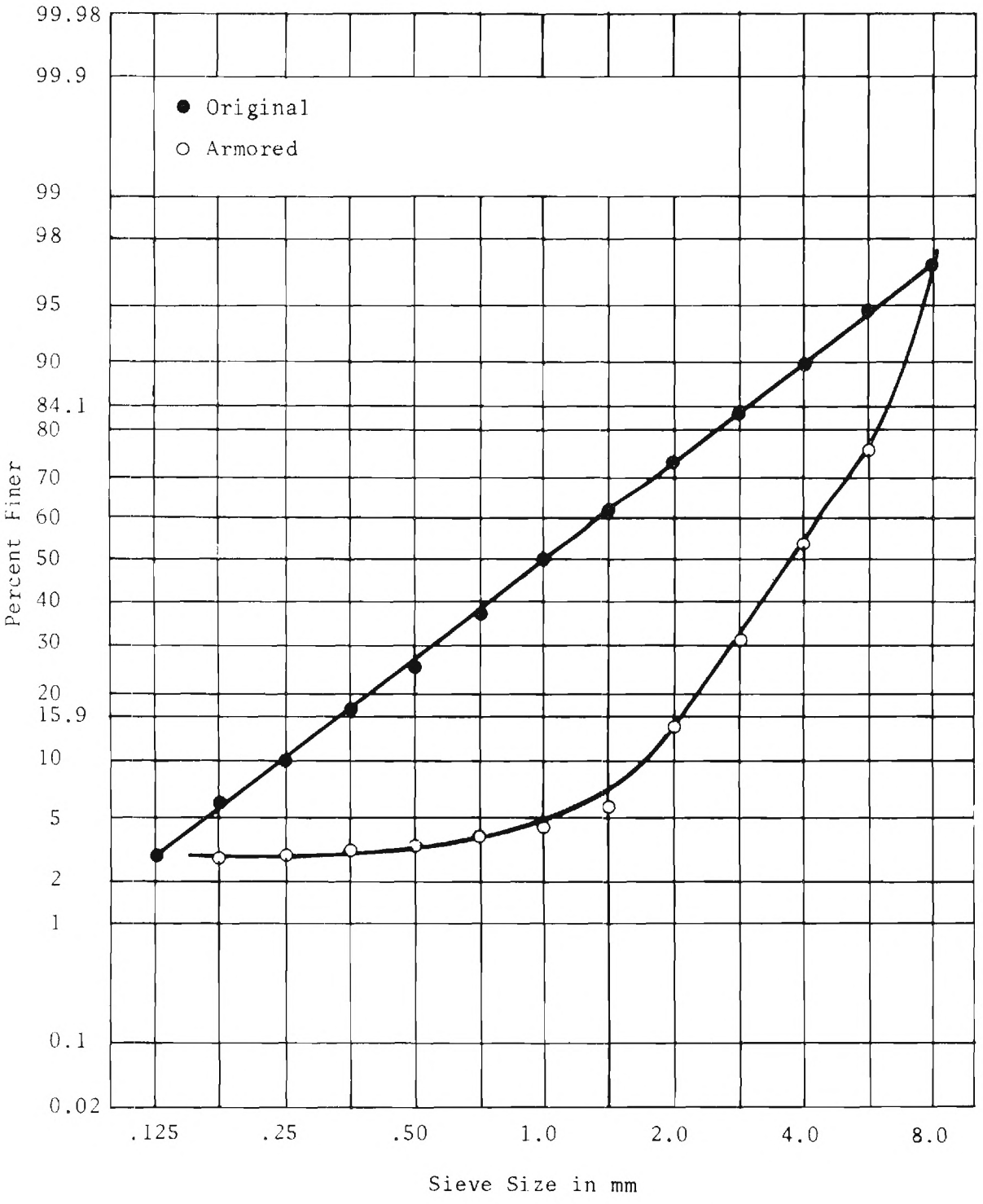

Figure 19. Plot of Original and Armored Distributions for Run 1-2

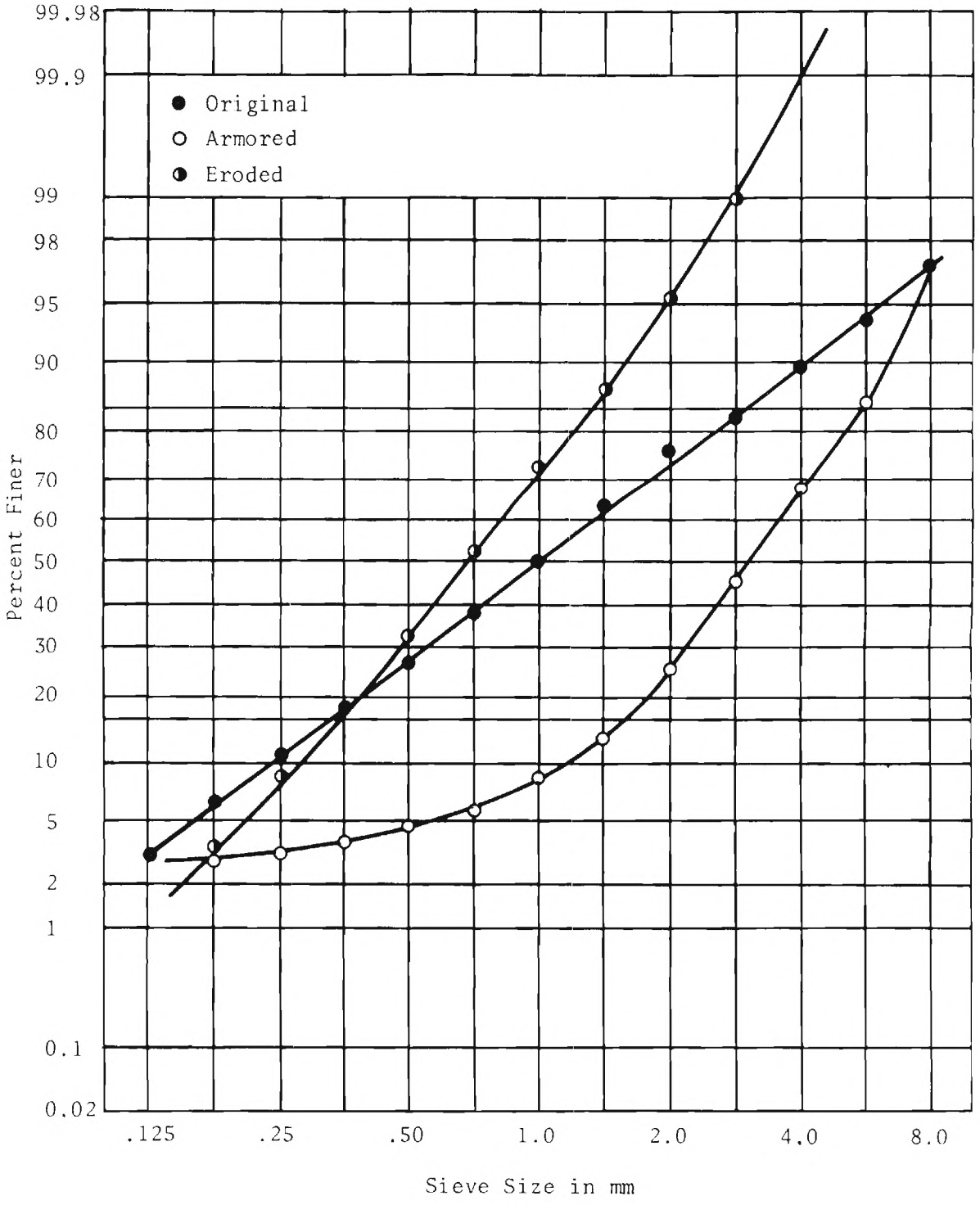

Figure 20. Plot of Original, Armored, and Eroded Distributions for Run 6-1

Table 6. Summary of Sediment Properties

Run Part	σ_{go}	d_{ga} mm	$\frac{d_{go}}{d_{ga}}$	σ_{ga}	$\frac{\sigma_{ga}}{\sigma_{go}}$	d_{ge} mm	σ_{ge}
4-1	1.50	1.42	0.704	1.42	0.95	0.99	1.45
4-2	1.50	1.52	.658	1.43	.95	.99	1.45
2-1	2.05	2.40	.417	1.65	.80	.90	1.70
2-2	2.05	2.60	.385	1.67	.81		
3-1	2.50	2.80	.357	1.73	.69	.89	1.67
3-2	2.50	3.05	.328	1.72	.69		
3-3	2.50	3.35	.299	1.73	.69		
3-4	2.50	3.05	.328	1.72	.69	.76	1.97
1-1	3.00	3.00	.333	1.75	.58	.78	1.73
1-2	3.00	3.75	.267	1.73	.58		
6-1	3.05	3.05	.328	1.72	.56	.67	1.94

Table 7. Summary of Flow Properties

Run Part	σ_{go}	Q cfs	y ft	S	$\overline{U}$ ft/sec	R ft	u_* ft/sec	τ lb/ft^2	d_{ga} mm	SP	R_*
5-1	1.12	0.097	0.061	0.0020	0.811	0.0574	0.0608	0.0072	IM[1]	0.0212	18.1
5-2	1.12	.252	.111	.0020	1.153	.0997	.0801	.0124	NA[2]	SM[3]	23.9
5-3	1.12	.351	.139	.0020	1.280	.1218	.0886	.0152	NA	SM	26.4
5-4	1.12	.452	.166	.0020	1.381	.1420	.0956	.0177	NA	SM	28.5
5-5	1.12	.552	.193	.0020	1.453	.1613	.1019	.0201	NA	SM	30.4
5-6	1.12	.205	.100	.0020	1.039	.0907	.0765	.0113	NA	SM	22.8
4-1	1.50	.220	.120	.0019	0.931	.1069	.0809	.0127	1.42	0.0264	39.7
4-2	1.50	.278	.130	.0019	1.086	.1148	.0838	.0136	1.52	.0265	44.0
2-1	2.05	.450	.184	.0020	1.242	.1550	.0999	.0193	2.40	.0239	82.8
2-2	2.05	.558	.213	.0020	1.328	.1751	.1062	.0219	2.60	.0249	95.3
3-1	2.50	.446	.186	.0019	1.219	.1564	.0978	.0185	2.80	.0196	94.6
3-2	2.50	.557	.215	.0019	1.315	.1764	.1039	.0209	3.05	.0203	109.4
3-3	2.50	.668	.242	.0020	1.402	.1942	.1118	.0242	3.35	.0214	129.4
3-4	2.50	.572	.217	.0019	1.338	.1778	.1043	.0211	3.05	.0205	109.8
1-1	3.00	.440	.184	.0019	1.214	.1550	.0974	.0184	3.00	.0181	87.1
1-2	3.00	.555	.192	.0025	1.468	.1606	.1137	.0251	3.75	.0198	127.2
6-1	3.05	.448	.184	.0020	1.236	.1550	.0999	.0193	3.05	.0188	90.9

[1] IM = Immobile
[2] NA = Not Applicable
[3] SM = Small

CHAPTER VI

DISCUSSION OF RESULTS

Relationship of Sediment Gradation and Armoring

The functional relationships derived by dimensional analysis in Chapter III were used to correlate the results of the armoring experiments. Least squares analysis was then used to statistically determine the best fitting functional relationship, that is, whether the functional forms correlate best linearly, exponentially, or in some other form.

The first two π-terms, Equations (7) and (8), correlated using a linear relationship; this can be seen in Figure 21 which shows the relationship of Shields' parameter versus the particle Reynolds number for various original standard deviations, σ_{go}. The best fit was of the form

$$\frac{\rho\, u_{*c}^2}{(\gamma_s-\gamma)\, d_{ga}} = a + bR_{*c} \tag{16}$$

where a and b are functions of the geometric standard deviation. Since there were so few data points for each geometric standard deviation, a least squares analysis was not run. As will be shown later, it was not necessary to determine the constants a and b for each geometric standard deviation. It was assumed that a linear relationship exists between the first two π-terms, the product of these two terms will now be related to the third π-term, $d_{ga}/d_{go}\ \sigma_{go}$. Tabulated values of the three π-terms are given in Table 8. Least squares analysis yielded the equation

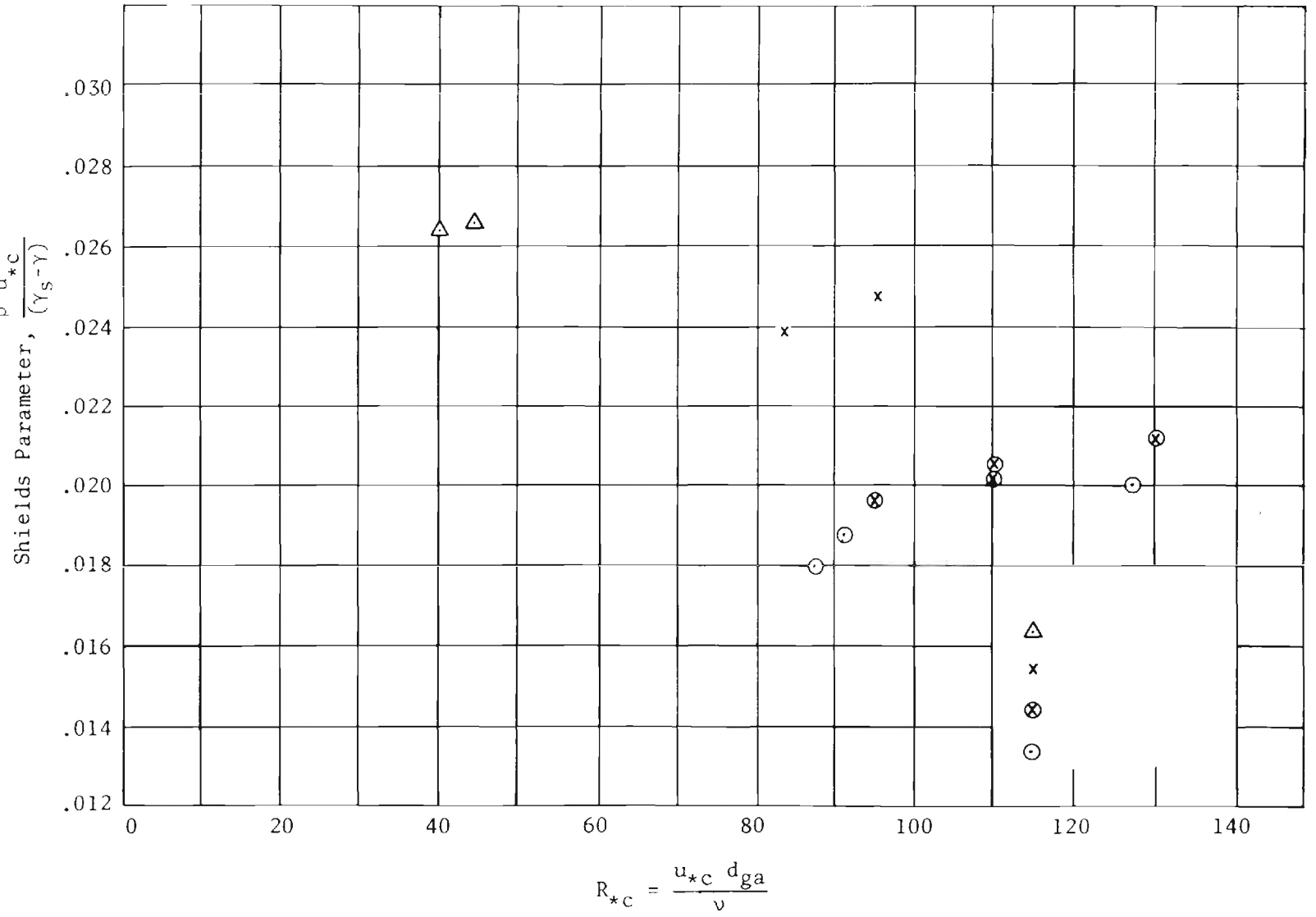

Figure 21. Shields' Parameter as a Function of R_*

$$\frac{d_{ga}}{d_{go}\ \sigma_{go}} = 0.908\ [(SP)(R_{*c})]^{0.353} \qquad (17)$$

The correlation coefficient was 0.93. Equation (17) is shown in Figure 22 with the measured data points superimposed.

Table 8. Summary of Sediment and Flow Dimensionless Parameters for Armored Sediments

σ_{go}	d_{ga} mm	$\frac{d_{ga}}{d_{go}\ \sigma_{go}}$	SP	R_{*c}	$(SP)(R_{*c})$
1.50	1.42	0.947	0.0264	39.7	1.048
1.50	1.52	1.013	.0265	44.0	1.166
2.05	2.40	1.171	.0239	82.8	1.979
2.05	2.60	1.268	.0249	95.3	2.373
2.50	2.80	1.120	.0196	94.6	1.854
2.50	3.05	1.22	.0203	109.4	2.221
2.50	3.35	1.34	.0214	129.4	2.769
2.50	3.05	1.22	.0205	109.8	2.251
3.00	3.00	1.00	.0181	87.1	1.577
3.00	3.75	1.25	.0198	127.2	2.519
3.05	3.05	1.00	.0188	90.9	1.709

The product of Shields' parameter and the critical particle Reynolds number is

$$(SP)(R_{*c}) = \left[\frac{\rho\ u_{*c}^2}{(\gamma_s-\gamma)d_{ga}}\right]\left[\frac{u_{*c}\ d_{ga}}{\nu}\right] = \frac{u_{*c}^3}{\nu(s-1)g} \qquad (18)$$

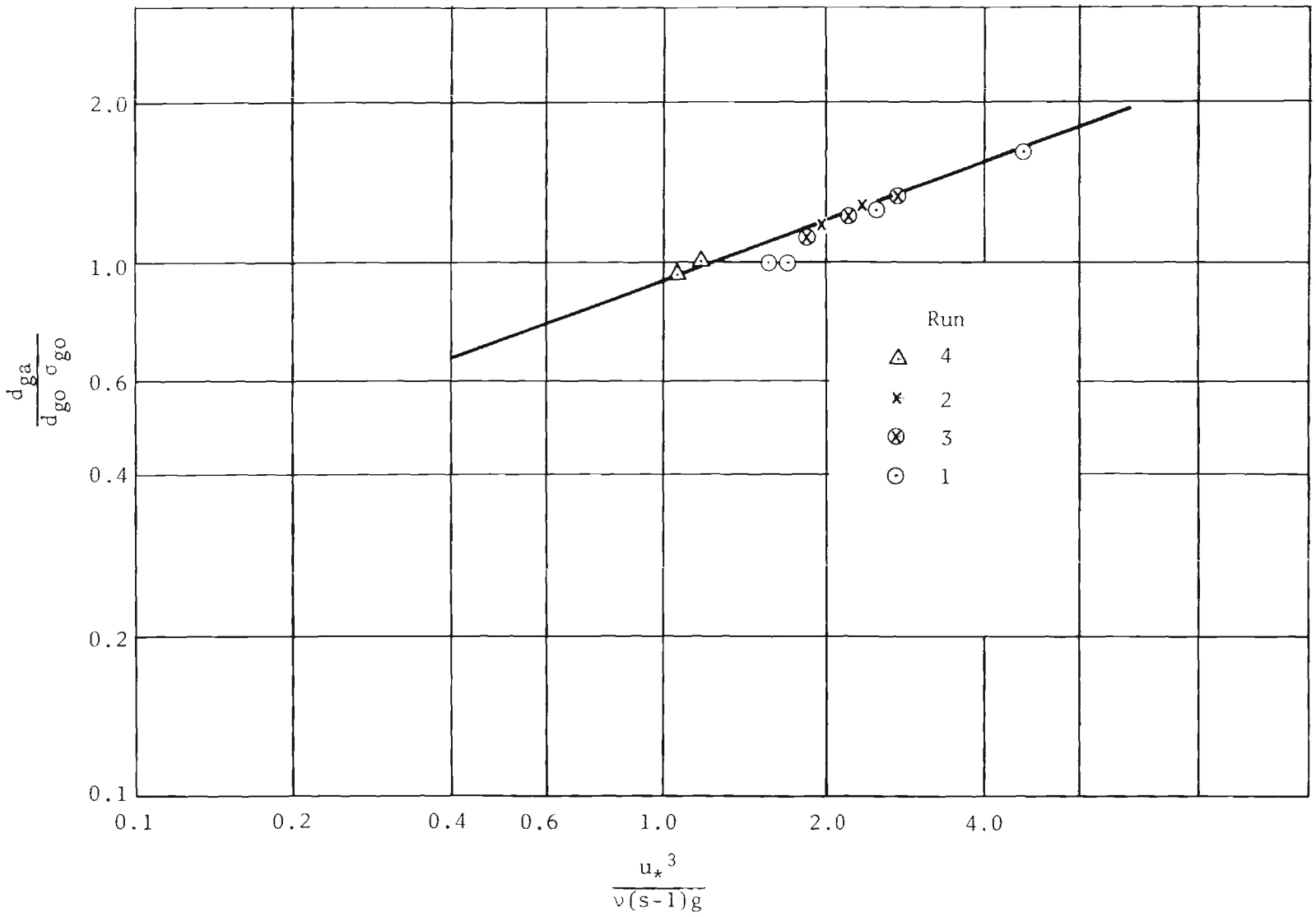

Figure 22. Plot of $d_{ga}/d_{go}\ \sigma_{go}$ Versus $(SP)(R_{*c})$

combining Equations (17) and (18) gives

$$\frac{d_{ga}}{d_{go}\,\sigma_{go}} = 0.908\left[\frac{u_{*c}^{3}}{\nu(s-1)g}\right]^{0.353} \tag{19}$$

The RHS of Equation (19) is seen to be functions only of fluid and flow properties and the specific gravity of the sediment, while the LHS of Equation (19) is a function of sediment properties only. Equation (19) fulfills objective two of this study in that it answers the question: If a sediment bed will armor, what is the mean size of the armored surface? However, Equation (19) does not answer the question: Will the sediment bed armor? Thus, another approach must be used to determine, for the given flow properties and original bed material, whether the channel will armor.

As a sediment bed armors, fine material from the original distribution is transported out, consequently, causing the distribution of sizes of the armored material to become more uniform. Flow conditions which are just below incipient motion of the largest particles contained in a mixture result in the most uniform distribution of the armored material. Therefore, incipient motion criteria for uniform sediments should be quite applicable to estimate the upper incipient motion point of broadly graded materials. Gessler (14) suggested that, considering the probabilistic nature of incipient motion, d_{95} size of the original material can be used as the controlling size for the upper incipient motion point. However, he pointed out that the d_{95} size would give a probability of movement of about 0.94. The incipient motion results of Mavis, Ho, and Tu (19) were analyzed and are plotted on Figure 23. By

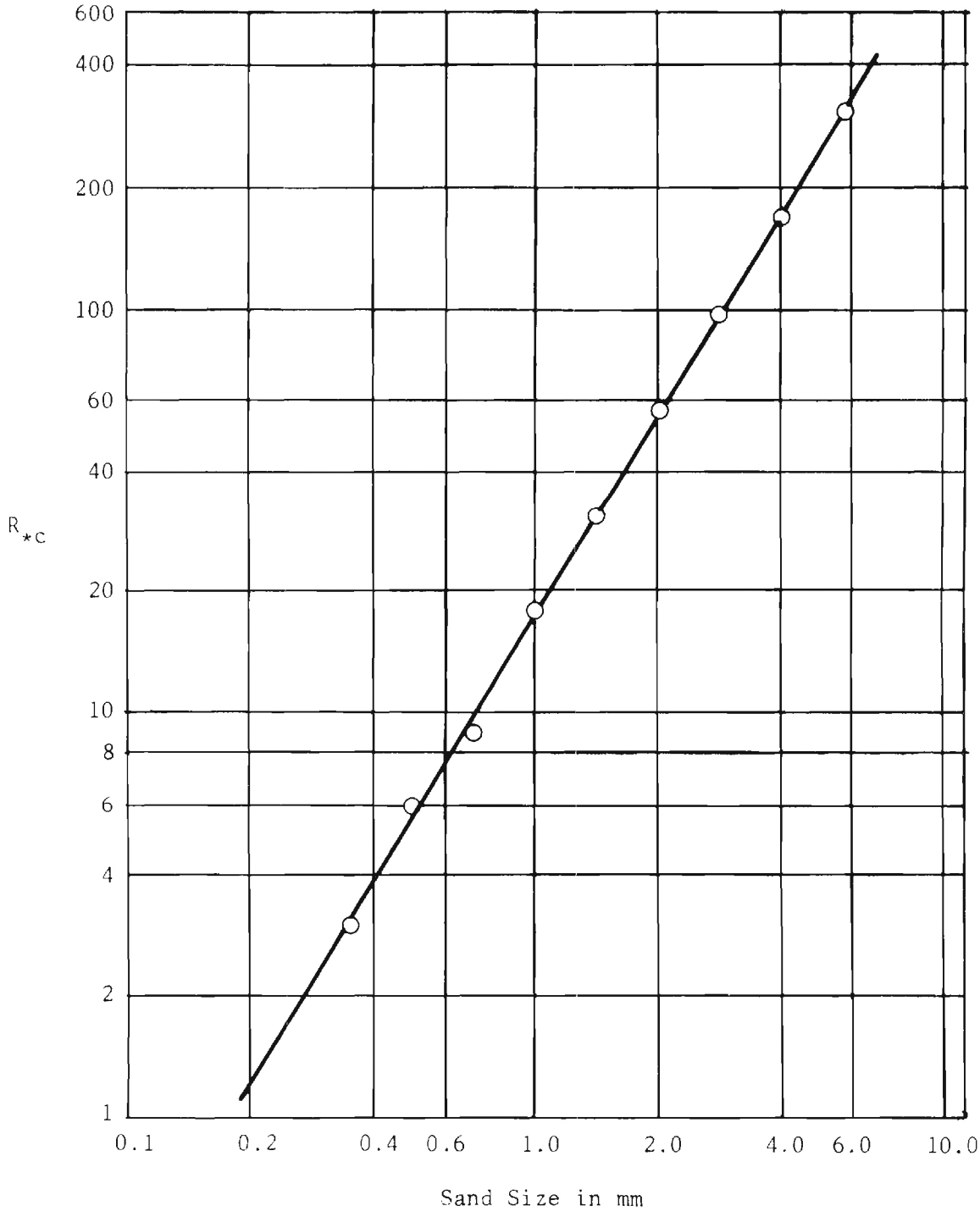

Figure 23. Incipient Motion Results for Uniform Materials

least squares analysis the Mavis data give a correlation coefficient of 0.997 when relating the critical particle Reynolds number to particle diameter in millimeters. The resulting nonhomogeneous equation was

$$R_{*c} = 17.878d^{1.5925} \tag{20}$$

For which 0.35 mm < d < 5.7 mm.

For any logarithmic-normal distribution of sediment, the d_{95} size (that particle size for which 95 percent by weight is finer) is defined by

$$d_{95} = d_{go}\ \sigma_{go}^{1.645} \tag{21}$$

Substituting d_{95}, as defined by Equation (21), for d in Equation (20) yields

$$R_{*c} = 17.878\ [d_{go}\ \sigma_{go}^{1.645}]^{1.5925} \tag{22}$$

where d_{go} is in millimeters. Equation (22) thus defines the upper incipient motion point as a function of the properties of the original sediment mixture.

For any logarithmic-normal distribution of sediment, the d_{05} size (that particle size for which five percent by weight is finer) is defined by

$$d_{05} = d_{go}\ \sigma_{go}^{-1.645} \tag{23}$$

Substituting d_{05}, as defined by Equation (23), for d in Equation (20) yields

$$R_{*c} = 17.878\ [d_{go}\ \sigma_{go}^{-1.645}]^{1.5925} \tag{24}$$

where d_{go} is in millimeters. Equation (24) thus defines the lower incipient motion point as a function of the properties of the original sediment mixture. The lower and upper critical particle Reynolds numbers for the particle gradations used in this study are listed in Table 9. The values of the lower and upper critical particle Reynolds numbers in Table 9 were calculated from Equations (24) and (22), respectively, and are plotted on Figure 24 along with the incipient motion results of the armored surfaces with d_{go}/d_{ga} as ordinate.

Table 9. Values of the Lower and Upper Critical Particle Reynolds Number

σ_{go}	d_{05}	Lower R_{*c}	d_{95}	Upper R_{*c}
1.12	0.83	13.3	1.21	24.1
1.50	.51	6.2	1.95	51.7
2.05	.31	2.7	3.26	117.2
2.50	.22	1.6	4.52	197.2
3.00	.16	1.0	6.09	317.8

The ratio d_{go}/d_{ga} is simply a measure of the degree of armoring. As d_{go}/d_{ga} decreases, the degree of armoring increases. For d_{go}/d_{ga} = 1.00, either of two conditions exists. First, if d_{go}/d_{ga} = 1.00, there are no particles moving (below lower incipient motion), or, secondly, all particles are moving (above upper incipient motion). Therefore, when d_{go}/d_{ga} = 1.00, there can be no armoring. As the ratio d_{go}/d_{ga} decreases, the bed surface becomes coarser. There is some minimum value to which d_{go}/d_{ga} can decrease, at which point all particles again go into motion,

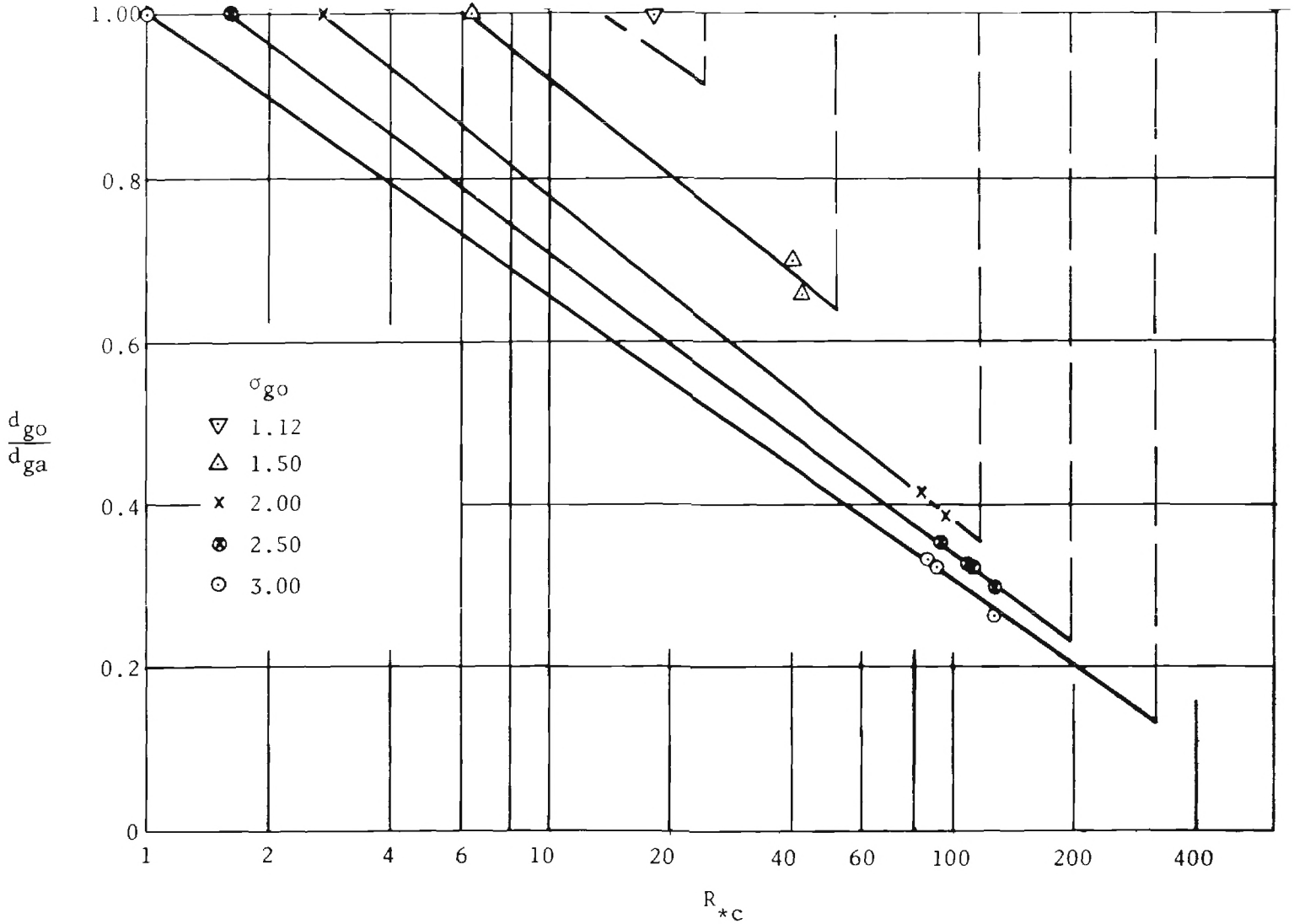

Figure 24. Plot of d_{go}/d_{ga} Versus R_{*c} for Armoring

and d_{go}/d_{ga} returns to 1.00.

Figure 24 depicts how the lower and upper incipient motion points are functions of the gradation of the original mixture. The triangular "envelope" describes the possible range of particle Reynolds numbers for which a given original mixture can armor as a function of the flow properties. Of course, the lower and upper incipient motion "points" are not necessarily unique values because of the random fluctuations of turbulence. The single point on Figure 24 at $d_{go}/d_{ga} = 1.00$ and $R_{*c} = 18$ is the measured incipient motion point for an original mixture with $d_{go} = 1.00$ and $\sigma_{go} = 1.12$ (very uniform). No armoring could be induced, of course, with this uniform distribution. However, using Equations (24) and (22) to determine the lower and upper incipient motion points, respectively, the triangular "envelope" depicted by the dashed line indicates the possible narrow range of armoring. Turbulence and experimental limitations, of course, preclude any possibility of armoring occurring for this uniform mixture. Significantly, the experimental value of $R_{*c} = 18$ is exactly the same value as that reported by Mavis et al. for 1.00 millimeter sand.

Equations (22) and (24) can be used thus to determine whether it is possible with given sediment and flow properties for the sediment bed to armor. Equation (19) can then be used to determine the geometric mean size of the armored material.

Figure 25 shows a plot of the ratio of armored to original geometric standard deviation versus the original geometric standard deviation. The armored geometric standard deviation may be obtained from Figure 25, from which the approximate armored distribution may be

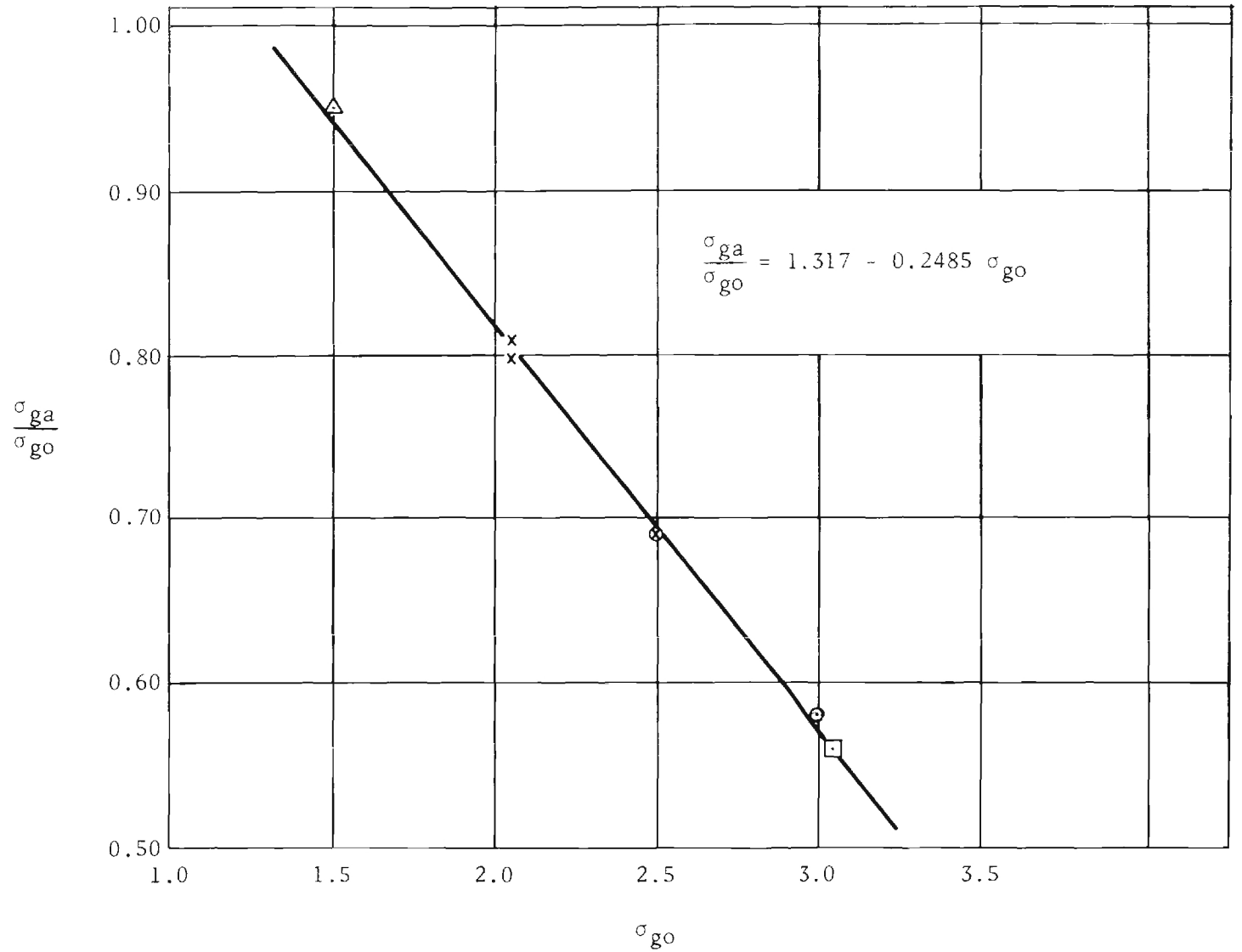

Figure 25. Plot of σ_{ga}/σ_{go} Versus σ_{go}

determined. In determining the armored geometric standard deviation from the plotted data, no attention was given to those particles smaller than d_{ga} since it is those particles greater than d_{ga} which gave the stabilizing influence to the armor coat. The smaller particles were either wedged between larger particles or were contained within a sheltered zone of separation and, thus, did not contribute to the stability of the bed.

Development of Armored Surface

At the beginning of an experimental run all sizes of material contained in the original distribution were available for transport. Since higher percentages of fine material are contained in distributions with large geometric standard deviations, more dune activity was observed with these mixtures than with those having more uniform gradations. (Dunes were larger and required more time to move off the flume.) Even without sediment inflow into the flume, dunes formed initially over the entire bed. As time progressed, dunes were observed to disappear first at the upper end of the flume since there was no sediment inflow. As the dunes began disappearing, armoring was immediately apparent. From the start of an experimental run, one to two hours were required for the dunes to move out of the flume. As the last dunes moved out, the sediment transport rate was reduced several orders of magnitude over a short period of time as shown best by Figure A.6 (Run 6-1, $\sigma_{go} = 3.05$). For low gradations, dunes were less pronounced, persisted longer, and the sediment transport rate decreased only gradually, as shown by Figures A.1 and A.2 (Runs 4-1 and 4-2, $\sigma_{go} = 1.50$).

As the surface armored and the sediment transport rate decreased,

the sediment transport was observed to be initially moved by local scour around larger non-moving particles. Even then, extremely fine material could be observed "hiding" in the wake or zone of separation of the large particles. Turbulence produced shifting of the zone of separation around the larger particles which caused small particles to become sporadically entrained into the flow. These would travel downstream until they were again trapped in another zone of separation. A cone of small particles would accumulate on the downstream side of all larger particles. Run 1-1, σ_{go} = 3.00, was continued for 19,925 minutes (almost 14 days), at which time there was still sediment outflow. After the first four days of that run, the sediment rate decreased very little, indicating that a very low sediment rate could exist for a very long period of time.

There was a question as to whether segregation of the starting surface mixture would cause a different armored distribution as compared to the prescribed original distribution as the starting mixture. This segregation could have been caused by mechanical segregation of the material while loading the flume or by the segregation which occurred during the armoring process of preceding part of an experiment run at a lower shear stress. Parts 2 and 4 of Run 3 were used to determine the effects of this presegregation on the size distribution of the armor coat for a given discharge. Figure 26 shows the armored distributions for Run 3, σ_{go} = 2.50, Parts 2 and 4. Part 2 had a discharge of 0.557 cfs and the starting surface was the armored surface from Part 1 with d_{ga} = 2.80 millimeters and σ_{ga} = 1.73. In Part 4, the armored surface of Part 3 was removed by the horizontal shear plate previously

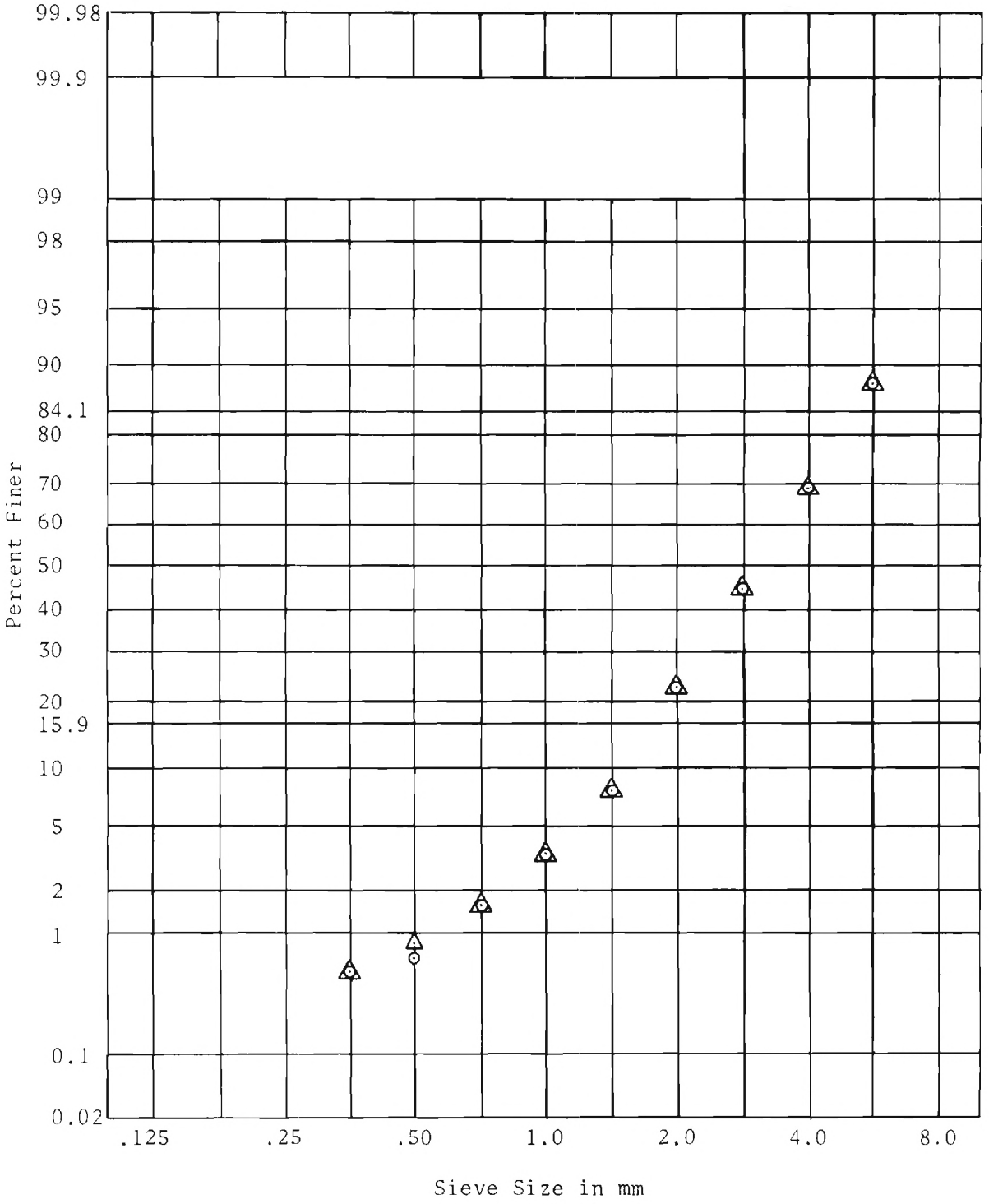

Figure 26. Plot of Armored Distributions for Run 3, Parts 2 and 4

described which gave a starting surface with d_{go} = 1.00 millimeter and σ_{go} = 2.50. Figure 26 shows the close agreement of the distributions because of the segregation of the finer material in the starting mixture.

Effect of Armoring on Depth of Flow and Slope

In this study, the initial bed slope for all experimental runs was set at 0.002. The depth of flow was measured as soon as constant depth conditions could be reached and long before any armoring had occurred. The adjustable end sill was used to follow the channel bed elevation and not to serve as a grade control structure during the armoring process. Changes in hydraulic radius and slope, before and after armoring, are given in Table 10. From the initial to the armored condition, there was an increase in hydraulic radius and a slight decrease in slope. The bed shear velocity was calculated from Equation (14), here repeated,

$$u_* = \sqrt{gRS} \tag{14}$$

and the calculated values are presented in Table 10 for the initial and final hydraulic radius and slope. The initial and final bed shear velocities for a given flow show that there was very little or no (statistical) change due to armoring. The time average bed shear stress is defined by

$$\tau = \rho\, u_*^2 \tag{25}$$

where τ is the time average bed shear stress, u_* is the bed shear velocity, and ρ is the mass density of water. Since the shear stress is

Table 10. Initial and Final Flow Conditions

Run-Part	Initial			Final		
	Hydraulic Radius R_i ft	Slope	Shear Velocity u_{*i} ft/sec	Hydraulic Radius R_f ft	Slope	Shear Velocity u_{*i} ft/sec
4-1	0.107	0.0020	0.0830	0.107	0.0019	0.0809
4-2	.115	.0020	.0861	.115	.0019	.0838
2-1	.146	.0020	.0970	.155	.0020	.0999
2-2	.169	.0020	.1043	.175	.0020	.1062
3-1	.145	.0020	.0966	.156	.0019	.0978
3-2	.170	.0020	.1046	.177	.0019	.1040
3-3	.192	.0020	.1112	.194	.0020	.1118
3-4	.172	.0020	.1052	.178	.0019	.1044
1-1	.145	.0020	.0966	.155	.0019	.0974
1-2	.156	.0020	.1121	.161	.0025	.1137
6-1	.144	.0020	.0963	.155	.0020	.0999

proportional to the bed shear velocity squared, and since for this study there was little change in bed shear velocity, there appeared to have been little change in the average bed shear stress from the initial to armored conditions. For experimental Runs 4-1 and 4-2, there was a decrease in bed shear velocity. This occurred because there was a decrease in slope and no change in hydraulic radius. These runs were made with bed material with a geometric standard deviation, $\sigma_{go} = 1.50$. This rather uniform material contained few large particles (compared to a material with $\sigma_{go} = 2.50$) and as the bed armored, the increase in mean particle size was relatively small and thus resulted in no increase in depth of flow.

In Runs 1-1 and 6-1, $\sigma_{go} = 3.00$, there was considerable dune activity within the first two hours. Even with the dunes developed early in the experiment, the flow depth increased eight to nine percent while there was a slight decrease in slope; the end result was a slight increase in bed shear velocity, u_*.

Comparison of Gessler's Method with Measured Data

Table 11 gives a comparison of the measured geometric mean diameter to that calculated by Gessler's (13) method utilizing the original sediment properties and flow properties of this study. Gessler recommended the value 0.047 be used for Shields' parameter and the value 0.57 be used for the standard deviation of the dimensionless shear stress, $\sigma_{\tau_c/\bar{\tau}}$, two variables which must be assumed as input to Gessler's method for calculating the armored surface size distribution. The differences between the measured and calculated values varied from 3.5 to 29.0 percent.

Table 11. Comparison of Gessler's Method with Measured Data

σ_{go}	Measured d_{ga} mm	Gessler's* d_{ga} mm	Difference %
1.50	1.42	1.37	3.5
1.50	1.52	1.38	9.2
2.05	2.40	1.90	20.8
2.05	2.60	1.95	25.0
2.50	2.80	2.12	24.3
2.50	3.05	2.23	27.1
2.50	3.35	2.38	29.0
2.50	3.05	2.23	27.1
3.00	3.00	2.35	21.7
3.00	3.75	2.70	28.0
3.05	3.05	2.41	21.2

* Calculated by Gessler's Method using Shields' Parameter = 0.047 and $\sigma_{\tau_c/\bar{\tau}} = 0.57$. These are Gessler's recommendations.

From Table 8, page 60, Shields' parameter, as calculated from the data of this study, varied from 0.018 to 0.026 which is considerably lower than 0.047, the value suggested by Gessler.

Values of Shields' parameter and $\sigma_{\tau_c/\bar{\tau}}$ were assumed by trial and error and used in Gessler's method to calculate a geometric mean diameter and geometric standard deviation of the armored surface which were approximately equal to the measured values. The values of Shields' parameter and $\sigma_{\tau_c/\bar{\tau}}$ necessary to force the measured and calculated values of the armored geometric diameter and standard deviations to be equal are given in Table 12. For most distributions used in this study an average value of Shields' parameter was 0.028 and of $\sigma_{\tau_c/\bar{\tau}}$ was 0.45. This value of Shields' parameter is on the same order of magnitude as those calculated from the measured data.

Apparently there are additional pertinent parameters in Gessler's method that have not been included which greatly affect the results.

Table 12. Values of Shields' Parameter and $\sigma_{\tau c/\bar{\tau}}$ Used in Gessler's Method to Force Equal Values of Calculated and Measured Armored Geometric Mean Diameters

Run	σ_{go}	R ft	S	Measured d_{ga} mm	Optimum Values of SP	Optimum Values of $\sigma_{\tau c/\bar{\tau}}$	σ_{ga}
4-1	1.50	0.1069	0.0019	1.42	0.040	0.57	1.43
4-2	1.50	.1148	.0019	1.52	.035	.45	1.43
2-1	2.05	.1550	.0020	2.40	.030	.45	1.67
2-2	2.05	.1751	.0020	2.60	.028	.42	1.67
3-1	2.50	.1564	.0019	2.80	.030	.44	1.75
3-2	2.50	.1764	.0019	3.05	.028	.45	1.75
3-3	2.50	.1942	.0020	3.35	.028	.40	1.70
3-4	2.50	.1778	.0019	3.05	.028	.45	1.75
1-1	3.00	.1550	.0019	3.00	.032	.45	1.81
1-2	3.00	.1606	.0025	3.75	.028	.45	1.67
6-1	3.05	.1550	.0020	3.05	.030	.45	1.81

CHAPTER VII

CONCLUSIONS

The pertinent conclusions of this study are summarized as follows:

1. An empirical technique was developed to determine, for a given logarithmic-normal sediment distribution and hydraulic flow properties, (1) if the sediment bed would armor, and (2) if the sediment bed should armor, the geometric mean diameter and standard deviation of the armored surface particles. The empirical equation relating sediment properties to flow properties was

$$\frac{d_{ga}}{d_{go}\,\sigma_{go}} = 0.908 \left[\frac{u_{*c}^3}{\nu(s-1)g}\right]^{0.353}$$

The criterion for determining if the sediment bed would armor was $d_{05} < d_{ga} < d_{95}$, where d_{05} and d_{95} are that particle size for which 5 and 95 percent by weight, respectively, is finer.

2. Dunes formed initially and as they moved off armoring became apparent. Armoring of the surface had no significant change on the average bed shear stress throughout the armoring process. For those distributions which armored, there was in most experiments a reduction in slope of approximately five percent and a corresponding increase in depth of approximately five percent. Since the average bed shear stress is proportional to the product of hydraulic radius and energy slope, there was little or no change in average bed shear stress.

3. After an "armor coat" had developed, a very low sediment

transport rate continued for long periods of time by local scour of fine material around larger particles.

4. For "broadly" graded materials, $\sigma_{go} \geq 2.00$, there was very little reduction in bed slope. The armored bed degraded essentially parallel to the original bed slope. This has been termed parallel degradation.

5. For "uniform" materials, $\sigma_{go} \leq 1.50$, little armoring could be induced. For $\sigma_{go} = 1.12$, no armoring could be induced under any flow conditions. This type of sediment bed can become stable only by a reduction in bed slope for a given flow condition.

APPENDIX

Table A.1. Cumulative Sediment Transport for Run 5-4

Sample No.	Cuml. Time min	Sample Weight gm	Cuml. Erosion lb
1	5	784.9	1.728
2	10	699.6	3.269
3	15	631.7	4.661
4	20	455.5	5.664
5	25	543.4	6.861
6	30	1005.1	9.075
7	35	505.9	10.189
8	40	326.1	10.907
9	45	1063.1	13.249
10	50	343.2	14.005
11	55	994.5	16.196
12	60	565.5	17.441
13	65	655.0	18.884
14	70	521.8	20.033
15	75	1032.7	22.308

Table A.2. Cumulative Sediment Transport for Run 4-1

Sample No.	Cuml. Time min	Sample Weight gm	Cuml. Erosion lb	Sample No.	Cuml. Time min	Sample Weight gm	Cuml. Erosion lb
1	10	113.6	.250	41	840	361.4	37.054
2	20	153.9	.589	42	870	302.6	37.720
3	30	151.9	.923	43	900	358.1	38.509
4	40	171.3	1.301	44	930	361.2	39.305
5	50	141.8	1.613	45	960	406.7	40.200
6	60	197.8	2.049	46	990	503.9	41.310
7	70	257.4	2.616	47	1020	436.9	42.273
8	80	239.7	3.144	48	1050	540.6	43.463
9	90	181.1	3.542	49	1080	429.0	44.408
10	100	160.4	3.896	50	1110	327.9	45.131
11	110	175.5	4.282	51	1140	289.8	45.769
12	120	219.8	4.766	52	1170	213.9	46.240
13	140	351.7	5.541	53	1200	152.1	46.575
14	160	383.5	6.386	54	1230	243.7	47.112
15	180	360.7	7.180	55	1260	457.0	48.118
16	200	368.0	7.991	56	1290	450.6	49.111
17	220	220.7	8.477	57	1320	375.0	49.937
18	240	269.0	9.070	58	1350	417.0	50.855
19	260	634.7	10.468	59	1380	321.0	51.562
20	280	512.3	11.596	60	1410	260.6	52.137
21	300	413.6	12.507	61	1440	290.4	52.776
22	320	284.2	13.133	62	1470	570.0	54.032
23	340	189.6	13.551	63	1500	583.5	55.317
24	360	369.7	14.365	64	1530	375.9	56.145
25	380	419.3	15.288	65	1560	310.9	56.830
26	400	384.1	16.135	66	1590	342.3	57.584
27	420	302.4	16.801	67	1620	392.6	58.448
28	450	679.5	18.297	68	1650	374.7	59.274
29	480	803.5	20.067	69	1680	262.0	59.851
30	510	829.1	21.893	70	1710	221.0	60.338
31	540	681.3	23.394	71	1740	212.8	60.806
32	570	658.5	24.844	72	1770	350.3	61.578
33	600	567.0	26.093	73	1800	297.4	62.235
34	630	552.4	27.310	74	1860	544.5	63.432
35	660	729.4	28.917	75	1920	694.9	64.963
36	690	811.2	30.703	76	1980	676.2	66.452
37	720	517.0	31.842	77	2040	464.7	67.475
38	750	680.7	33.342	78	2100	691.2	68.998
39	780	642.3	34.756	79	2160	528.3	70.162
40	810	681.6	36.258	80	2220	676.1	71.651

Table A.2. (Continued)

Sample No.	Cuml. Time min	Sample Weight gm	Cuml. Erosion lb	Sample No.	Cuml. Time min	Sample Weight gm	Cuml. Erosion lb
81	2280	539.5	72.840	121	4700	353.3	114.692
82	2340	469.6	73.874	122	4760	371.9	115.511
83	2400	366.0	74.680	123	4820	596.3	116.825
84	2460	438.3	75.646	124	4880	598.5	118.143
85	2520	347.2	76.410	125	4940	453.6	119.142
86	2580	313.5	77.101	126	5000	520.4	120.288
87	2640	330.6	77.829	127	5060	551.5	121.503
88	2700	469.9	78.864	128	5120	531.5	122.674
89	2760	469.4	79.898	129	5180	415.9	123.590
90	2820	461.1	80.914	130	5240	278.2	124.203
91	2880	441.2	81.885	131	5300	320.5	124.909
92	2940	778.7	83.601	132	5360	386.2	125.759
93	3000	466.9	84.629	133	5480	806.2	127.535
94	3060	418.3	85.550	134	5600	615.0	128.890
95	3120	566.6	86.798	135	5720	543.8	130.087
96	3180	569.8	88.053				
97	3240	528.6	89.218				
98	3300	552.3	90.434				
99	3360	662.0	91.892				
100	3420	446.2	92.875				
101	3500	464.7	93.899				
102	3560	483.2	94.963				
103	3620	443.6	95.940				
104	3680	428.5	96.884				
105	3740	437.8	97.848				
106	3800	391.3	98.710				
107	3860	682.1	100.213				
108	3920	618.9	101.576				
109	3980	420.7	102.503				
110	4040	334.7	103.240				
111	4100	343.9	103.997				
112	4160	364.8	104.801				
113	4220	462.4	105.819				
114	4280	470.2	106.855				
115	4340	638.8	108.262				
116	4400	625.0	109.639				
117	4460	658.1	111.088				
118	4520	549.8	112.299				
119	4580	388.3	113.155				
120	4640	344.7	113.914				

Table A.3. Cumulative Sediment Transport for Run 4-2

Sample No.	Cuml. Time min	Sample Weight gm	Cuml. Erosion lb	Sample No.	Cuml. Time min	Sample Weight gm	Cuml. Erosion lb
1	10	326.4	.718	41	620	967.3	55.240
2	20	480.6	1.777	42	650	933.5	57.296
3	30	357.3	2.564	43	680	1617.6	60.859
4	40	389.4	3.422	44	710	1854.1	64.943
5	50	596.5	4.736	45	740	1872.7	69.068
6	60	537.5	5.920	46	770	1450.1	72.262
7	70	323.3	6.632	47	800	1600.8	75.788
8	80	523.1	7.784	48	830	1556.1	79.215
9	90	464.1	8.806	49	860	1133.4	81.712
10	100	414.5	9.719	50	890	813.7	83.504
11	110	593.7	11.027	51	920	940.7	85.576
12	120	471.9	12.066	52	950	823.4	87.390
13	130	542.1	13.260	53	980	957.4	89.498
14	140	461.1	14.276	54	1010	827.2	91.320
15	150	491.8	15.359	55	1040	882.1	93.263
16	160	557.5	16.587	56	1070	853.0	95.142
17	170	516.9	17.726	57	1100	908.4	97.143
18	180	600.3	19.048	58	1130	857.6	99.032
19	190	400.4	19.930	59	1160	903.6	101.022
20	200	361.8	20.727	60	1190	1032.7	103.297
21	210	310.5	21.411	61	1220	969.7	105.433
22	220	301.4	22.075	62	1250	919.3	107.458
23	230	501.7	23.180	63	1280	868.4	109.371
24	240	483.7	24.245	64	1310	862.1	111.270
25	260	629.7	25.632	65	1340	935.6	113.330
26	280	941.2	27.705	66	1370	945.6	115.413
27	300	964.8	29.830	67	1400	879.9	117.351
28	320	832.9	31.665	68	1430	782.0	119.074
29	340	857.2	33.553	69	1460	799.8	120.835
30	360	842.2	35.408	70	1490	736.0	122.457
31	380	887.6	37.363	71	1520	776.9	124.168
32	400	746.6	39.008	72	1550	863.7	126.070
33	420	760.2	40.682	73	1580	807.0	127.848
34	440	818.8	42.486	74	1610	737.0	129.471
35	460	610.3	43.830	75	1640	623.3	130.844
36	480	720.5	45.417	76	1670	638.3	132.250
37	500	697.8	46.954	77	1700	681.9	133.752
38	530	987.6	49.129	78	1730	644.3	135.171
39	560	946.6	51.214	79	1760	625.4	136.549
40	590	860.2	53.109	80	1790	584.8	137.837

Table A.3. (Continued)

Sample No.	Cuml. Time min	Sample Weight gm	Cuml. Erosion lb
81	1820	558.0	139.066
82	1850	593.8	140.374
83	1880	619.5	141.738
84	1910	566.8	142.987
85	1940	558.2	144.216
86	1970	512.2	145.344
87	2000	526.6	146.504
88	2030	499.1	147.604
89	2060	523.4	148.757
90	2090	531.8	149.928
91	2120	543.6	151.125
92	2150	490.4	152.205
93	2180	494.8	153.295
94	2210	491.0	154.377
95	2240	511.5	155.503
96	2270	469.1	156.537

Table A.4. Cumulative Sediment Transport for Run 2-1

Sample No.	Cuml. Time min	Sample Weight gm	Cuml. Erosion lb	Sample No.	Cuml. Time min	Sample Weight gm	Cuml. Erosion lb
1	10	591.0	1.301	41	450	672.3	43.919
2	20	577.1	2.572	42	510	812.2	45.708
3	30	554.5	3.794	43	540	565.2	46.953
4	40	590.0	5.093	44	570	751.9	48.609
5	50	599.4	6.414	45	600	765.0	50.294
6	60	574.6	7.679	46	630	719.6	51.879
7	70	557.3	8.907	47	660	782.4	53.602
8	80	572.2	10.167	48	690	676.4	55.092
9	90	554.3	11.388	49	720	544.1	56.291
10	100	518.2	12.529	50	750	587.5	57.585
11	110	494.3	13.618	51	780	562.0	58.823
12	120	526.7	14.778	52	810	610.0	60.166
13	130	438.5	15.744	53	840	606.4	61.502
14	140	688.5	17.261	54	870	510.4	62.626
15	150	604.5	18.592	55	900	464.3	63.649
16	160	549.0	19.801	56	960	860.1	65.543
17	170	540.4	20.992	57	1020	813.0	67.334
18	180	424.0	21.926	58	1080	818.1	69.136
19	190	512.4	23.054	59	1140	781.8	70.858
20	200	631.4	24.445	60	1200	670.3	72.335
21	210	460.7	25.460	61	1260	661.6	73.792
22	220	511.7	26.587	62	1320	511.5	74.918
23	230	496.0	27.679	63	1350	340.0	75.667
24	240	362.5	28.478	64	1410	608.6	77.008
25	250	438.0	29.443	65	1470	572.3	78.268
26	260	456.8	30.449	66	1530	703.5	79.818
27	270	393.7	31.316	67	1590	551.4	81.033
28	280	316.1	32.012	68	1650	582.0	82.314
29	290	401.3	32.896	69	1710	437.4	83.278
30	300	396.8	33.770	70	1770	670.7	84.755
31	310	365.7	34.576	71	1830	419.7	85.680
32	320	313.0	35.265	72	1890	332.5	86.412
33	330	305.3	35.938	73	1950	304.7	87.083
34	340	326.6	36.657	74	2070	625.1	88.460
35	350	308.3	37.336	75	2190	596.1	89.773
36	360	295.5	37.987	76	2310	532.5	90.946
37	370	241.2	38.518	77	2430	544.2	92.145
38	390	480.3	39.576	78	2550	568.6	93.397
39	410	624.3	40.951	79	2730	758.1	95.067
40	430	675.0	42.438	80	2970	838.6	96.914

Table A.4. (Continued)

Sample No.	Cuml. Time min	Sample Weight gm	Cuml. Erosion lb
81	3210	763.4	98.595
82	3450	692.4	100.120
83	3690	840.9	101.972
84	3930	639.6	103.381
85	4290	629.2	104.767
86	4650	644.5	106.187
87	5010	681.5	107.688
88	5370	611.1	109.034
89	5730	494.2	110.122
90	6090	431.3	111.072
91	6570	544.7	112.272
92	6810	306.5	112.947
93	7170	504.4	114.058
94	7590	607.8	115.397
95	8070	461.0	116.412
96	8490	408.5	117.312
97	8970	608.0	118.651
98	9450	423.0	119.583
99	9930	433.5	120.538
100	10110	162.7	120.896

Table A.5. Cumulative Sediment Transport for Run 3-1

Sample No.	Cuml. Time min	Sample Weight gm	Cuml. Erosion lb	Sample No.	Cuml. Time min	Sample Weight gm	Cuml. Erosion lb
1	10	456.6	1.005	34	1320	462.1	19.180
2	20	310.5	1.689	35	1440	507.7	20.307
3	30	286.3	2.320	36	1560	453.8	21.307
4	40	219.8	2.804	37	1680	276.0	21.915
5	50	167.6	3.173	38	1800	289.2	22.552
6	60	130.7	3.461	39	2040	703.3	24.101
7	70	123.0	3.732	40	2280	691.0	25.623
8	80	113.3	3.981	41	2520	728.9	27.228
9	90	103.3	4.209	42	2760	661.8	28.686
10	100	99.5	4.428	43	3000	706.2	30.242
11	110	97.8	4.644	44	3240	476.1	31.290
12	120	97.3	4.858	45	3480	250.0	31.841
13	140	163.3	5.218	46	3720	260.0	32.414
14	160	113.0	5.466	47	3960	218.0	32.894
15	180	120.5	5.732	48	4200	324.6	33.609
16	210	153.1	6.069	49	4440	297.6	34.264
17	240	180.0	6.466	50	4920	495.2	35.355
18	270	248.6	7.013	51	5400	472.4	36.396
19	300	216.6	7.490	52	5880	402.2	37.281
20	330	211.7	7.957	53	6360	738.5	38.908
21	360	193.5	8.383	54	6840	479.2	39.964
22	390	235.0	8.900	55	7320	384.1	40.810
23	420	193.7	9.327	56	7620	257.5	41.377
24	450	317.4	10.026	57	8100	338.0	42.121
25	480	271.2	10.624	58	8580	330.8	42.850
26	540	410.6	11.528	59	9060	322.7	43.561
27	600	261.5	12.104	60	9540	351.2	44.334
28	660	264.1	12.686	61	10260	493.4	45.421
29	720	290.4	13.325	62	10980	420.9	46.348
30	840	733.7	14.941	63	11700	405.6	47.242
31	960	620.9	16.309	64	12600	390.4	48.101
32	1080	467.6	17.339	65	13380	318.3	48.803
33	1200	377.8	18.171	66	14820	599.6	50.123

Table A.6. Cumulative Sediment Transport for Run 3-4

Sample No.	Cuml. Time min	Sample Weight gm	Cuml. Erosion lb	Sample No.	Cuml. Time min	Sample Weight gm	Cuml. Erosion lb
1	5	1391.1	3.064	41	205	349.7	87.072
2	10	1064.1	5.407	42	210	372.5	87.892
3	15	1006.5	7.624	43	220	625.9	89.271
4	20	1210.4	10.290	44	230	617.2	90.630
5	25	1193.1	12.918	45	240	525.2	91.787
6	30	1152.7	15.457	46	250	457.8	92.795
7	35	1680.3	19.159	47	260	519.4	93.939
8	40	1034.6	21.437	48	270	502.8	95.047
9	45	1367.5	24.449	49	280	439.3	96.014
10	50	1232.2	27.164	50	290	340.5	96.764
11	55	1331.5	30.096	51	300	303.5	97.433
12	60	1755.6	33.963	52	310	399.7	98.313
13	65	999.7	36.165	53	320	419.1	99.237
14	70	574.9	37.432	54	330	339.9	99.985
15	75	693.7	38.960	55	340	268.7	100.577
16	80	2008.2	43.383	56	350	311.4	101.263
17	85	2577.2	49.060	57	360	304.0	101.933
18	90	1742.4	52.898	58	370	226.5	102.431
19	95	1381.0	55.939	59	380	230.4	102.939
20	100	1212.0	58.609	60	390	294.2	103.587
21	105	1142.7	61.126	61	420	742.3	105.222
22	110	931.9	63.179	62	450	602.5	106.549
23	115	778.5	64.893	63	480	606.2	107.884
24	120	876.8	66.825	64	510	670.4	109.361
25	125	831.4	68.656	65	540	468.8	110.394
26	130	703.0	70.204	66	570	390.2	111.253
27	135	648.4	71.633	67	600	393.8	112.120
28	140	630.8	73.022	68	630	394.6	112.990
29	145	644.8	74.442	69	660	381.9	113.831
30	150	652.9	75.880	70	690	404.6	114.722
31	155	581.6	77.161	71	720	400.7	115.605
32	160	448.2	78.149	72	750	402.6	116.491
33	165	397.7	79.025	73	780	345.2	117.252
34	170	512.4	80.153	74	810	304.7	117.923
35	176	677.9	81.646	75	840	307.4	118.600
36	180	382.4	82.489	76	870	277.3	119.211
37	185	451.3	83.483	77	900	348.1	119.977
38	190	447.9	84.469	78	930	276.2	120.586
39	195	433.0	85.423	79	960	287.1	121.218
40	200	398.7	86.301	80	990	232.4	121.730

Table A.6. (Continued)

Sample No.	Cuml. Time min	Sample Weight gm	Cuml. Erosion lb
81	1020	280.0	122.347
82	1050	260.8	122.921
83	1080	223.5	123.414
84	1110	147.1	123.738
85	1170	445.6	124.719
86	1230	437.2	125.682
87	1290	357.9	126.470
88	1350	337.2	127.213
89	1470	819.4	129.018
90	1590	579.4	130.294
91	1710	527.2	131.455
92	1830	452.5	132.452
93	1950	540.0	133.642
94	2070	427.9	134.584
95	2190	471.5	135.623
96	2310	449.2	136.612
97	2430	382.6	137.455
98	2550	327.0	138.175
99	2670	427.0	139.116
100	2790	420.0	140.041
101	2910	343.2	140.797
102	3030	240.4	141.326
103	3150	318.4	142.027
104	3330	467.0	143.056
105	3510	366.1	143.862
106	3690	382.9	144.706
107	3890	328.9	145.430
108	4110	375.6	146.258
109	4350	376.7	147.087
110	4530	240.0	147.616

Table A.7. Cumulative Sediment Transport for Run 1-1

Sample No.	Cuml. Time min	Sample Weight gm	Cuml. Erosion lb	Sample No.	Cuml. Time min	Sample Weight gm	Cuml. Erosion lb
1	10	292.3	.643	41	410	37.8	12.609
2	20	399.9	1.524	42	420	37.1	12.691
3	30	382.5	2.367	43	430	38.7	12.776
4	40	350.6	3.139	44	440	38.6	12.861
5	50	254.3	3.699	45	450	40.2	12.950
6	60	179.4	4.094	46	460	54.3	13.070
7	70	129.2	4.379	47	470	43.3	13.165
8	80	123.9	4.652	48	480	47.9	13.270
9	90	222.3	5.141	49	490	48.0	13.376
10	100	292.2	5.785	50	610	564.7	14.620
11	110	283.0	6.408	51	730	411.0	15.525
12	120	206.1	6.862	52	850	357.1	16.312
13	130	224.4	7.357	53	970	355.2	17.094
14	140	234.8	7.874	54	1090	352.3	17.870
15	150	224.8	8.369	55	1135	188.8	18.286
16	160	148.3	8.696	56	1255	261.1	18.861
17	170	125.8	8.973	57	1375	330.5	19.589
18	180	113.6	9.223	58	1615	500.2	20.691
19	190	104.5	9.453	59	1855	374.4	21.516
20	200	87.9	9.647	60	2215	566.8	22.764
21	210	72.3	9.806	61	2695	546.1	23.967
22	220	81.6	9.986	62	3175	526.0	25.125
23	230	83.2	10.169	63	3655	524.7	26.281
24	240	76.9	10.338	64	4135	479.5	27.337
25	250	71.4	10.496	65	4615	314.3	28.030
26	260	79.8	10.671	66	5065	241.9	28.562
27	270	73.1	10.832	67	5545	259.5	29.134
28	280	79.3	11.007	68	6025	278.0	29.746
29	290	77.3	11.177	69	6505	246.8	30.290
30	300	94.0	11.384	70	6985	215.7	30.765
31	310	97.0	11.598	71	7465	213.6	31.236
32	320	83.4	11.782	72	7945	236.2	31.756
33	330	59.5	11.913	73	8425	240.7	32.286
34	340	44.8	12.011	74	8905	233.7	32.801
35	350	35.7	12.090	75	9385	268.0	33.391
36	360	41.1	12.181	76	9865	222.5	33.881
37	370	42.2	12.274	77	10345	237.9	34.405
38	380	38.1	12.357	78	10795	237.5	34.928
39	390	39.6	12.445	79	11255	222.5	35.418
40	400	37.0	12.526	80	11885	230.1	35.925

Table A.7. (Continued)

Sample No.	Cuml. Time min	Sample Weight gm	Cuml. Erosion lb
81	12605	202.6	36.372
82	13325	288.0	37.006
83	14045	256.0	37.570
84	14945	238.7	38.096
85	15545	197.4	38.530
86	16265	228.1	39.033
87	16985	214.3	39.505
88	17645	226.5	40.004
89	18425	200.0	40.444
90	19145	263.0	41.024
91	19925	167.7	41.393

Table A.8. Cumulative Sediment Transport for Run 6-1

Sample No.	Cuml. Time min	Sample Weight gm	Cuml. Erosion lb	Sample No.	Cuml. Time min	Sample Weight gm	Cuml. Erosion lb
1	5	1392.8	3.067	41	230	376.8	82.198
2	10	1055.8	5.393	42	240	414.4	83.111
3	15	1193.0	8.021	43	250	405.0	84.003
4	20	1344.9	10.983	44	260	401.6	84.887
5	25	1237.0	13.708	45	270	351.7	85.662
6	30	933.2	15.763	46	280	275.8	86.270
7	35	1033.2	18.039	47	290	278.0	86.882
8	40	1491.2	21.324	48	300	268.6	87.474
9	45	1111.7	23.772	49	320	524.6	88.629
10	50	506.5	24.888	50	340	424.3	89.564
11	55	1991.7	29.275	51	360	359.9	90.356
12	60	1305.8	32.151	52	380	361.9	91.153
13	65	849.6	34.022	53	400	287.6	91.787
14	70	848.8	35.892	54	420	254.1	92.347
15	75	1106.6	38.329	55	450	320.2	93.052
16	80	1444.0	41.510	56	480	288.2	93.687
17	85	1961.0	45.829	57	510	231.1	94.196
18	90	1463.0	49.052	58	540	232.4	94.708
19	95	1204.9	51.706	59	570	229.2	95.212
20	100	1210.7	54.373	60	630	283.8	95.838
21	105	910.3	56.378	61	690	493.0	96.924
22	110	963.3	58.499	62	750	408.2	97.823
23	115	850.8	60.374	63	810	348.0	98.589
24	120	740.0	62.003	64	870	347.0	99.353
25	125	731.4	63.614	65	930	261.9	99.930
26	130	801.2	65.379	66	990	254.8	100.492
27	135	740.0	67.009	67	1050	296.1	101.144
28	140	650.1	68.441	68	1110	218.7	101.625
29	145	585.2	69.730	69	1170	207.8	102.083
30	150	532.4	70.903	70	1230	224.0	102.577
31	155	499.8	72.004	71	1290	169.3	102.949
32	160	426.8	72.944	72	1410	358.2	103.738
33	165	429.0	73.889	73	1530	315.2	104.433
34	170	399.7	74.769	74	1650	298.9	105.091
35	175	381.7	75.610	75	1770	236.3	105.612
36	180	363.4	76.410	76	1890	225.4	106.108
37	190	579.4	77.687	77	2010	246.4	106.651
38	200	583.3	78.971	78	2250	391.1	107.512
39	210	582.0	80.253	79	2490	514.3	108.645
40	220	506.1	81.368	80	2730	345.9	109.407

Table A.8. (Continued)

Sample No.	Cuml. Time min	Sample Weight gm	Cuml. Erosion lb
81	2970	385.5	110.256
82	3210	242.6	110.790
83	3450	250.5	111.342
84	3690	270.9	111.939
85	3930	246.3	112.481
86	4170	245.7	113.023
87	4410	268.6	113.614
88	4650	279.1	114.229
89	5130	447.9	115.216
90	5610	432.6	116.168
91	6090	410.3	117.072
92	6570	433.8	118.028
93	7050	395.9	118.900
94	7530	364.2	119.702
95	8010	358.7	120.492
96	8490	349.6	121.262

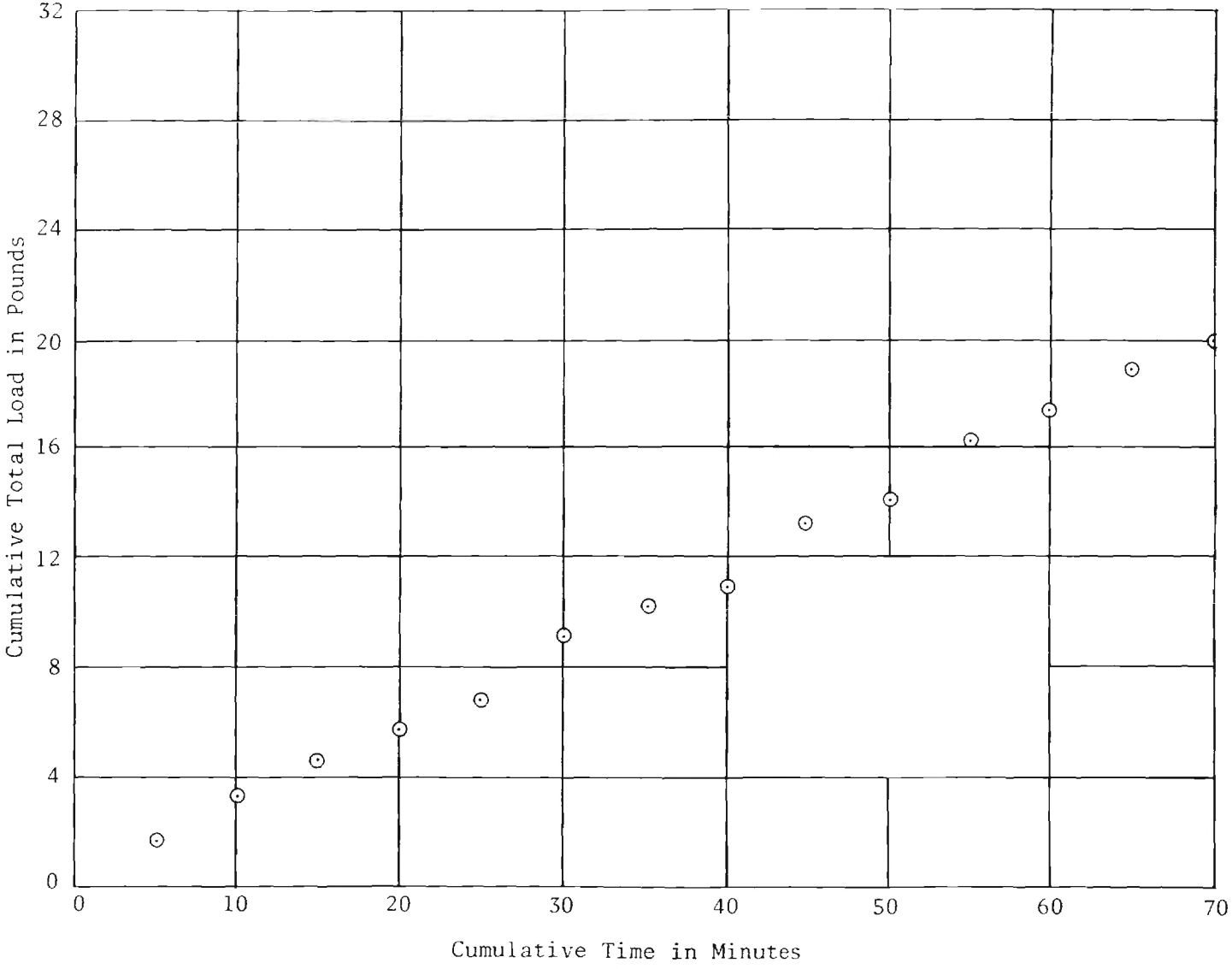

Figure A.1. Cumulative Total Load as a Function of Time for Run 5-4

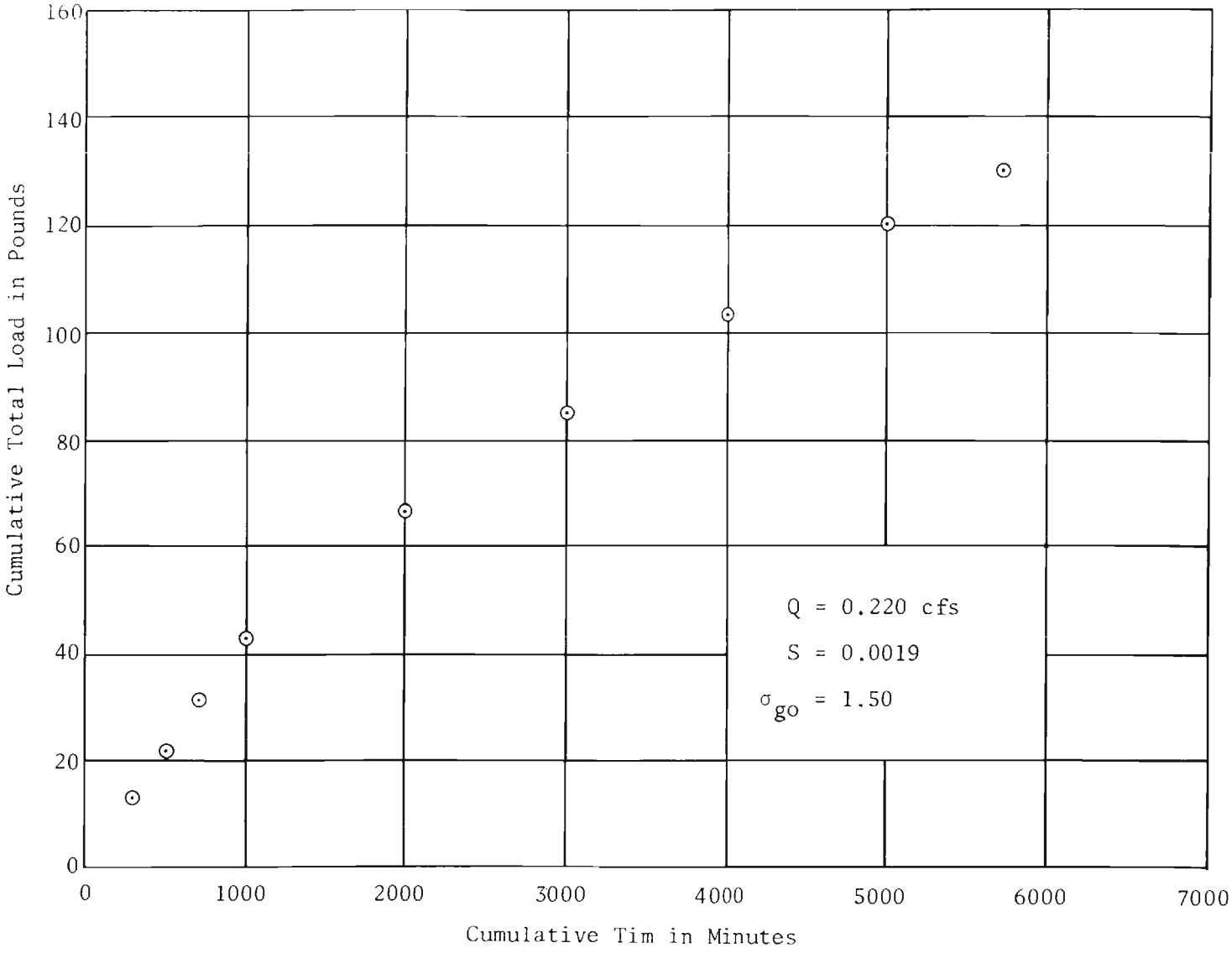

Figure A.2. Cumulative Total Load as a Function of Time for Run 4-1

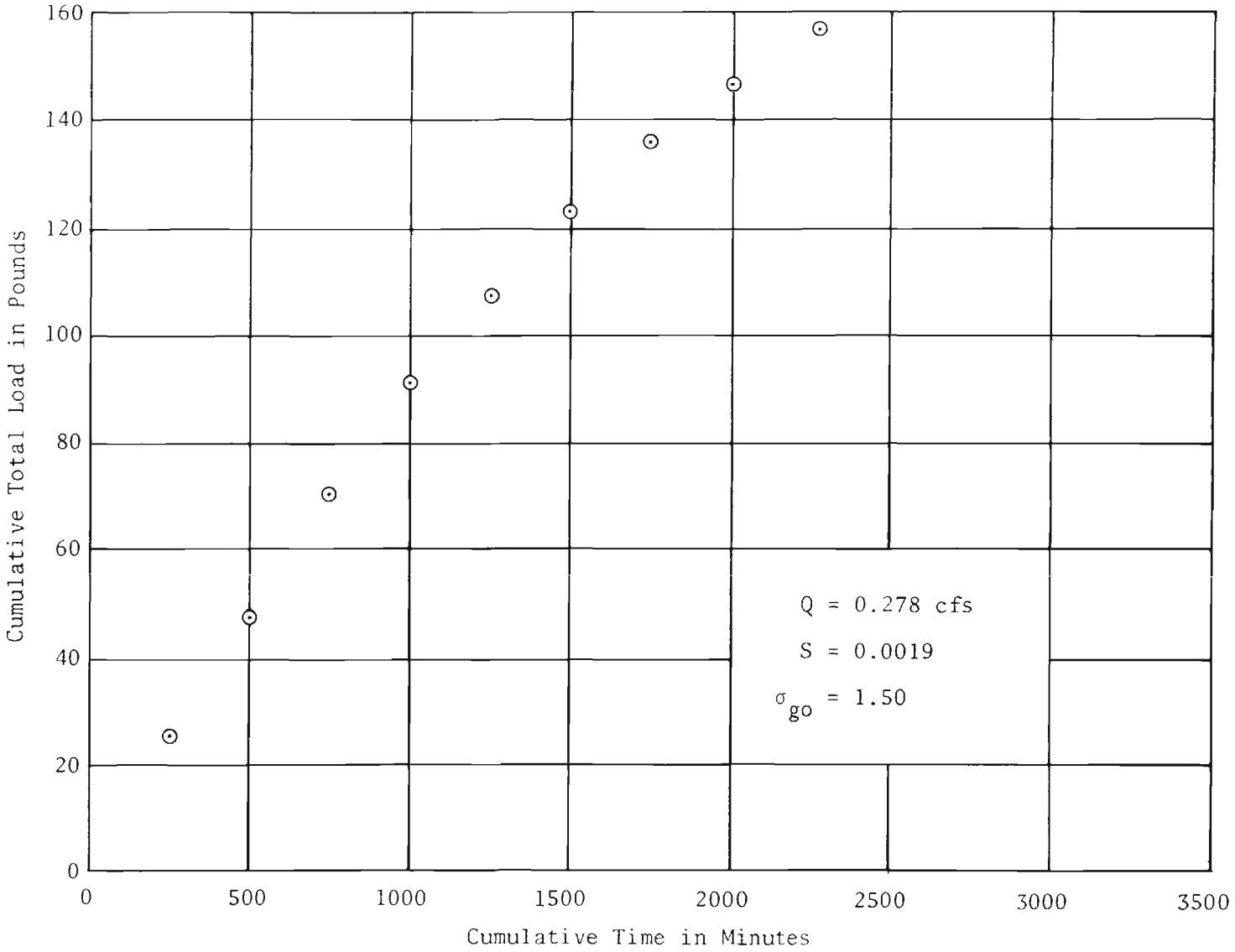

Figure A.3. Cumulative Total Load as a Function of Time for Run 4-2

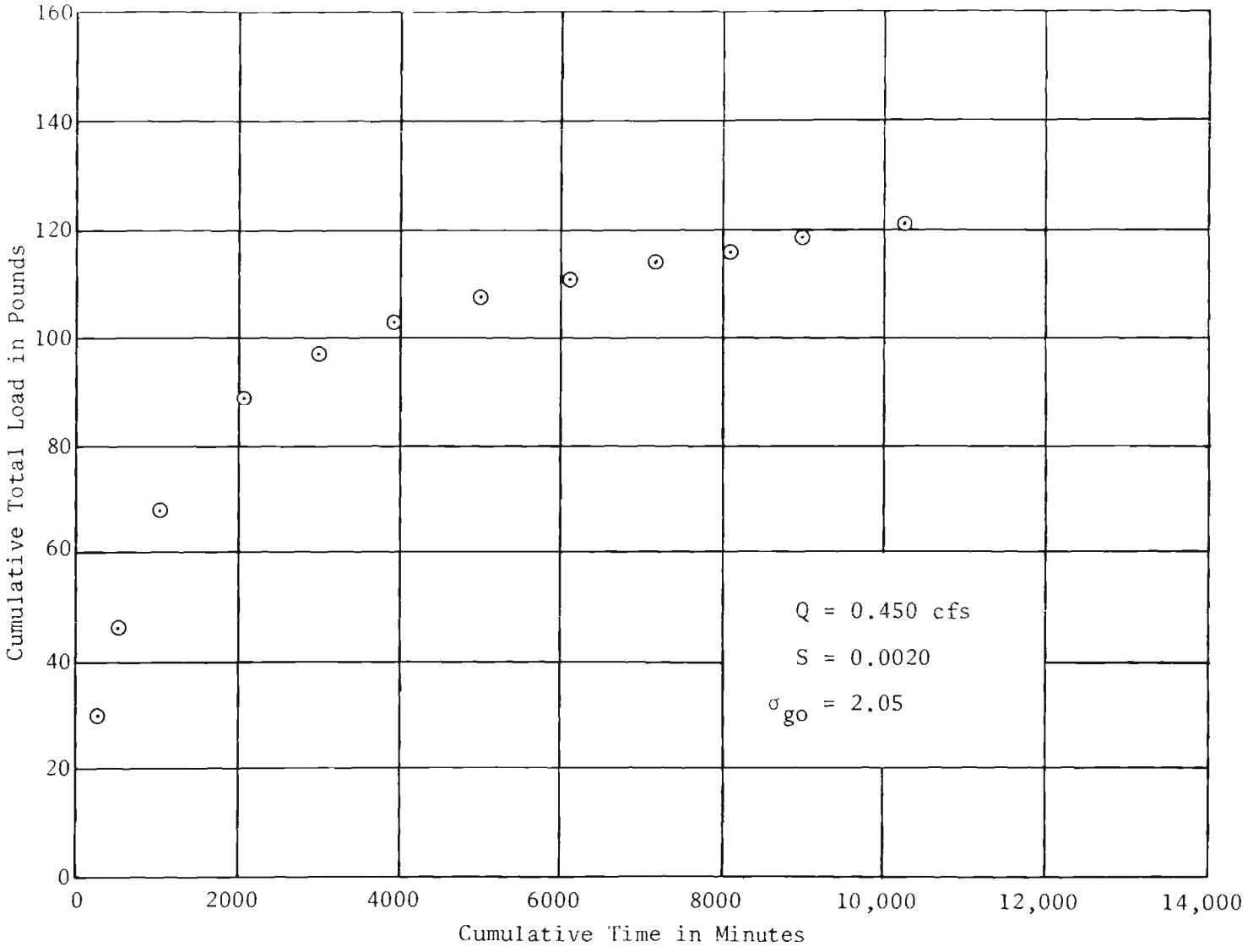

Figure A.4. Cumulative Total Load as a Function of Time for Run 2-1

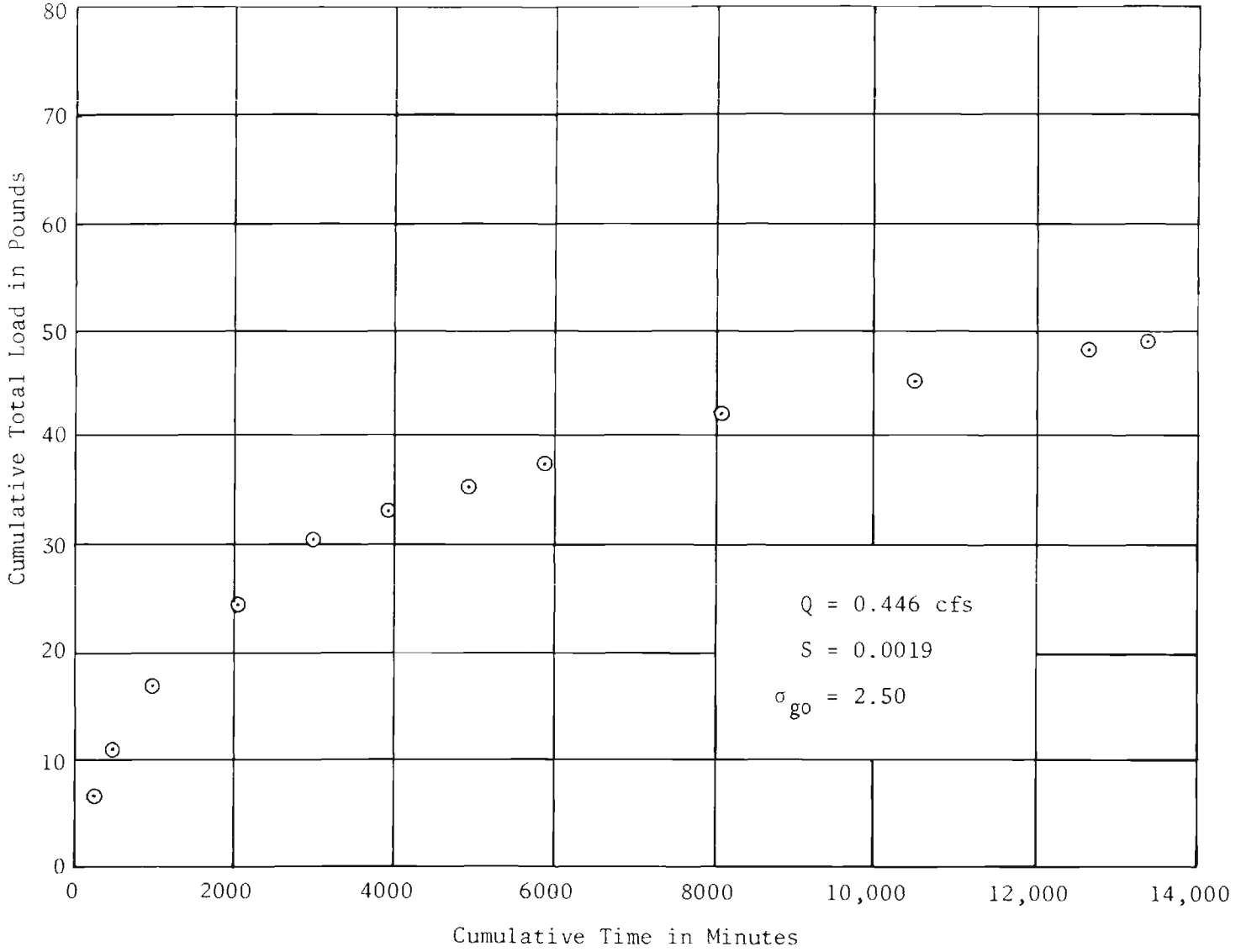

Figure A.5. Cumulative Total Load as a Function of Time for Run 3-1

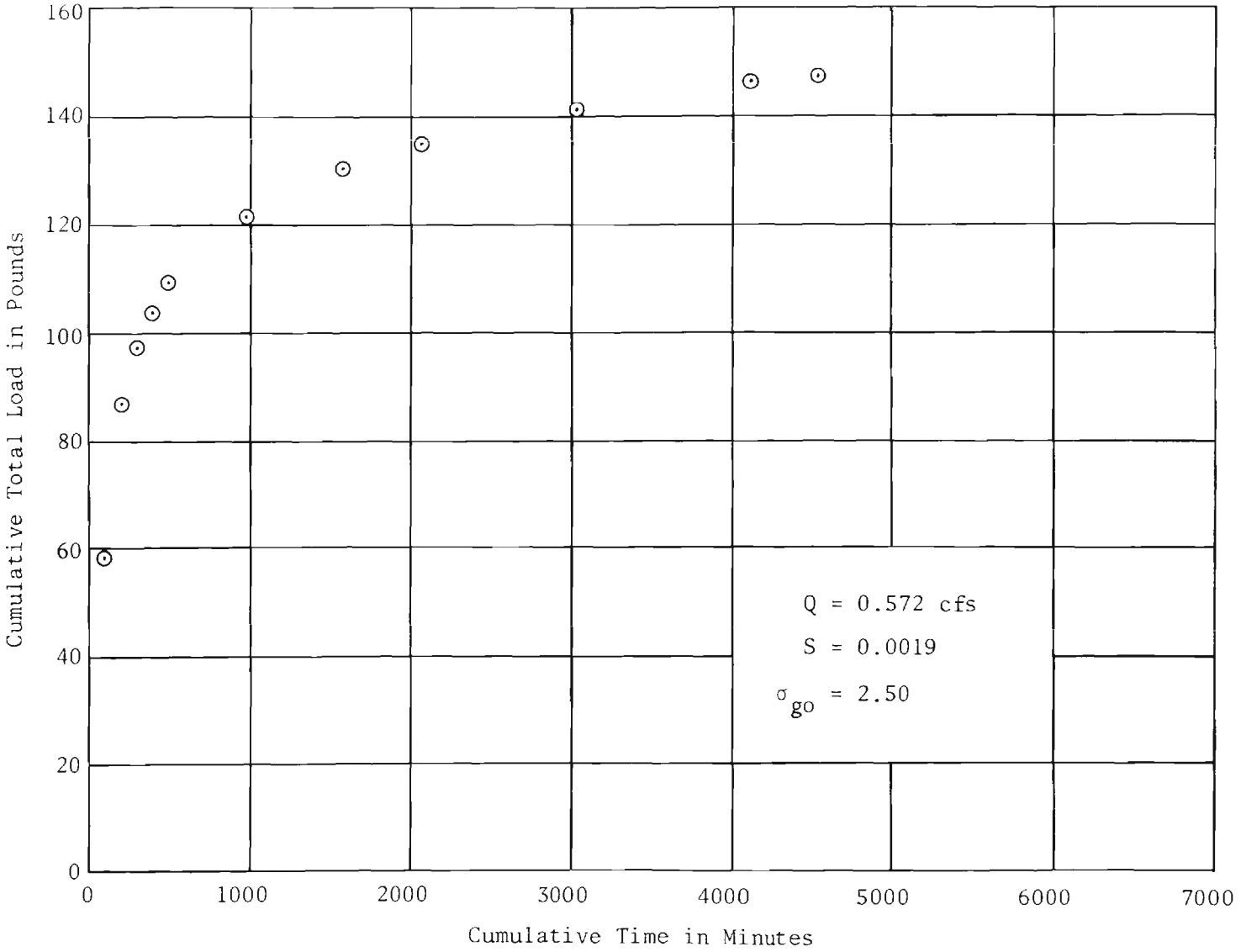

Figure A.6. Cumulative Total Load as a Function of Time for Run 3-4

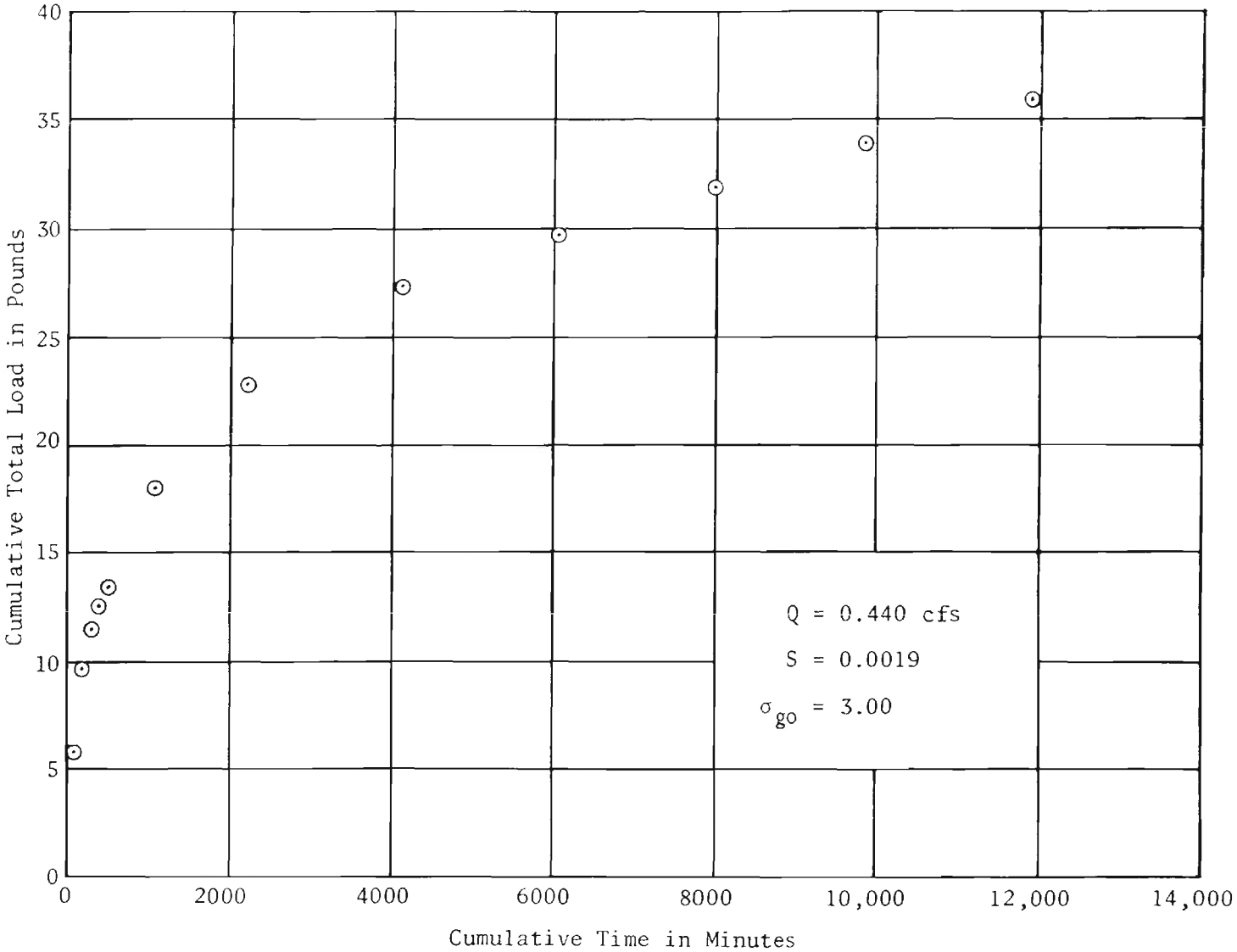

Figure A.7. Cumulative Total Load as a Function of Time for Run 1-1

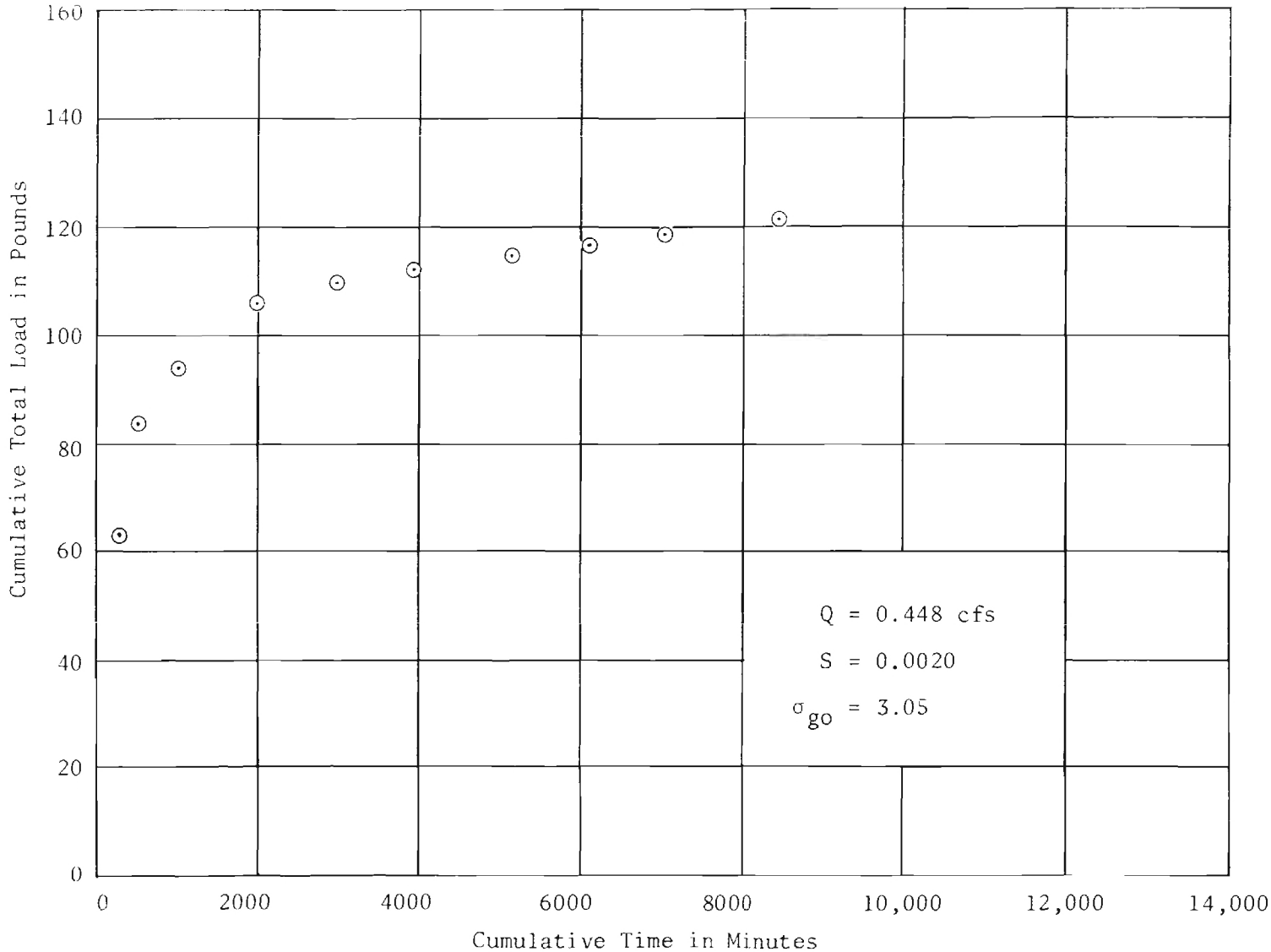

Figure A.8. Cumulative Total Load as a Function of Time for Run 6-1

REFERENCES

1. ASTM Standards, "Sieve Analysis of Fine and Coarse Aggregation," Part 3, ASTM Designation C136-46, American Society for Testing Materials, Philadelphia, 1955.

2. Bagnold, R. A., "Sediment Discharge and Stream Power, A Preliminary Announcement," U. S. Geological Survey, Circular 421, 1960, 23 p.

3. Bishop, A. A., "Sediment Transport in Alluvial Channels, A Critical Examination of Einstein's Theory," Ph.D. Dissertation, Colorado State University, July 1961, 138 p.

4. Chen, Charng Ning, "Removal of a Spherical Particle from a Flat Bed," Ph.D. Dissertation, School of Civil Engineering, Georgia Institute of Technology, October 1970, 98 p.

5. Cheng, E. D. H., "Incipient Motion of Large Roughness Elements in Open Channel Flow," Ph.D. Dissertation in Civil Engineering, Utah State University, Logan, Utah, 1969, 179 p.

6. Colby, B. R., and Hubbell, D. W., "Simplified Methods for Computing Total Sediment Discharge with the Modified Einstein Procedure," U. S. Geological Survey, Water-Supply Paper, No. 1593, 1961, 17 p.

7. Coleman, Neil L., "Laboratory Experiments in Selective Grain Transport," Ph.D. Dissertation, Department of Geology, The University of Chicago, June 1960, 49 p.

8. Daranandana, N., "A Preliminary Study of the Effect of Gradation of Bed Material on Flow Phenomenon in Alluvial Channels," Ph.D. Dissertation, Colorado State University, May 1962, 167 p.

9. Einstein, H. A., "The Bed-Load Function for Sediment Transportation in Open Channel Flows," Technical Bulletin No. 1026, U. S. Dept. of Agriculture, Washington, D. C., 1950.

10. Einstein, H. A., and Chen, Ning, "Transport of Sediment Mixtures with Large Ranges of Grain Sizes," University of California, Missouri River Division Sediment Series No. 2, June 1953.

11. Garde, R. J., and Hasan, S. M., "An Experimental Investigation of Degradation in Alluvial Channels," Proceedings of the 12th Congress, International Association for Hydraulic Research, Vol. 3, Fort Collins, Colorado, 1967, pp. 38-45.

12. Gessler, Johannes, "The Beginning of Bedload Movement of Mixtures Investigated as Natural Armoring in Channels," (1965) Translated by E. A. Prych. Translation T-5, W. M. Keck Laboratory of Hydraulics and Water Resources, California Institute of Technology, Pasadena, California. (Revised October 1968).

13. Gessler, J., "Self-Stabilizing Tendencies of Alluvial Channels," Journal of the Waterways and Harbors Division, ASCE, Vol. 96, No. WW2, May 1970, pp. 235-249.

14. Gessler, J., "Critical Shear Stress for Sediment Mixtures," Proceedings of the 14th Congress, International Association for Hydraulic Research, Vol. 3, Paper No. C1, Paris, 1971, pp. 1-8.

15. Harrison, Alfred S., "The Segregation of Grain Sizes in a Degrading Bed," Master of Science Thesis, Department of Civil Engineering, University of California, Sept. 1950, 205 p.

16. Kalinske, A. A., "Movement of Sediment as Bedload in Rivers," American Geophysical Union, Transactions, Vol. 28, August 1947, pp. 615-620.

17. Lane, E. W., and Carlson, E. J., "Some Factors Affecting the Stability of Canals Constructed in Coarse Granular Material," Proceedings, International Association for Hydraulic Research, Minnesota International Hydraulics Convention, 1953.

18. Martin, Charles S., "The Role of a Permeable Bed in Incipient Sediment Motion," Ph.D. Dissertation, School of Civil Engineering, Georgia Institute of Technology, May 1964, 150 p.

19. Mavis, F. C. Ho, and Tu, Y., "The Transportation of Detritus by Flowing Water-I," Bulletin 5, University of Iowa Studies in Engineering, Iowa City, Iowa, March 1935, 53 p.

20. Vanoni, V. A., Brooks, N. H., and Kennedy, J. F., "Lecture Notes on Sediment Transportation and Channel Stability," Publication No. KHWR-1, W. M. Keck Laboratory of Hydraulics and Water Resources, California Institute of Technology, Sept. 1960.

21. White, C. M., "The Equilibrium of Grains on the Bed of a Stream," Proceedings of the Royal Scoeity of London, Vol. 174A, 1940, pp. 322-324.

VITA

William Campbell Little was born in Remlap, Alabama, on March 23, 1930. He attended elementary and junior high school, Pinson, Alabama, and was graduated from Phillips High School, Birmingham, Alabama, in May 1948. In September of the same year, he entered Auburn University and attended until June 1950. He entered the United States Air Force in August 1950 and was honorably discharged in August 1954. He re-entered Auburn University in January 1955 and received the degree of Bachelor of Science in Agricultural Engineering in June 1957.

He was then employed by the U. S. Department of Agriculture, Agricultural Research Service, at Auburn University where he participated in several irrigation research projects with the Agricultural Engineering Department. He received the Master of Science degree from Auburn University in March 1962. From March 1962 to September 1965 he was on the staff of the Southern Piedmont Conservation Research Center where he participated in water management systems research. In 1965, he entered Georgia Institute of Technology in pursuit of a Doctor of Philosophy degree. Academic requirements were completed in June 1967. He then returned to Southern Piedmont Conservation Research Center to begin the study herein reported.

He is a member of Gamma Sigma Delta, Phi Kappa Phi, and Sigma Xi.

He and his wife, Stephanie (Farris), have four children.